

AD-A268 189



Estimated average number of copies per report, including the time for reviewing instructions, searching existing data sources, gathering and reviewing the collection of information, and comments regarding this burden estimate or any other aspect of this collection of information, including suggestions for reducing this burden, should be sent to Washington Headquarters Services, Directorate for Information Operations and Reports, 1215 Jefferson Davis Highway, Suite 1204, Arlington, VA 22202-4302, and to the Office of Management and Budget, Paperwork Reduction Project (0704-0188), Washington, DC 20503.

REPORT DATE: 27 July 1992  
3. REPORT TYPE AND DATES COVERED: Annual Technical Report - 2nd Year  
1 April 1992 - 31 March 1993

4. TITLE AND SUBTITLE  
Cellular and Molecular Level Responses After Radiofrequency Radiation Exposure, Alone or in Combination with X-rays or Chemicals.

5. FUNDING NUMBERS  
G-AFOSR-91-0206  
61102F  
2312  
AS

6. AUTHOR(S)  
Martin L. Meltz, Ph.D.

7. PERFORMING ORGANIZATION NAME(S) AND ADDRESS(ES)  
The University of Texas Health Science Center at S.A.  
7703 Floyd Curl Drive  
San Antonio, Texas 78284-7800

8. PERFORMING ORGANIZATION REPORT NUMBER  
K-GAUO-00-030-102  
AFOSR-TR- 93 0580

9. SPONSORING / MONITORING AGENCY NAME(S) AND ADDRESS(ES)  
AFOSR/NL  
110 DUNCAN AVENUE, STE B115  
BOLLING AFB DC 20332-0001

10. SPONSORING / MONITORING AGENCY REPORT NUMBER

DTIC  
SELECTE  
AUG 12 1993  
S C D

11. SUPPLEMENTARY NOTES

12a. DISTRIBUTION / AVAILABILITY STATEMENT  
Approved for public release; distribution unlimited.  
93-18857  
94pj

13. ABSTRACT (Maximum 200 words)  
The focus of the second years' activities has been to establish, for the human 244B human lymphoblastoid cell line, selected biological effects of standard dose rate ionizing radiation (over the same low total dose range as to be used for combined microwave/ionizing radiation experiments) and hyperthermia (at the same temperature as will be used in the combined studies). The endpoints which have been examined, and for which alterations have been observed after either ionizing radiation exposure or heat treatment (for different times and temperatures), include cell proliferation and viability, cell cycle distribution, cell surface membrane markers, stress protein synthesis, DNA binding protein induction (NF-kB), and proto-oncogene induction. The observation of the two latter endpoints, at low doses, was unexpected. An interaction of ionizing radiation and hyperthermia, reducing stress protein synthesis, was also unexpected. Of the final 10 surface markers examined, 4 have been identified for their potential use in detecting either ionizing radiation or hyperthermia effects.

14. SUBJECT TERMS  
Radiofrequency Radiation,  
Mammalian Cells, Lymphoblastoid Cells, Surface Markers, DNA  
Binding Proteins, Proto-Oncogenes, Stress Proteins

15. NUMBER OF PAGES

16. PRICE CODE

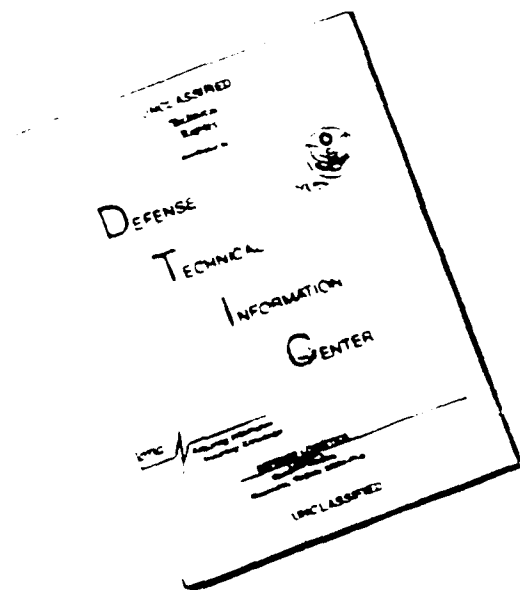
17. SECURITY CLASSIFICATION OF REPORT  
(U)

18. SECURITY CLASSIFICATION OF THIS PAGE  
(U)

19. SECURITY CLASSIFICATION OF ABSTRACT  
(U)

20. LIMITATION OF ABSTRACT  
(U)

# DISCLAIMER NOTICE



THIS DOCUMENT IS BEST QUALITY AVAILABLE. THE COPY FURNISHED TO DTIC CONTAINED A SIGNIFICANT NUMBER OF PAGES WHICH DO NOT REPRODUCE LEGIBLY.

TABLE OF CONTENTS - PART A

	<u>Page</u>
INTRODUCTION.....	3
MATERIALS AND METHODS.....	5
Cell Culture.....	5
Mycoplasma Treatment.....	5
EBV Detection.....	5
Exposures.....	5
Hyperthermia.....	6
Irradiation.....	6
Cell Growth Kinetics.....	6
Cell Cycle.....	6
Cell Surface Markers.....	7
Total Protein.....	7
Western Blot Analysis.....	8
Gel-Retardation Assay.....	9
Statistical Analysis.....	9
RESULTS.....	10
Cell Growth Kinetics.....	10
Hyperthermia.....	10
Ionizing Radiation.....	10
Hyperthermia/Ionizing Radiation.....	11
Cell Cycle Analysis.....	11
Fixation Methods for DNA Analysis.....	11
Control Cell Cycle Distribution.....	12
Cell Cycle Distribution Following Ionizing Radiation Exposure..	12

Accession For	
NTIS CRA&I	✓
DTIC TAB	
Unannounced	
Justification	
By _____	
Distribution /	
Availability Co	
Dist	Avail and / Special
A-1	

<b>Cell Cycle Distribution Following Sequential Hyperthermia</b>	
Treatment and Ionizing Radiation Exposure.....	13
<b>Cell Surface Markers.....</b>	<b>13</b>
Selection.....	13
244B Cell Surface Phenotype.....	14
Cell Fixation Methods to Optimize Cell Surface Marker Analysis.	14
<b>Cell Surface Marker Response to Hyperthermia, Ionizing Radiation</b>	
<b>Exposure and Sequential Hyperthermia/Ionizing Radiation</b>	
Exposure.....	15
Total Protein.....	16
Proliferating Cell Nuclear Antigen (PCNA) Protein.....	16
Heat Shock Proteins (HSPs).....	16
Effect of Cell Concentration on HSP Expression and Induction...	16
HSP Expression as a Function of Ionizing Radiation Dose.....	17
HSP Expression as a Function of the Ionizing Radiation	
Exposure / Hyperthermia Treatment Sequence.....	18
HSP Expression as a Function of Hyperthermia Treatment Time	
and Ionizing Radiation Dose.....	18
Analysis of HSP 90 Expression.....	19
Heat Shock Transcription Factor (HSTF).....	19
<b>DISCUSSION AND CONCLUSIONS.....</b>	<b>20</b>
Cell Growth Kinetics and Cell Cycle Kinetics.....	20
Cell Surface Marker.....	20
Heat Shock Proteins.....	20
Proliferating Nuclear Cell Antigen.....	21
<b>REFERENCES.....</b>	<b>22</b>

## LIST OF TABLES

- Table 1: Fold Increase in 244B Cell Growth as an Index of Proliferation Following Hyperthermia Treatment
- Table 2: Fold Increase in 244B Cell Growth as an Index of Proliferation Following SDRR Exposure and Hyperthermia Treatment Followed by SDRR Exposure
- Table 3: Effect of Fixation on Flow Cytometric DNA Analysis of 244B Cells
- Table 4: Flow Cytometric DNA Analysis of 244B Cell Line
- Table 5: Percent Cell Cycle Compartment Distribution of 244B at 24 and 120 Hours Following Exposures
- Table 6: B-Cell Associated Cell Surface Markers
- Table 7: Phenotypic Cell Surface Characteristics of 244B Cell Line
- Table 8: Effect of Fixation on 244B Cell Surface Markers
- Table 9: 244B Cell Surface Marker Analysis 4 Hours Post Exposure
- Table 10: 244B Cell Surface Marker Analysis 24 Hours Post Exposure
- Table 11: 244B Cell Surface Marker Analysis 120 Hours Post Exposure
- Table 12: Statistical Profile of 244B Cell Surface Marker Panel

## LIST OF FIGURES

- Fig. 1. Effect of hyperthermia on the proliferation of 244B cells.
- Fig. 2. Effect of standard dose rate ionizing radiation on the proliferation and percent of control viability of 244b cells.
- Fig. 3. Effect of hyperthermia on 42 degrees C, followed by standard dose ionizing radiation, on the proliferation and percent of control viability of 244B cells.

- Fig. 4. Low cytometric analysis of 244B cells analyzed as live cells or after using different fixative methods.
- Fig. 5. Flow cytometric analysis of 244B cells following standard dose rate ionizing radiation exposure.
- Fig. 6. Flow cytometric analysis of 244B cells after 42 degree C hyperthermia treatment for 1.5 h, followed by standard dose rate ionizing radiation exposure.
- Fig. 7. Histogram of SR101 and FITC-anti-HLA-DR dual-labeled 244B cells for determination of total protein and cell surface marker.
- Fig. 8. Expression of proliferating nuclear antigen (PCNA) after ionizing radiation and sequential hyperthermia/ionizing radiation exposures (Western blot).
- Fig. 9. Effect of cell concentration on the expression of Heat Shock Proteins (HSPs) p70 and p27 in 244B cells following hyperthermia treatment, low dose rate ionizing radiation exposure, and standard dose rate ionizing radiation exposure.
- Fig. 10. The expression of HSPs p70 and p27 following 50-1000 cGy ionizing radiation exposure.
- Fig. 11. The expression of HSPs p70 and p27 following different sequences of hyperthermia treatment and ionizing radiation exposure.
- Fig. 12A The expression of HSPs p70 and p27 in 244B cells at 4 hrs after standard dose rate exposures of cells following hyperthermia treatment at 42 degrees C. Hyperthermia time: 30 min.

12B Hyperthermia treatment time: 1 hr

12C Hyperthermia treatment time: 1.5 hr

12D Hyperthermia treatment time: 2 hr

Fig. 13 The expression of HSP 90 in 244B cells after 42 degree C hyperthermia treatment for 1.5 hr, followed by 50-1000 cGy ionizing radiation exposures.

Fig. 14 Heat shock Transcription Factor (HSTF) analyzed by gel retardation assay following 42 degree C hyperthermia for 1.5 hr, and sequential hyperthermia/ionizing radiation exposure at standard dose rate.

**TABLE OF CONTENTS - PART B**

	<b><u>Page</u></b>
<b>BACKGROUND</b> .....	54
Biological Response to Low-Dose Ionizing Radiation.....	54
Nuclear/Factor $\kappa$ B ((NF- $\kappa$ B)).....	54
Ionizing Radiation and NF- $\kappa$ B.....	55
Ionizing Radiation and Immediate Early Genes.....	55
Effect of Cell Density on the Expression of NF- $\kappa$ B.....	56
<b>OBJECTIVES</b> .....	56
Induction of NF- $\kappa$ B by Low Dose Ionized Radiation.....	56
Induction of Immediate Early Genes by Low Dose Ionizing Radiation.	56
High Cell Density and NF- $\kappa$ B Expression.....	56
<b>EXPERIMENTAL DESIGNS AND METHODS</b> .....	57
Reagents and Chemicals.....	57
Cell Culture.....	57
Exposure to Ionizing Radiation.....	57
Second Messenger System Inducer and Inhibitors.....	57
Cell Harvest.....	57
Electrophoretic Mobility-Shift Assays (EMSAs).....	58
Antibodies/Western Blotting.....	58
Densitometric Analysis.....	59
RNA Isolation and Northern Blot Analysis.....	59
<b>RESULTS</b> .....	59
Dose Response Expression of NF- $\kappa$ B In Low Dose Ionizing Radiation..	59
Time-course Expression of NF- $\kappa$ B.....	60
Dose-dependent Response of NF- $\kappa$ B Subunits p65 and p50.....	60

Signal Transduction of NF- $\kappa$ B Expression After a 0.5 Gy Exposure, and Comparison to PMA Induction.....	61
Induction of Immediate Early Genes by Low Dose Ionizing Radiation..	61
Dependence of NF- $\kappa$ B Expression on Cell Density.....	62
Kinetics of NF- $\kappa$ B Expression At Different Cell Densities.....	63
Experimental Methods.....	64
Expression of NF- $\kappa$ B Subunit p50 and p65 at Different Cell Densities	64

#### DISCUSSION

Induction of NF- $\kappa$ B By Low Dose Ionized Radiation.....	64
Signal Transduction.....	65
Ionizing Radiation and NF- $\kappa$ B Subunit p65 and p50 Expression.....	65
High Cell Density Stress and NF- $\kappa$ B Expression.....	66

REFERENCES.....	68
-----------------	----

#### LIST OF FIGURES

- Fig. 1. Dose dependent activation of NF- $\kappa$ B by low dose ionizing radiation.
- Fig. 2. Densitometric analysis of dose dependent activation of NF- $\kappa$ B.
- Fig. 3. Kinetics of NF- $\kappa$ B expression by low dose ionizing radiation.
- Fig. 4. Differential regulation of NF- $\kappa$ B subunit p50 and p65 by low dose ionizing radiation.
- Fig. 5. Densitometric analysis of NF- $\kappa$ B subunit p50/p65 expression after low dose ionized radiation.
- Fig. 6. The effect of low dose ionizing radiation on signal transduction.
- Fig. 7. Densitometric analysis of NF- $\kappa$ B expression in the presence of signal transduction inhibitors.
- Fig. 8. Kinetics of *c-fos*, *c-jun*, *c-myc* and *c-Ha-ras* expression after low dose ionizing radiation exposure.

- Fig. 9. Induction of immediate early gene transcripts (*c-fos*, *c-jun*, *c-myc* and *c-Ha-ras*) by low dose ionizing radiation.
- Fig. 10. Immediate early genes. Signal transduction mechanism in response to low dose ionizing radiation.
- Fig. 11 Density dependent NF- $\kappa$ B protein expression in 244B human lymphoblastoid cells.
- Fig. 12 Densitometric analysis of cell density dependent NF- $\kappa$ B expression.
- Fig. 13 Kinetics of transcription factor NF- $\kappa$ B expression in different cell densities.
- Fig. 14 Effect of cell density on NF- $\kappa$ B subunit expression p50 and p65.

# Cellular and Molecular Level Responses After Radiofrequency Radiation

## Exposure, Alone or in Combination with X-rays or Chemicals

Martin L. Meltz, Principal Investigator

### General Introduction

The contents of this report are presented in two parts, A and B. Part A focuses on the growth and viability of the 244B human lymphoblastoid cell line, and its cell cycle distribution, as well as the characterization of the surface markers of this human immune system derived cell. It then describes how each of these parameters is effected by exposure to ionizing radiation and hyperthermia treatment, including the dose range to which the cells will subsequently be exposed to in combined microwave and ionizing radiation exposures (at similar temperatures). The induction of heat shock protein is also examined, and an interaction between hyperthermia and ionizing radiation is described.

Part B focuses on the molecular biology of the cell, including the induction of a specific DNA binding protein, NF- $\kappa$ B. The effect of incubation at high cell density on the induction of this nuclear factor is examined, to ensure that future experiments are performed at the correct cell density. The mechanism of its induction by standard dose rate ionizing radiation, at low doses (an unexpected observation), is explored. Also examined is the induction of selected proto-oncogenes. The doses chosen were those to be used in the simultaneous low dose rate and microwave radiation exposures planned for year three of this project.

PART A

STUDIES OF CELL GROWTH, SURFACE RECEPTORS, AND  
STRESS PROTEINS, AFTER HYPERTHERMIA TREATMENT AND  
IONIZING RADIATION EXPOSURE

Co-Authors: Sandra L. Schneider, Dr. P.H.

Martin L. Meltz, Ph.D.

## AFSOR IMMUNOLOGY REPORT

### INTRODUCTION

An investigation of potentially adverse health effects of different agents used in the clinical setting or present in the environment must consider not only genotoxic and carcinogenic outcomes, but also the physiologic alteration of the immune system. The activation of human peripheral blood B-cells in  $G_0$  and their subsequent progression through the cell cycle is regulated by cellular events, some of which may induce or modulate the expression of cell surface antigens. These markers may be important in the induction and regulation of cell proliferation and differentiation (Kehrl, Muraguchi, & Fauci, 1984). Ionizing radiation or microwave radiation exposure and/or treatment at elevated temperatures may alter the cellular events in B-cell antigen presentation, cell proliferation or differentiation. Epstein-Barr Virus (EBV)-transformed lymphoblastoid cell lines of non-neoplastic (normal) origin have normal diploid karyotype, are polyclonal, and vary in size, morphology and Ig expression. The membrane glycoproteins expressed by EBV-transformed cell lines are similar to mitogen-activated, mature, normal B lymphocytes (Åman, Ehlin-Henriksson, & Klein, 1984)). The cell surface marker CD22, which plays a role in early B-cell activation, is present within the cytoplasm of all B-cells, but expressed only on the surface of a subpopulation of those cells. CD22 is an activation receptor associated with cell proliferation of small resting B-cells, and acts as an adhesion molecule mediating the binding of B-cells to other hematopoietic cells (Stamenkovic & Seed, 1990). The CD22 surface glycoprotein is the putative extracellular ligand of the protein tyrosine phosphatase CD45. The human cytokine interleukin-2 plays a critical role in the mediation of the immune response as cells bearing specific IL-2 (CD25) receptor are signaled for activation of T cells and natural killer cells, and for proliferation and functional differentiation of B-cells. B-cell specific antigens CD19, CD20, CD21, and CD23, as well as surface immunoglobulin (Ig), have been defined as having receptor function in cell activation (Pezzutto, Dörken, Moldenhaus, & Clark, 1987). CD20 is also involved in early cell activation (Clark, Shu, & Ledbetter, 1985). Modulation of cell surface markers by ionizing or microwave radiation, or by hyperthermia associated with microwave radiation, could therefore have considerable immunological significance.

To determine any pathogenetic significance of exposure to ionizing and microwave radiation, the ideal situation would be to expose primary human lymphocytes, both unstimulated and primarily in  $G_0$  stage, and in cycle after *in vitro* stimulation with a mitogen. However, the inherent variability and sample requirements in primary human lymphocyte culture makes them unsuitable as a initial model to investigate bioeffects which may be very subtle in nature (Schwartz 1990). Therefore, a continuously cultured cell line representative of the human lymphocyte

system, the 244B EBV-transformed human lymphoblastoid B-cell line, was used to initiate our immunological cell surface marker and cell line characterization studies.

A universally observed response of organisms to heat treatment is the induction of a special set of proteins. These heat shock or "stress" proteins (HSPs) are grouped into five families by molecular weight (MW): ~15-30 kDa (low MW HSPs), ~60 kDa (HSP 60), ~70 kDa (HSP 70), ~90 kDa (HSP 90), and ~110 kDa (HSP 110). The HSPs are present in multigene families, and can be expressed in unstressed, as well as heat treated cells (Lindquist & Craig, 1988). There is also a closely related set of "glucose regulated proteins" or stress proteins induced by stresses such as glucose deprivation and anoxia. Cells exposed to various forms of environmental stress respond by increasing the rate of synthesis of a group of highly conserved HSPs. Many of these proteins, including HSP 70 and HSP 60, are also constitutively expressed and function as "molecular chaperones" (Ellis, 1991). Most conditions that induce the HSP response result in an accumulation of denatured proteins (Hightower, 1980). However, little is known about the mechanism by which HSPs function in preventing denaturation of protein or in renaturing damaged protein (Lindquist & Craig, 1988). HSP 70 in the mitochondrial matrix functions to transport and fold proteins, guide the assembly of oligomeric structures and assist in the degradation of proteolytic enzymes (Kang, et al 1990). It has been suggested that the HSP 70 and HSP 60 systems cooperate in preventing protein denaturation under stress conditions (Manning-Krieg et al., 1991; Langer et al., 1992). The small HSPs share the property of being induced at specific stages in development at normal temperatures (Lindquist & Craig, 1988).

In addition to HSPs, proteins that regulate B-cell growth are likely to undergo transient changes in expression during the time interval extending through peak proliferation to the onset of growth arrest. None of the known B-cell activation antigens are known to demonstrate "unique" expression during this time. The HSP 28 was suggested as likely to be directly involved in down-regulating B-cell growth, since it was demonstrated to be expressed as activated B-cells stop proliferating and undergo growth arrest (Spector, Samson, Ryan, et al 1992). A direct relationship between the level of heat inducible HSP 27 (HSP 24) and neoplasia has been demonstrated (Fuqua, Blum-Salingaros, & McGuire 1989). The ability to determine the levels of HSPs and other regulatory proteins, immediately and at later times after microwave and ionizing radiation exposure, would be important information to have to determine non-genotoxic effects in cells of the immune system.

The normal human lymphoblastoid cell line 244B has been characterized in our laboratory for use as an *in vitro* B-cell model to determine which cell surface markers, associated with immune function, could be used in future studies to examine the effects of ionizing radiation and microwave exposures. Cell growth kinetics including proliferation and cell cycle, heat shock proteins and proliferating nuclear antigen (PCNA) proteins were examined after hyperthermia treatment and ionizing radiation exposure. The general hypothesis, in the original design of

these studies, is that the exposure of cells of human lymphocyte origin to simultaneous low dose rate x-ray and microwave radiation will result in alteration of cellular membrane receptor(s), and alteration of molecular level proteins(s) important to immune function. This alteration(s) to cell membrane receptors(s) and cellular protein(s) is expected to vary with the temperature achieved during microwave exposure. The studies as reported here present data specific for hyperthermia induced by convection heating and ionizing radiation at standard dose rate (>100 cGy/min) which will allow us to select specific cell characteristics and experimental conditions to study the combined low dose rate ionizing radiation and microwave radiation effects on human lymphoblastoid cells *in vitro*.

## MATERIALS AND METHODS

### Cell Culture

The lymphoblastoid cell line 244 B, derived from Epstein-Barr virus (EBV) transformed normal human peripheral blood lymphocytes, was obtained from Dr JL Schwartz, Argonne Laboratory, The University of Chicago, Il. (Schwartz, Turkula, Sagher, & Strauss, 1989). An "in-our-laboratory" passage number was assigned upon receipt of the 244B cells in our laboratory. The 244B cells were cultured as a suspension cell line at 37°C in 6% CO<sub>2</sub>•94% air in RPMI 1640 medium supplemented with 10% heat-inactivated Hyclone defined fetal bovine serum (FBS) [Sterile Systems, Logan UT], 2mM L-glutamine, 10mM HEPES and 25µg/ml gentamycin sulfate (Sigma, St Louis). Cells were subcultured at 2.5X10<sup>5</sup> cells/ml every 72 h to maintain exponential growth conditions. Media and serum lots were tested for optimum growth conditions. The same lot number of media, serum, and chemicals was used throughout this study to standardize experimental reagents.

*Mycoplasma Treatment:* Cultures were treated with 40µg/ml ciprofloxacin (Sigma, St Louis) to remove mycoplasma contamination (Schmitt, Däubener, Bitter-Suermann, & Hadding, 1988), and tested at various passages for mycoplasma by culture and DNA staining as previously reported (Zeltzer, Schneider, & Von Hoff, 1984).

*EBV Detection:* The production of EBV virus in 244B cells was determined by incubating washed human cord blood cells with supernatant from 244B cells cultured for 3-4 days (Chang, Hsieh, & Blankenship, 1971). Transformation of cord cells was observed after 6 weeks in culture, indicating the presence of EBV virus. Level 2 biosafety precautions were used in all procedures using 244B cells.

### Exposures

The experimental exposure conditions described in this report include hyperthermia treatment (H) at 37°C - 42.5°C, standard dose rate ionizing radiation (SDRR) exposure at 117 cGy/min over the dose range of 50 cGy - 1000 cGy, or a combination of 42°C hyperthermia treatment

followed by standard dose rate radiation exposure (42°C/50 cGy -1000 cGy). Control cell flasks were mock treated. Control cell flasks and post-exposure experimental cell flasks were incubated at 37°C until assayed. Cultures to be assayed at time points greater than 4 hours post exposure were adjusted to  $2.5 \times 10^5$  cells/ml at 4 hr with fresh media. These cultures were fed with fresh media every 24 h to control for nutrient depletion. Mean cell count and viability were determined by direct cell count in a hemacytometer using trypan blue dye exclusion.

#### *Hyperthermia*

Flasks containing  $1 \times 10^6$  cells/ml of media were gassed with 5% CO<sub>2</sub>•95% air, sealed in 17X19 mm polyester/polyethylene bags, and equilibrated for 30 minutes at 37°C in an incubator. The sealed bags were then placed in covered, weighted baskets designed to allow a distributed flow of water around each flask when they were totally immersed in plexiglas waterbaths with Hethotherm controller/circulators (37°C - 42.5°C ±0.3C). The waterbath temperatures were calibrated and preset by certified thermometer #87-1756 (National Bureau of Standards). After the incubations of 1.5 h -2 hr (as noted for each experiment), the flasks were immediately immersed into a 37°C waterbath for 5 minutes. Flasks were then removed from the bags and returned to the 37°C incubator if additional incubation was required. The flasks for 42°C/SDRR experiments were equilibrated for 20 minutes at 37°C before ionizing radiation exposure.

#### *Irradiation*

A <sup>137</sup>Cs GammaCell-40 Irradiator (Atomic Energy of Canada, Ltd.) was used for standard dose rate radiation (SDRR) exposures. The gamma ray dose rate for this unit was 116.7-115.1 cGy/min during the interval of these experiments. Flasks containing  $1 \times 10^6$  cells/ml media were gassed with 5% CO<sub>2</sub>•95% air, and equilibrated for 30 minutes at 37°C before ionizing radiation exposures. Flasks for low dose rate (LDRR) exposures were placed in the field of a Maxitron Orthovoltage x-ray unit operated at 150 KV, 4 mA, 4mm copper filtration in a specially designed temperature controlled warm room. The LDRR dose rate was 0.5 cGy/minute. The warm room housing the x-ray unit was set to maintain the temperature in the medium in the flasks at 37°C during the LDRR exposure.

#### *Cell Growth Kinetics*

Following exposure the control and treated cells were adjusted to a density of  $2.5 \times 10^5$  cells/ml with fresh media. Volumes of 2 ml were seeded into 24mm tissue culture wells (Costar, Cambridge, MA). Triplicate wells were harvested at each time point and the mean cell count and viability were determined by direct cell count in a hemacytometer using trypan blue dye exclusion. Cell proliferation was determined as mean viable cells or percent of control viable cells as previously reported (Zeltzer, Schneider, & Von Hoff, 1984).

#### *Cell Cycle*

The cell cycle distributions in G<sub>0</sub>G<sub>1</sub>, S, and G<sub>2</sub>M compartmental fractions were obtained using a modified Krishan technique (Krishan, A,

1975). A total of  $2 \times 10^6$  PBS washed cells were centrifuged at  $200 \times g$  for 6 minutes at  $4^\circ\text{C}$ . The cell pellets were resuspended in 1ml of 3mM citrate buffer containing 1mg/ml RNase A, 0.3%NP-40, 50  $\mu\text{g}/\text{ml}$  propidium iodide, and were then vortexed and allowed to stain for 30 min at room temperature in the dark. Prior to flow cytometry measurement (FCM), samples were filtered through a  $37\mu\text{m}$  nylon mesh into 12X75 mm tubes and stored at  $4^\circ\text{C}$ . Stained cells were analysed using FCM on a dual laser EPICS 753 instrument (Coulter Corp, Hialeah, Fl.) with an argon-ion laser. Red fluorescence from the propidium iodide (peak fluorescence 610 nm) was collected through 515 nm and 610 nm long pass filters. Compartmental analysis of DNA histograms was done on  $5 \times 10^4$  cells using \*MODFIT software (Verity Software House, Inc. Topsham, ME). Percent CV was within 3-5% for each assay.

#### **Cell Surface Markers**

Cell surface markers were analyzed on live cells following exposure or additional incubation using an indirect fluorescein-5-isothiocyanate (FITC) immunofluorescence assay adapted to flow cytometry measurements. This technique was decided upon comparison analysis of various fixation procedures. The cell surface marker panel of B-cell monoclonal antibodies (MoAb) included: HLA-DR (clone DK22, Dako Corp), CD19 (clone HD37, Dako Corp), CD21 (clone IF8, Dako Corp), CD10 (clone J5 [calla], Coulter Corp), CD20 (clone B1, Coulter Corp), CD22 (clone 4KB128, Dako Corp), CD23 (clone MHM6, Dako Corp), CD25 (clone 1HT44H3 [IL-2R1], Coulter Corp), CD45RA (clone 4KB5, Dako Corp), IgG (clone R10Z8E9, Boehringer Mannheim Biochemicals), IgM (clone R1/69, Dako Corp), IgD (clone IgD26, Dako Corp), and Kappa (clone DK22, Dako Corp). Antibodies were centrifuged at  $100,000 \times g$  for 10 min to remove aggregated material and to optimize staining. A total of  $1 \times 10^6$  cells in 12X75 glass tubes were washed twice in phosphate buffered saline (PBS) and resuspended in 50  $\mu\text{l}$  1% bovine serum albumin (BSA)•PBS for 30 minutes at room temperature. MoAb or control antibody was added at  $5\mu\text{g}/10^6$  cells for 30 min at  $4^\circ\text{C}$ , washed three times in 2% FBS•PBS, resuspended in 50 $\mu\text{l}$  FITC-conjugated goat affinity purified anti-mouse F(ab')<sub>2</sub> (Organon Teknika, Durham, NC), diluted 1:20 in PBS, and incubated for 30 min at  $4^\circ\text{C}$ . The FITC labelled cells were washed as above in PBS and resuspended in 1ml of freshly prepared, methanol-free, formaldehyde EM grade 1% paraformaldehyde (Electron Microscopy Sciences, Ft Washington, Pa.) in PBS. The cells were kept covered to avoid light at  $4^\circ\text{C}$ , and filtered through a  $37\mu\text{m}$  nylon mesh just prior to FCM. Fluorescence was read on a dual laser EPICS 753 instrument (Coulter Corp, Hialeah, Fl.) with an argon-ion laser tuned to 488nm and 400 mW of power. The percent positive cells were calculated as the percent of the marker population in excess of the FITC only control derived by channel for channel subtraction (Baker, Wiebe, Koester, et al., 1992).

#### **Total Protein**

Total protein was determined as modified from Engelhard, Krupa & Bauer, 1991. Cells were fixed in freshly prepared methanol-free formaldehyde EM-grade 0.5% paraformaldehyde (Electron Microscopy Sciences, Ft Washington, Pa.) in PBS and analyzed using a direct dual fluorescent

dye assay of <sup>3</sup>Sulforhodamine 101 (SR101) and FITC labeled Moab. Cells stained with FITC labeled Moab were fixed for 30 min with 0.5% paraformaldehyde, centrifuged, and washed twice with PBS. The washed cells were resuspended in 0.1% Triton-X 100 for 3 min at 1x10<sup>6</sup>/ml, centrifuged, and resuspended in 1ml 0.1M Tris, 0.1M NaCl pH7.6 buffer containing 3µg/ml SR101 for 30 min at 4°C. The cells were kept covered to avoid light at 4°C and were then filtered through a 37 µm nylon mesh just prior to FCM. Fluorescence was read as above for simultaneous measurement of FITC and SR101. The 488 nm laser line was used to excite FITC and SR101 using a 560nm s.p. dichroic filter. The patterns of total protein and/or cell surface marker were determined from analysis of the FCM histograms.

#### *Western Blot Analysis*

Western blot analysis for the p90, p70, and p27 HSPs, and proliferating nuclear antigen (PCNA) was done as previously described (Schneider, Fuqua, Speeg, Tandon, & McGuire, 1990). Cells exposed to SDRR or 42°C/SDRR were incubated for 4 hours at 37°C after exposure, unless noted, to allow for the maximal expression of the HSPs. The cells were harvested immediately after the timed incubation by centrifugation at 4°C at 400-450 x g for 5 min. Cell pellets were harvested in 2ml self-locking Eppendorf tubes, immediately frozen in a liquid nitrogen dry ice bath, and stored at -70°C until assayed. Total protein was isolated from the cell pellets by suspending the pellet in a small amount of 5% SDS solution, homogenization of the pellet material by repeated passage through a 22 gauge needle, and solubilization by boiling. The clear supernatant was collected after centrifugation for 2 min at 13,000 x g. Protein concentration in the SDS-extract was determined by the BCA method (Pierce Chemical Co.). Equal amounts of protein (100 µg/lane) were electrophoresed on a 12.5% (unless noted) polyacrylamide gel (PAGE) under denaturing, reducing conditions (Laemmli, 1970). Molecular weight markers were used to identify kilobase sizes. Resolved proteins were transferred to a nitrocellulose membrane at 200 mA for 16 h at 10°C (Kartner, 1985). Unsaturated protein binding sites on the membrane were blocked with 5% Carnation milk, and incubated overnight at 4°C with antibody cocktail. The p27 and p70 antibody were generously supplied by Dr. S. Fuque, Department of Medicine/Oncology UTHSCSA, and consisted of anti-27kD heat shock protein G3.1 monoclonal antibody diluted 1:100 (Ciocca, Adams, Bjerke, Edwards & McGuire, 1982; Fuqua, Blum-Salingaros, & McGuire, 1989) and anti-72kD C92F3A-5 monoclonal antibody diluted 1:500 (Riabowol, Mizzen & Welch, 1988). The anti-90kD monoclonal antibody (StressGen. Biotech Corp.) was diluted 1:1500. The anti-PCNA (clone PC10 Dako Corp) was diluted 1:100 as above. Following the incubation with antibody, the cellulose membranes were washed in PBS and then incubated overnight at 4°C with <sup>125</sup>I labeled goat anti-mouse IgG (NEN-Dupont). The blots were washed as above and exposed to X-OMAT X-ray film at -70°C using intensifying screens. HSP bands were observed visually and compared with controls.

### ***Gel-Retardation Assay***

Heat Shock Transcription Factor (HSTF) levels were determined by gel-retardation assay, as reported by Zimarino, Tsai, & Wu, 1990, using a double stranded synthetic oligonucleotide consensus heat shock element (5'-GTCGACGGATCCGAGCGGCCCTCGAATGTTCTAGAAAAGG-3'). The oligonucleotides were synthesized by Genosys (Houston, TX) and labeled using T4 polynucleotide kinase and gamma-<sup>32</sup>P-dATP. Cellular heat shock proteins were induced with 42°C hyperthermia for the times indicated. Cells were homogenized in 20mM Tris HCL pH 7.5, 2mM DTT, 20% glycerol, and 0.4M KCL solution with the addition of proteolytic inhibitors (aprotinin, antipain, leupeptin, and pepstatin, 2.5 µg/ml (Sigma, St Louis, MO). Protein extracts were prepared by centrifugation at 100,000 x g for 1 h at 4°C. Protein was determined using a Bio Rad Protein assay kit and 10µg of the protein extract was mixed with 0.2 ng of labeled double stranded oligonucleotide and 3µg of poly (dAdT)•poly (dAdT) in 0.1M Tris HCL (pH7.5), 1mM DTT, 0.1M KCL, and 4% glycerol. After incubation at room temperature for 30 minutes, the samples were loaded onto a 5% polyacrylamide gel in 6.7mM Tris HCL (pH 7.5), 3.3mM sodium acetate, and 1mM EDTA, and electrophoresed with buffer recirculation for 2 hours. The gel was then dried for autoradiography.

### ***Statistical Analysis***

Cell surface marker FCM data measures were assessed as the percentage of positive cells in excess of the FITC only control derived by channel for channel subtraction. A variance stabilizing transformation (arcsin) was applied to the percentage scores prior to statistical analysis. The transformed data was subjected to univariate three way analysis of variance (ANOVA) to test for mean differences associated with the hour, temperature, and standard dose rate ionizing radiation dose. The three levels of hour (4 h, 24 h, and 120 h), two levels of temperature (37°C and 42°C), and three levels of dose (0, 100 cGy and 500 cGy) formed 18 cells in the completely crossed design. The three main effects and all three two level interaction terms were included in the linear model, with the residual mean square as the error term. The interaction effects were tested using a Student Newman-Keuls (SNK) procedure and *post-hoc* comparisons were interpreted to determine which levels differed significantly from one another in the presence of a significant main effect associated with the ANOVA. Since F-tests of the interaction effects inherently have less statistical power than the main effects tests, we used an alpha ≤ 0.10 before interpreting interactions and the standard alpha ≤ 0.05 before interpreting main effects tests. In all, 10 univariate ANOVA models were fit (Table 7). Multiple comparison procedures such as the Newman-Keuls ensure that too many falsely significant differences are not declared when a number of potential comparisons are possible. The basic procedure is to ensure that the overall probability of declaring any significant differences between all possible pairs of groups is maintained at some fixed significance level ( $\alpha$ ). (Rosner, 1990, and Kleinbaum, Kupper, & Muller, 1988).

## RESULTS

### Cell Growth Kinetics

The maintenance and growth conditions of the human lymphoid cell line 244B were optimized and characterized for use in studying the *in vitro* immunological function of B-cells exposed to hyperthermia (37°C - 42.5°C/2h), ionizing radiation (50 cGy - 1000 cGy), and hyperthermia at 42°C/1.5h followed within 30 minutes by standard dose rate ionizing radiation (50 cGy - 1000 cGy). Cell growth kinetics over a period of 24-120 h following exposure were reported as total numbers of viable cells and percent viability. Earlier hyperthermia growth kinetic experiments in our laboratory had demonstrated a decrease in cell growth and viability with increasing time post exposure (Holahan, Eagan, Meltz, 1991). After standardization of cell culture media and experimental conditions, including treatment of the cells for eradication of mycoplasma, the observation of decreased viability could not be replicated, although the inhibition of cell growth after heat treatment was similar. The studies described here with the 244B cell line allowed us to select optimal heat and radiation exposure conditions for our planned studies to determine potential interactions between microwave radiation and ionizing radiation. A preliminary presentation of these results has been made (Schneider, Szekeresova, & Meltz, 1993, Schneider et al., 1993).

### Hyperthermia

The proliferation of 244B cells as total viable cells after heat treatment at 37°C - 42.5°C for 2h was determined and plotted against time (24-120 h) using a computerized quadratic fit  $Y = a + bX + cX^2$  where  $a$  is a constant and  $b$  and  $c$  are slope coefficients (Figure 1). A statistically (Pearson's Correlation) significant decrease in the number of viable cells at each time point was observed with increasing temperature ( $r = -0.342$ ,  $p < .002$ ). The viability for all temperatures at all time points exceeded 96% of control, except after the 42.5°C incubation at the 24h and 48 h time points (86% and 84% respectively, data not shown). The fold increase in cell growth was determined as an index of proliferation following the 2 hr hyperthermia treatments (Table 1). Mock 37°C control cells had a 5.7 and 14.7 fold increase after 72h and 120 h in culture, respectively, while a temperature dependent decrease in proliferation of cells was observed. For example, after the 42°C treatment only a 3.7 and 8.4 fold increase was observed at 72h and 120 h respectively. This temperature dependent decrease in cell proliferation corresponded to 65% and 57% of control cell growth at 72 h and 120 h, respectively.

### Ionizing Radiation

The proliferation of 244B cells as total viable cells and percent of control viability after SDRR exposures (50 cGy - 1000 cGy) were determined and plotted against time (24-120 h) using a computerized quadratic fit  $Y = a + bX + cX^2$  where  $a$  is a constant and  $b$  and  $c$  are slope coefficients (Figure 2 A, B). At the 50 cGy - 100 cGy dose a quadratic to near linear function is observed with cell proliferation

over time, and at the 250 cGy dose there is progression to a flat curve (500 cGy - 1000 cGy). A statistically (Pearson's Correlation) significant decrease in the number of viable cells at each time point was observed with increasing dose ( $r = -.590$ ,  $p < .001$ ) (Figure 2 A). The cell viability for all doses at each time point was  $\geq 92\%$  of control, except for the 1000 cGy dose at 120 h post exposure, which decreased to 87% of control (Figure 2 B). The fold increase in cell number was determined as an index of proliferation following ionizing radiation exposure (Table 2). There is a dose dependent decrease in cell proliferation for all time points compared to mock treated 37°C control cells, which becomes more evident with increased time post-exposure. For example at 72 h there is a 3.9 fold increase after 50 cGy exposure compared to the control fold increase of 4.4, and after 120 h the irradiated cells have only increased by 9.9 fold compared to the control cell fold increase of 15.2. The cell proliferation after 500 cGy and 1000 cGy exposures is minimal from 24 -120 h post exposure. Since cell viability at these times after these exposures remained high, it is evident that the cell proliferation mechanism has been effected.

#### *Hyperthermia/Ionizing Radiation*

The proliferation of 244B cells as total viable cells and percent of viability after hyperthermia treatment at 42°C for 1.5h, followed within 30 minutes by ionizing radiation exposures of 50 cGy - 1000 cGy, was determined and plotted against time (24-120 h) using a computerized quadratic fit  $Y = a + bX + cX^2$  where  $a$  is a constant and  $b$  and  $c$  are slope coefficients (Figure 3 A, B). A similar dose curve to ionizing radiation only exposure is observed, where at the 50 cGy -100 cGy dose a quadratic to near linear function is observed with cell proliferation over time, and at the 250 cGy dose there is progression to a flat curve (500 cGy - 1000 cGy). The cell viability for 42°C/50 cGy and 42°C/100 cGy, at all time points, was  $\geq 92\%$ . The cell viability was decreased for 42°C/250 cGy and 42°C/500 cGy exposures, at 96 hours, to 88% and 77% of control respectively; and for 42°C/1000 cGy at all time points (24-120 h) to 82%, 89%, 83% 82% and 71% of control, respectively. The fold increase in cell growth was determined as an index of proliferation following the sequential hyperthermia / ionizing radiation exposures (Table 2). There is a dose dependent decrease in cell proliferation for 42C/SDRR exposed cell at all time points in comparison to the mock treated control cells, although it was minimal for all doses at 24 h compared to the 42°C unirradiated control. The 42°C only treated cells appear to have a slightly higher fold increase at 72 h and 96 h (5.6 and 9.0) in comparison to the 37°C control cells (4.4 and 8.2). The 42°C/SDRR exposure sequence does not appear to change the cell proliferation rate very much from that observed for the cells exposed only to radiation; there is little evidence for a synergistic effect on cell proliferation at later times post-exposure.

#### **Cell Cycle Analysis**

##### *Fixation Methods for DNA Analysis*

The effect of cell fixation, prior to the addition of propidium iodide, by the fixatives 0.5% paraformaldehyde, 2% paraformaldehyde•70% ETOH,

or 70% ETOH on the percent cell cycle compartment was determined in comparison to a live cell (or no fixation) method (Table 3). Histograms comparing the fixation methods are presented in Figure 4. All fixation methods tested show a disproportionate percent of the G2M cell cycle compartment in comparison to the non-fixed cells. This relationship is best seen by looking at the histograms (Figure 4). The live cell or non-fixed cell method (A) has a very sharp, distinct and narrow GoG1 band and clear separation of the G2M-band. Of the fixation methods, 0.5% paraformaldehyde (C) would be the best method, followed by the 70% ETOH method (D). The 2% paraformaldehyde+70% ETOH (B) is the least desirable method due to the flat, wide GoG1 and G2m compartments. The live cell (no fixation) method was selected for all DNA cell cycle analysis of the 244B cells.

#### *Control Cell Cycle Distribution*

Cell cycle DNA analysis was performed for 244B cells by EPICS 753 dual laser flow cytometric analysis (FCM). The control cell cycle distribution, based on DNA content, is reported as percent GoG1, S-phase, and G2M cell cycle compartments. Data from 8 separate experiments (cell passages 15-47) is summarized in Table 4. The median cell cycle distribution in the GoG1, S-phase, and G2M cell cycle compartment is 74.8%, 12.5%, and 8.2% respectively. The greatest range of cell cycle compartment variability between experiments was observed in the GoG1. The G2M D/A ratio is consistent across passage, demonstrating that the staining of the cells by propidium iodide is stoichiometric, and that the instrument response check is linear.

#### *Cell Cycle Distribution following Ionizing Radiation Exposure*

The cell cycle distribution was determined for 244B cells exposed to SDRR (Figure 5 and Table 5). Cells were exposed to 50 cGy - 1000 cGy doses and then analysed for percent cell cycle compartment distribution at 24 -120 h following exposure. The 37°C mock control cells at 24h demonstrate a percent cell cycle distribution for GoG1, S, and G2M of 77.6%, 13.8%, and 8.6%, respectively, and at 120h a percent cell cycle distribution of 87.3%, 6.5%, and 6.2% respectively. The increase in distribution of GoG1 in the control cells corresponds to the cell cycle pattern seen with cells reaching confluence (unpublished observations). After 120 hours, only cells exposed to the lowest dose of 50 cGy approach the control cell cycle distribution. After all doses tested, the major observations are an increase in the G2M cell cycle compartment, and a decrease in the S compartment. The increase in G2M varies with dose for all time points with peak levels occurring for G2M at 500 cGy and declining at 1000 cGy. At 24 h, the increase in G2M after 50 cGy is associated with an increase in GoG1 and a decrease in S compared to control compartment levels. After 250 cGy and 500 cGy, the further increase in G2M is associated mainly with a decrease in S. In this experiment, the results after 100 cGy are not consistent with a dose-dependent pattern. There does not appear to be a dose dependent decrease in S in the 250 -1000 cGy exposure range. The decrease of G2M after 1000 cGy is associated with an increase in GoG1. At 120 h, the dose dependent (50 cGy - 500 cGy) increase in G2M is associated with dose dependent decreases in both GoG1 and S. The dose dependent

prolongation out to 120 h of the cell cycle alterations is associated with the dose dependent decrease in cell proliferation. The possible block in G2, as well as a possible block at the G1/S boundary, may be responsible for the observed decrease in cell proliferation. Interphase cell death is not responsible, due to the high cell viability observed for all doses through the 120 h time point.

#### *Cell Cycle Distribution Following Sequential Hyperthermia Treatment and Ionizing Radiation Exposure*

The cell cycle distribution as percent cell cycle compartment distribution was determined on 244B cells after 42°C hyperthermia treatment for 1.5 hours, or after the hyperthermia treatment followed by 50 cGy - 1000 cGy ionizing radiation exposures (Figure 6 and Table 5). The 42°C hyperthermia treated cells demonstrate after 24 h a percent cell cycle distribution in GoG1, S, and G2M of 77.3%, 12.7%, and 10.0%, respectively, and after 120 h a percent cell cycle distribution of 83.9%, 7.6%, and 8.5%, respectively. This corresponds at 120h to a slight increase in G2M, a slight increase in S, and a decrease in GoG1 compared to 37°C control levels. After hyperthermia and 50 cGy exposure the redistribution back to control level, as was observed after the ionizing radiation exposure only at 50 cGy, was not observed. As was observed with SDRR only exposures, there was a dose dependent increase in G2M, but with peak levels after 42°C/250 cGy as compared to the peak level after 500 cGy as seen in SDRR only exposed cells. This increase in G2M over the 50-500 cGy range, was associated with a small dose dependent increase in GoG1 and obvious decrease in S, as occurred after exposure to radiation alone. The differences in the pattern of response of the sequential hyperthermia/ radiation vs. radiation only are relatively minor. While the cell cycle distribution following 42°C/SDRR is predominantly due to the effects of increasing ionizing dose, there is some interaction between hyperthermia and ionizing radiation on the cell cycle progression.

#### **Cell Surface Markers**

##### *Selection*

Preliminary studies describing 244B cell surface markers as described in our first annual report were obtained using a clinical FAC-SCAN flow cytometer. Although these studies allowed us insight into the types of markers associated with 244B, they were limited by the use of equipment designed for clinical application (i.e. limited gating and fluorescent dye filter range). The present cell surface marker studies were standardized on an EPICS 753 dual laser FAC with the availability of a wide range of gating and filter options necessary for experimental application. A panel of 13 B-cell associated markers was selected from 28 potential markers examined in year one of this project (Table 6). The markers selected were chosen in the categories of Control Markers: HLA-DR, CD19(B4), CD21(B2), CD10; Cell Type Markers: CD20(B1), CD22, CD23, CD25(IL-2R), CD45; and Cell Function Markers: IgG, IGM, IGD, Kappa. The panel consisted of pan B-cell markers (P) and B-cell restricted markers (R) as noted in Table 6. The positive and negative markers in the control category were presumed to be associated with stable characteristics of 244B lymphoblastoid cell line. Cell type and

cell function markers were selected that would allow us to determine if markers associated with human lymphocyte cell function or cell differentiation would be altered immediately or at a later time after standard dose rate ionizing radiation exposure. Cell surface markers showing alterations associated with these ionizing radiation exposures, as well as surface markers showing alterations associated with hyperthermia, will be used in upcoming studies to assay for alterations associated with simultaneous low dose rate x-ray and microwave radiation exposures.

#### *244B Cell Surface Phenotype*

The selected panel of cell surface markers (HLA-DR, CD19, CD21, CD20, CD10, CD22, CD23, CD25, CD45, IgG, IgM, IgD and kappa) was tested on 244B cells, passages 15-43, to determine the cell line phenotype (Table 7). The phenotype (positive or negative) of 244B was determined from the median score of percent positive cells from FAC analysis. The immuno-globulin nonsecretor, terminal deoxynucleotidyltransferase (TdT) negative, 244B cell line was consistently positive for HLA-DR, CD19, CD21, CD20, CD22, CD23, CD45, IgG and kappa. The CD21 marker was variable in reactivity, and it is noted that this marker is extremely sensitive to cell cycle stage (Åman, 1976). The cells were consistently negative with the IgM and IgD markers. The 244B phenotype for the CD10 and CD25 markers, at control experimental conditions, is considered negative even though one positive reaction was observed with CD10 and CD25 in one out of the 5 repeated assays. We did not pursue this one time point discrepancy except to note that the percent positive cells are in the low range, indicating weak (few receptors) cell reaction. The EBV-transformed 244B B-cell line, of normal lymphocytic origin, is representative of active normal lymphocytes with the phenotype CD20 (B1)+, CD21 (B2)+, CD45+, CD23 (B6)+ (Anderson, Boyd, Fisher, et al., 1985).

#### *Cell Fixation Methods to Optimize Cell Surface Marker Analysis*

Several flow cytometric cell fixation assays were tested to optimize FCM cell surface marker analysis (Table 8). A cell fixation method, which gave results comparable to a live cell analysis, would allow flexibility of cell surface marker analysis following varied timed exposure. Live cell, 0.5% paraformaldehyde and 70% ethanol (ETOH) fixed cell methods were tested. The live cell analysis method was optimum or equivalent for the HLA-DR, CD19, CD20, CD22, CD23, CD45, and IgD markers. The live cell and 0.5% paraformaldehyde methods were comparable for CD22, CD45, IgG, IgM, IgD, and kappa markers. There was no percent positive cell surface marker correlation, except for IgD and possibly kappa, among the tested fixation methods. This pilot study, to select potential cell surface markers to determine exposure effect on lymphocytes, did not propose to optimize the monoclonal antibody reagents with respect to fixation methods. Therefore, the live cell (no fixation of cells prior to addition of cell surface antibody) assay was chosen as the method of analysis for cell surface markers. The cell surface marker immunofluorescent staining and flow cytometric method used for these studies is as described in the materials and methods section.

*Cell Surface Marker Response to Hyperthermia, Ionizing Radiation Exposure and Sequential Hyperthermia/Ionizing Radiation Exposure*

Cell surface markers were determined by FCM on 244B cells (passages 22-29) at 4h, 24 h, and 120 h following exposure to 42°C for 1.5 h, 100 cGy and 500 cGy ionizing radiation or to hyperthermia at 42°C for 1.5 h followed by 100 cGy (42°/100 cGy) or 500 cGy (42°/500 cGy) (Tables 9-11). The 100 cGy and 500 cGy doses were selected since it was determined in a preliminary experiment that exposure at 100 cGy and below did not appear to significantly alter cell surface markers, and that the 500 cGy exposure would demonstrate changes and still allow for cell proliferation. The flow cytometric analysis of the panel of markers is presented as percent positive cells for the variables time (4h, 24h, and 120h), temperature (37°C and 42°C), and dose (100 cGy and 500 cGy ionizing radiation), and the interactions time•temperature, time•dose, and temperature•dose. (Tables 9-11). Due to the complexity of the raw data, as percent positive cells, a statistical approach was used to examine the relationship of cell surface marker changes in relationship to exposure dose and time points post exposure. To interpret the relationship of marker status, FCM data was arcsin transformed and analysed by ANOVA and a Student Newman-Keuls test for multiple comparison. A statistical profile of the 244B cell surface marker panel was determined (Table 12). Statistical significance of  $\alpha \leq .05$  indicates a very strong marker association and  $\alpha \leq .10$  indicates a weak marker association. Markers CD10, IgM and IgD were negative at all time points tested and could not be statistically analysed. Of the 13 markers tested, 10 markers were selected by ANOVA analysis as associated with changes following hyperthermia or SDRR, or associated with inter-actions of time, temperature or dose. Cell surface marker changes in HLA-DR, CD45RA, and IgG were significant ( $\alpha \leq .05$ ) for time (120 h) only. There were no significant associations to change in these markers, due to hyperthermia or to ionizing radiation. A decrease in the kappa marker was significant ( $\alpha \leq .05$ ) for time (120 h) and temperature (42°C), and significant ( $\alpha \leq .10$ ) for a temperature•SRDD dose interaction. A decrease in CD20 was observed and was significant ( $\alpha \leq .05$ ) for time (120 h) and SDRR dose (500 cGy). The markers CD22 ( $\alpha \leq .10$ ), CD19 ( $\alpha \leq .05$ ) and CD23 ( $\alpha \leq .05$ ) were significant for time (120 h), temperature (42°C) and dose (500 cGy). The CD19 marker demonstrated a time•SDRR dose interaction and a temperature•dose interaction, and the CD23 marker was associated with a time•dose interaction. The CD21 marker was significant ( $\alpha \leq .05$ ) for temperature, and a time•temperature interaction was also observed. The effect of radiation exposure on CD25 was significant ( $\alpha \leq .05$ ) for dose (500 cGy) with a time•dose interaction. It is difficult to interpret this interaction because an increase in CD25 marker was observed at 4 and 24 hours, and a decrease in this marker was observed at 120 h. From the 10 possible markers selected by ANOVA, 4 markers CD20, CD19, CD23 and CD25 demonstrate a strong association ( $\alpha \leq .05$ ) with a decrease in percent positive cells following ionizing radiation exposure. The interleukin-2 receptor, CD25, clearly has the "cleanest" association with ionizing radiation exposure. Future experiments will need to rigidly control for temperature and time when examining the ionizing radiation response with the CD20, CD19, CD23, and CD25 cell surface

markers. Selection of cell surface markers associated with ionizing radiation and hyper-thermia, ie kappa, would be useful to monitor combined low dose rate ionizing and microwave radiation (Schneider, Koester, et al 1993).

#### **Total Protein**

A dual label fluorescent probe assay was used to simultaneously determine 244B cells total protein and specific cell surface marker by FCM methodology. Preliminary data demonstrating the <sup>3</sup>Sulforhodamine 101 (SR101) labeled cells for total protein and the FITC labeled anti-HLA-DR specific cell surface marker probe is shown in Figure 7. Electronic gating was used to correct for doublets and aggregates. Panel A is a histogram of the FITC labeled control cells which had also been counter labeled with the SR101 total protein probe. Panel B is a histogram of cells labeled with FITC • anti-HLA-DR counter labeled with SR101. The normal distribution of cells that labeled with the total protein probe in relation to the FITC control cells is shown in panel A. The normal distribution of cells positive for the HLA-DR marker probe is shown in panel B. The total protein peak distribution is equivalent in both the control stained (A) and marker stained (B) cells. This technique may provide a rapid quantitative approach to investigate alterations in cellular growth as indicated by cell protein distribution (SR101)/ or specific cell surface marker. The test will also allow us to determine which markers are not changed if there is an alteration in total cellular protein.

#### **Proliferating Cell Nuclear Antigen (PCNA) Protein**

The highly conserved and cell cycle associated 36 kD nuclear protein, proliferating cell nuclear antigen (PCNA), was determined in cells either exposed to SDRR (50 cGy - 1000 cGy) at 37°C, treated with 42°C hyperthermia alone, or treated for 1.5 hr at 42°C followed by SDRR exposure. Exposed cells were reincubated for 4 hours at 37°C after each exposure to allow for protein expression. Control cells (0 dose) were tested at 0 and 4 hour time points (Figure 8). PCNA was present in all of the 37°C samples tested, with an observed increase of PCNA at all ionizing radiation exposures  $\geq 100$  cGy. When cells were treated at 42°C for 1.5 hours, the PCNA level appeared to be similar to that observed in the 37°C control cells. PCNA levels in cells which were incubated at 42°C for 1.5 h before receiving an ionizing radiation exposure, appeared to be lower at each dose when compared with cells that received an ionizing radiation exposure alone (at 37°C).

#### **Heat Shock Proteins (HSPs)**

##### **Effect of Cell Concentration on HSP<sub>i</sub> Expression and Induction**

The constitutive expression of the heat shock proteins (HSPs) p70 and p27, the induction of these HSP's in cells that had been treated at 42°C hyperthermia for 2 hours; or in cells exposed to low dose rate ionizing radiation (LDRR) at 0.5 cGy/min., or to standard dose rate ionizing radiation (SDRR) at 100 cGy/min., was examined in cells either at moderate or high cell densities at the time of treatment (Figure 9). The cell concentrations tested were  $1 \times 10^6$  cells/ml and  $5 \times 10^6$  cells/ml.

The constitutive expression of p70 and p27 in 37°C mock treated control cells at  $1 \times 10^6$  cells/ml and at  $5 \times 10^6$  cells/ml are shown in Lane 1 and Lane 2, respectively. In these control cells, the  $5 \times 10^6$  cells/ml concentration showed higher levels of p70 and p27 than cells at the  $1 \times 10^6$  cells/ml concentration, indicating that cell stress occurs at the higher ( $5 \times 10^6$  cells/ml) cell concentration under these experimental conditions.

The 42°C heat treated cells at  $1 \times 10^6$  cells/ml and  $5 \times 10^6$  cells/ml are shown in Lane 3 and Lane 4, respectively. The induced 42°C HSP levels are greater at the  $1 \times 10^6$  cells/ml concentration than at the  $5 \times 10^6$  cells/ml concentration. At the higher cell density ( $5 \times 10^6$  cells/ml), the 42°C HSP induced p70 level appeared to be equivalent to the 37°C p70 levels, with the p27 levels still being greater than the constitutive level in the 37°C control cells at the  $1 \times 10^6$  cells/ml concentration.

The expression of HSP's in cells exposed to low dose rate ionizing radiation (LDRR) at  $1 \times 10^6$  cells/ml and  $5 \times 10^6$  cells/ml are shown in Lane 5 and Lane 6, respectively, and the HSP expression in cells exposed to standard dose rate ionizing radiation (SDRR) at  $1 \times 10^6$  cells/ml and  $5 \times 10^6$  cells/ml are shown in Lane 7 and Lane 8, respectively. The expression of p70 after LDRR exposure at  $1 \times 10^6$  cells/ml and  $5 \times 10^6$  cells/ml, and after SDRR exposure at  $1 \times 10^6$  cells/ml appears to be equivalent to the expressions observed with the 37°C control cells at the  $1 \times 10^6$  cells/ml concentration. After SDRR exposure at  $5 \times 10^6$  cells/ml, the HSP 70 level appears to be decreased. The expression of p27 after LDRR exposure at the  $1 \times 10^6$  cells/ml concentration, and SDRR at  $1 \times 10^6$  cells/ml, appears to be slightly greater than the constitutive level in cells at that density, and equivalent to the expression observed with the 37°C control cells at the  $5 \times 10^6$  cells/ml concentration. The expression of p27 after SDRR exposure at  $5 \times 10^6$  cells/ml appears to be less than the levels expressed at the  $1 \times 10^6$  cells/ml concentration after SDRR and after the LDRR exposures of both cell concentrations; the level was equivalent to that observed for the 37°C control cells at the  $1 \times 10^6$  cells/ml concentration. These preliminary results suggested that a very high dose of ionizing radiation at standard dose rate may inhibit constitutive HSP synthesis. A cell density of  $1 \times 10^6$  cells/ml should be the maximum used in future experiments to minimize the expression of HSPs associated with cell "stress" at high cell concentration. The effects of LDRR and SDRR exposure on the expression of HSP will be further examined during proposed combined low dose rate ionizing radiation and microwave radiation exposures; the SDRR exposure will be used as a control during the LDRR/microwave exposure experiments.

#### *HSP Expression as a Function of Ionizing Radiation Dose*

The expression of the heat shock proteins (HSP) p70 and p27 following 50 cGy - 1000 cGy ionizing radiation was determined (Figure 10). Cells were tested immediately after exposure (0 h) as a baseline cell control. A 4 hour incubation at 37°C following hyperthermia was used to obtain positive control HSP expression. The constitutive levels of

p70 and p27 for cells maintained at control conditions (4 h) are shown in Lane 1, the expression of HSPs induced by 42°C hyperthermia treatment for 1.5 h are shown in Lane 2. The expression of HSP p70 and p27 for all doses tested (50 cGy - 1000 cGy) were  $\leq$  control levels. This data provides evidence that standard dose rate ionizing radiation, over a broad dose range, does not induce HSPs.

#### *HSP Expression as a Function of the Ionizing Radiation Exposure / Hyperthermia Treatment Sequence*

The effect of a 100 cGy ionizing radiation exposure before, at the end of, or 4 hr after a 2 h hyperthermia treatment at 42°C on the expression of heat shock proteins (HSP) p70 and p27 was determined (Figure 11). The 37°C and 42°C treated control cells were tested immediately after exposure (0 h) as baseline controls. A 4 hour incubation at 37°C following 42°C hyperthermia was used to obtain positive HSP expression. The constitutive levels in mock treated 37°C control cells (0 h and 4 h) are shown in Lane 7 and Lane 8; the 42°C treated cells at the 0 h (Lane 9) are equivalent. The positive expression of p70 and p27 at 4 h after the 42°C/2h treatment is observed in Lane 1. If cells are exposed to 100 cGy at the end of that 4 h period at 37°C, the HSP expression is equivalent (Lane 2). The result is also the same when the 100 cGy exposure immediately precedes the 42°C treatment and the subsequent 37°C post exposure incubation (Lane 5). However, when the 100 cGy ionizing radiation dose is given within 30 min after the 42°C treatment, and prior to the 37°C 4 h post exposure incubation, the HSP levels are decreased to control levels. They are the same as for the 100 cGy radiation only control, no hyperthermia treatment, (Lane 4) and cell baseline levels (Lanes 7 and 8). This same inhibition of HSP was observed when the 42°C treated cells were irradiated at 42°C at the end of the heat treatment and then incubated for 4 h at 37°C post exposure (Lane 6). Inhibition of the HSP p70 and p27 is only observed when the irradiation immediately or closely (within 30 min) follows hyperthermia treatment under the experimental conditions as described.

#### *HSP Expression as a Function of Hyperthermia Treatment Time and Ionizing Radiation Dose*

Studies on other human and mammalian cell lines have shown that the time of hyperthermia treatment is critical for the induction and expression of heat shock proteins (Lindquist & Craig 1988). The expression of the heat shock proteins p70 and p27 in 244B cells after heat treatment at 42°C for 30 minutes (A), 1 hour (B), 1.5 hours (C), 2 hours (D), and then irradiated with 50 cGy - 1000 cGy doses was determined (Figure 12A-D). The expression of p70 and p27 in cells that had been heat treated at 42°C for 30 minutes (12A) and then incubated for 4 h at 37°C is shown in Lane 2. If irradiated immediately after the 30 min heat treatment with a dose of 50 cGy or higher, the HSP induction does not occur. The expression seen is equal to that observed for the 42°C control (0 cGy) at time 0 h. After heat treatment at 42°C for 1 hour (B), the expression of p70 was equivalent after all doses to both the 0 h and 4 h 42°C control levels. The level of p27 in cells exposed to 50 cGy - 250 cGy appeared increased over the

42°C positive (4 h) control. At 500 cGy and higher, the p27 expression appeared to be less than after the lower doses. The greatest induction and expression of p70 and p27 compared to other heating times, was observed after heat treatment at 42°C for 1.5 h (12C). The HSP level expressed after 50 cGy and 100 cGy were equivalent to that that observed for the 42°C 4 h control (i.e., no radiation inhibition of expression; an inhibition of both p70 and p27 was observed, however, following exposures of 250 cGy - 1000 cGy. After heat treatment at 42°C for 2 h (12D), the expression of p70 and p27 is again evident, although the levels are greatly reduced compared to the 1.5 h heat treatment. After the 2 h treatment, the inhibition of p70 is not demonstrated after any radiation dose. An inhibition of the low level of p27 is observed starting with the 50 cGy dose. This reduction in the expression of HSP with increasing incubation time at 42°C may be due to increased cellular damage occurring at the longer treatment time (2 h vs. 1.5 h). Of great interest is the observation that depending on the time of treatment (at this temperature), ionizing radiation exposure may increase or decrease specific HSP expression, if given at the end of the heat treatment.

#### *Analysis of HSP 90 Expression*

The initial broad spectrum HSP cocktail used to select heat shock proteins associated with the 244B cell line, failed to demonstrate a reaction to the HSP p 90. The use of "cocktail" probes, while being efficient in screening multiple HSPs, may fail to select proteins that compete or have a lower binding affinity. Since we had expected to find p90 associated with lymphoblastoid cells, the 42°C/1.5 h 50 -1000 cGy ionizing radiation exposure gel (see Figure 12C) was reprobbed with a specific anti-p90 monoclonal probe (Figure 13). The heat shock induced levels of p90 HSP in the 42°C 0 and 4 h controls are  $\geq$  levels observed with p70 at this treatment and time points. Although the p90 proteins, at this concentration of antibody used, appear to be present in greater amounts than that observed for the p70 cocktail probe antibody dilution, the same pattern of HSP expression following the 250 cGy dose is observed. The pattern of the HSP p90 present in 42°C heat induced cells is similar to that observed with p70. There was no specific advantage in the additional selection of the p90 protein as a HSP probe, and the p70 and p27 will be assayed in our future studies.

#### *Heat Shock Transcription Factor (HSTF)*

A gel retardation assay for HSTF was done on cells harvested immediately after 42°C hyperthermia (1.5 h treatment) or after 42°C/1.5 h followed by 250 cGy ionizing radiation (Figure 14). The HSTF is not observed in the 37°C mock control cells (Lane 1), but it is observed as expected in the 42°C hyperthermia only control (0 dose) cells (Lane 2). Following the 42°C/250 cGy exposure (Lane 3), the HSTF is present in  $\geq$ 42°C control amounts. This data suggests that the inhibition of HSP p 70 and p 27 following  $\geq$ 250 cGy ionizing radiation is not due to inhibition of the activity necessary to initiate transcription of the messenger RNA for HSP synthesis (i.e., no decrease in the presence of HSTF in the cells). It is likely due to alteration of a subsequent

transcriptional or post-transcriptional event involved in protein synthesis.

## DISCUSSION AND CONCLUSIONS

### *Cell Growth Kinetics and Cell Cycle Kinetics*

Cell kinetic and viability studies after hyperthermia treatment or ionizing radiation exposure (50 cGy - 1000 cGy) demonstrate, in 244B cells as expected, that temperatures or exposure to increasing radiation doses results in decreased cell proliferation. Cell death in the 244B cells is observed only at the highest temperature (42.5°C) and the highest dose (1000 cGy) examined within 120 hours post-exposure. The effect of a 42°C hyperthermia treatment, sequentially followed by ionizing radiation exposure on 244B cell kinetics is similar to that observed with ionizing radiation alone, i.e., there is no significant additional effect of the combined hyperthermia/ionizing radiation exposure with respect to cell proliferation, and evidence for only a small interaction on cell cycle compartment distribution.

### *Cell Surface Marker*

The lymphoblastoid cell line 244B, which has a phenotype similar to that of activated peripheral blood cells and expresses B-cell surface makers, can be used as an *in vitro* model to study the immunological and molecular effects of low dose rate and standard dose rate ionizing radiation exposures, microwave exposures, and hyperthermia treatments. Analysis of cell surface markers by FCM can not discriminate whether a modulation in protein expression would be due to a change of a specific protein (cell surface marker) or due to a general change in total cellular protein reflecting cell growth and/or proliferation differences in the cell population (Englehard, Krupka, Bauer, 1991). Conditions to incorporate the FITC labeled Moab cell surface marker and SR101, and staining assay for simultaneous analysis of cell surface markers, total protein, and DNA respectively, as previously reported (Englehard, 1991), are currently being optimized for the 244B cell line. We have gone to considerable lengths to statistically examine alterations in cell surface markers as a function of effect of temperature, time of analysis, radiation dose, and the possible interaction thereof. From a panel of 28 potential markers examined in year 1 of the project, 13 of these B-cell associated markers were examined. The results of our studies indicate that, as a minimum, our future research should include examination of CD20, CD19, CD23, and CD25 cell surface markers.

### *Heat Shock Proteins*

244B cells express HSP 70 and HSP 27 under conditions of 42°C/1.5 h hyperthermia, but not standard dose rate ionizing radiation. The inhibition of HSP 70 and HSP 27 following SDRR is a possibly important, and definitely unexpected observation. Preliminary evidence suggests that it is not due to a very early step in the transcription mechanism, as evidenced by lack of effect on heat shock transcription factor

measured using the gel retardation assay. Therefore, this inhibition of HSP may be due to inhibition of transcription at a later step, or due to postranscriptional or another mechanism regulating synthesis and expression of the HSP in this system. The phenomena of HSP inhibition following ionizing radiation may alternatively be due to some mechanism involved in x-ray induced G2M cell accumulation. In HeLa cells HSP 70 is not detected when cells are heat shocked in G2. It has been suggested that the epitope recognized by the antibody is inaccessible due to the association of other proteins (Milarski, Welch & Morimoto 1989). It could therefore be hypothesized that a similar complex of proteins occurs after radiation exposure of the 244B cells (which would be independent of cell cycle stage).

#### *Proliferating Nuclear Cell Antigen*

The mechanism for the increased expression of PCNA following  $\geq 100$  cGy is unknown. PCNA is directly involved in DNA synthesis (Mathews, Bernstein, Franza, Garrels, 1984) and recently PCNA has been identified as the polymerase delta accessory protein (Lee, Hurwitz, 1990). In vitro, stimulated peripheral blood mononuclear cells, unlike established cell lines, show a correlation between the number of cells with PCNA expression and the number of cells incorporating bromodeoxyuridine (Hall, Levinson, Woods, et al 1990). The gene for PCNA is transcribed efficiently in both quiescent and proliferating cells, but PCNA mRNA normally only accumulates in proliferating cells (Ottavio, et al 1990). Accumulation of PCNA mRNA and high levels of protein synthesis is stimulated by growth factors, such as PDGF, but is not necessarily associated with DNA synthesis. PCNA also accumulates in the presence of hydroxyurea, which inhibits DNA synthesis (Jaskulski Gatti, Travalli, et al, 1988; and Bravo, MacDonald, -Bravo, 1985). The increased levels of PCNA observed following  $\geq 100$  cGy may be due to accumulation of this cell cycle associated protein or to an alteration of the cell cycle associated proteins. The latter is suggested, as this may explain the increase of the G2M cell cycle compartment observed following SDRR exposure. It is hypothesized that hyperthermia at 42°C inactivates PCNA receptor or inhibits PCNA synthesis, as no accumulation following 42°/SDRR was observed. Understanding the general controls of initiation and inhibition of HSP and PCNA at the molecular level may help define the effector mechanism which regulates cellular proliferation rate and "programed cell death" following SDRR. A speculative hypothesis is that under conditions of hyperthermia/SDRR, the HSPs and PCNA proteins cooperate and participate in a complex system to regulate DNA replication and subsequent cell division.

## REFERENCES

- Aman, P, Ehlin-Henriksson, B, Klein, G. Epstein-Barr virus susceptibility of normal human B lymphocyte populations. *J Exp Med* 159:208-220;1984.
- Anderson, KC, Boyd, AW, Fisher, DC, Slaughenhaupt, B, Groopman, JE, O'Hara, J, Daley, JF, Schlossman, SF, Nadler, LM. Isolation and functional analysis of human B cell populations. I. Characterization of the B1<sup>+</sup>B2<sup>+</sup> and B1<sup>+</sup>B2<sup>-</sup> subsets. *J. Immunology* 134:820-827;1985.
- Baker, WJ, Wiebe, VJ, Koester, SK, Emsholl, VD, Maenpaa, JU, Wurz, GT, DeGregorio, MW. Monitoring the chemosensitizing effects of toremifene with flow cytometry in estrogen receptor negative multidrug resistant human breast cancer cells. *Breast Cancer Research and Treatment* 24: 43-49, 1992.
- Bravo, R., MacDonald-Bravo, H. Changes in the nuclear distribution of cyclin (PCNA) but not its synthesis depends on DNA replication. *EMBO J* 4:655-661;1985
- Chang, RS, Hsieh, MW, Blankenship, W. Initiation from cord blood leucocytes treated with viruses, chemicals and radiation. *J. Natl Cancer Inst.* 47:479-483, 1971.
- Ciocca, DR, Adams, DJ, Bjerke, RJ, Edwards, DP, McGuire, WL. Immunohistochemical detection of an estrogen-regulated protein by monoclonal antibodies. *Cancer Res* 42:4256-4258.
- Clark, EA, Shu, G, Ledbetter, JA. Role of BB p35 cell surface polypeptide in human B cell activation. *Proc Natl Acad Sci U.S.A.* 82:1766-1772; 1985.
- Ellis, RJ. Molecular chaperones. *Annu Rev Biochem* 60:321-347;1991.
- Englehard, HH III, Krupa, JL, Bauer, KD. Simultaneous quantification of c-myc oncoprotein, total cellular protein, and DNA content using multiparameter flow cytometry. *Cytometry* 12:68-76;1991.
- Fox, MH. A model for computer analysis of synchronous DNA distribution obtained by flow cytometry. *Cytometry* 1:71-77; 1980.
- Fuqua, SAW, Blum-Salingaros, M, McGuire, WL. Induction of the estrogen-regulated "24K" protein by heat shock. *Cancer Res* 49:4126-4129;1989.
- Hall, PA., Levinson, DA., Woods, AL., Yu, C. C-W., Kellock, D.B. Watkins, JA., Barnes, DM., Gillett, CE., Camplyokins, R., Dover, R., Waseem, NH., Lane, DP. Proliferating cell nuclear antigen (PCNA) immunolocalization in paraffin sections: an index of cell proliferation with evidence of deregulated expression in some neoplasma. *J Pathology* 162:285-294;1990.

Haugland, RP. (1992) Handbook of fluorescent probes and research chemicals (5th edition). Eugene, Oregon: Molecular Probes, Inc.

Hightower, LE. Cultured animal cells exposed to amino acid analogues or puromycin rapidly synthesize several polypeptides. J Cellular Physiology 102:407-427;1980

Holahan, PK, Eagan, P, Meltz, L. Hyperthermic effects on viability and growth kinetics of human lymphoblastoid cells. International Journal Hyperthermia 7(6):849-856, 1991.

Jaskulski, D., Gatti, G., Tavalli, S., Calabretta, B., Baserga, R. Regulation of the proliferating cell nuclear antigen cyclin and thymidine kinase mRNA levels by growth factors. J Biol Chem 263:10175-10179;1988

Kang, P-J, Ostermann, J, Shilling, J., Neuoert, W., Craig, EA, Pfanner N. Requirement for hsp70 in the mitochondrial matrix for translocation and folding of precursor proteins. Nature 348:137-142;1990.

Kartner, N. Detection of P-glycoprotein in multidrug-resistant cell lines by monoclonal antibodies. Nature 316:820-823;1985.

Kehrl, JH, Muraguchi, A, Fauci, AS. Differential expression of cell activation markers after stimulation of resting human B lymphocytes. J Immunology 132; 2857-2861;1984.

Kleinbaum, DG, Kupper, LL, Muller, KE. Applied Regression Analysis and Other Multivariable Methods. PWS-Kent Publishing Co. Boston, 1988.

Krishan, A. Rapid flow cytofluorometric analysis of mammalian cell cycle by propidium iodide staining. J Cell Biol 66:188-195;1975.

Laemmli, UK. Cleavage of structural proteins during the assembly of the head of bacteriophage T4. Nature 227:680-685; 1970.

Langer, T, Lu, C, Echols, H, Flanagan, J, Hayer, MK, Hartl, FU. Successive action of DnaK, DnaJ and GroEL along the pathway of chaperone-mediated protein folding. Nature 356:683-689;1992.

Lee, SH, Hurwitz, J, Mechanism of elongation of primed DNA by DNA polymerase delta, proliferating cell nuclear antigen and activator. Proc Natl Acad Sci (USA) 87:5672-5676;1990.

Lindquist, S., Craig, EA. The heat-shock proteins. Annu Rev Genet 22:631-677;1988

Manning-Krieg, UC, Scherer, PE, Schatz, G. Sequential action of mitochondrial chaperones in protein import into the matrix. EMBO J 10:3273-3280; 1991.

Mathews, MB, Bernstein, RM, Franza, BR, Garrels, JI. Identity of the proliferating cell nuclear antigen and cyclin. Nature 303:374-376;1984

Milarski, KL, Welch, WJ, Morimoto, RI. Cell cycle-dependent association of HSP70 with specific cellular proteins. *J Cell Biology* 108:413-423;1989.

Ottavio, L., Chang, CD, Rizzo, MG., Travelli, S., Casadevall, C., Baserga, R. Importance of introns in the growth regulation of mRNA levels of the proliferating cell nuclear antigen gene. *Mol Cell Biology* 10:303-309; 1990.

Pezzutto, A, Dörken, B, Moldenhauer, G, Clark, EA. Amplification of human B cell activation by a monoclonal antibody to the B cell-specific antigen CD22, Bp 130/140<sup>1</sup>. *J Immunology* 138:98-103;1987.

Riabowol, KT, Mizzen, LA, Welch, WJ. Heat shock is lethal to fibroblasts microinjected with antibodies against HSP70. *Science* 242:433-436;1988.

Rosner, B. Fundamentals of Biostatistics. PWS-Kent Publishing Co Boston, 1990.

Schmitt, K, Däubener, W, Bitter-Suermann, D, Hadding, U. A safe and efficient method for elimination of cell culture mycoplasma using ciprofloxacin. *J. Immunological Methods* 109:17-25; 1988.

Schneider, SL, Fuqua, SL, Speeg, KV, Tandon, AK, McGuire, WL. Isolation and characterization of an adriamycin-resistant breast tumor cell line. *In Vitro Cell Dev Biol* 26:621-628;1990.

Schneider, SL, Koester, S, Mitzel, H, Szekeresova, M, Infante, AJ, Meltz, ML. Expression of B-cell surface markers as indicators of immune function response to hyperthermia and radiation exposure. Manuscript In Preparation 1993. Abstract *In Vitro Cellular and Developmental Biology* 29A:125A;1993.

Presented at the Congress on Cell and Tissue Culture June 4-9, 1993 San Diego Calif.

Schneider, SL, Fuqua, SAW, Szekeresova, M, Meltz, ML. Heat shock proteins associated with exposure to hyperthermia and ionizing radiation in a normal human lymphoblastoid cell line. Manuscript In Preparation 1993.

Schneider, SL, Szekeresova, M, Meltz, ML. Characterization of a normal human peripheral blood B-cell line to study the immunological effects of hyperthermia and ionizing radiation exposure. Manuscript In Preparation. Abstract in Forty First Annual Meeting of the Radiation Research Society, page 37, 1993. Presented at the Radiation Research Society and the North American Hyperthermia Society Meeting March 20-25, 1993 Dallas, Tx., page 37, 1993.

Schwartz, JL, Turkula, T, Sagher, D, Strauss, B. The relationship between O<sup>6</sup> - alkylguanine alkyltransferase activity and sensitivity to alkylation induced sister chromatid exchanges in human lymphoblastoid cell lines. *Carcinogenesis* 10(4): 681-685; 1989.

Schwartz, GG. Chromosome Aberrations (1990). In Hulka, BS, Wilcosky, TC, & Griffith, JD (Eds) *Biologic Markers in Epidemiology* (pp147-172). New York, Oxford: CRC Press, Oxford University Press.

Stamenkovic, I Seed, B. The B-cell antigen CD22 mediates monocyte and erythrocyte adhesion. *Nature* 345:74-77;1990.

Spector, NL, Samson, W, Ryan, C, Gribben, J, Urba, W, Weklch, WJ, Nadler, LM. Growth arrest of human B lymphocytes is accompanied by induction of the low molecular weight mammalian heat shock protein (Hsp28). *J Immunology* 148:1668-1673;1992.

Zeltzer, PM, Schneider, SL, Von Hoff, DD. Morphologic, cytologic and neurochemical characterization of the human medulloblastoma cell line TE671. *J. Neuro-Oncology* 2:35-45;1984.

Zimarino, V., Tsai, C., and Wu, C. Complex modes of heat shock factor activation. *Molecular Cell Biology* 10:752-759; 1990.

**Table 1**  
**Fold Increase in 244B Cell Growth as an Index of Proliferation Following Hyperthermia Treatment**

Temperature °C <sup>b</sup>	72 Hours		120 Hours	
	Fold Increase	% Control	Fold Increase	% Control
37	5.7	100	14.7	100
39	5.1	89	11.3	77
40	5.6	99	11.1	76
41	5.5	96	10.5	72
41.5	4.3	75	11.0	75
42	3.7	65	8.4	57
42.5	2.1	37	3.8	26

<sup>a</sup>Cell viability at 72 and 120 hrs was 95-100%

<sup>b</sup>Heat treatment for 2 hours

**Table 2**  
**Fold Increase in 244B Cell Growth as an Index of Proliferation Following SDRR Exposure and Hyperthermia Treatment Followed by SDRR Exposure.**

Exposure <sup>b</sup>	Fold Increase <sup>a</sup>			
	24 Hour	72 Hour	96 Hour	120 Hour
37°C Control	1.9	4.4	8.2	15.2
50 cGy	1.8	3.9	7.3	9.9
100 cGy	1.5	3.4	5.1	7.0
250 cGy	1.5	2.4	3.0	3.4
500 cGy	1.4	1.9	2.3	2
1000 cGy	1.2	1.5	1.6	1.5
42°C Control	0.9	5.6	9.0	14.8
42°C/50 cGy	0.9	3.9	6.7	9.4
42°C/100 cGy	1.0	3.0	4.0	6.1
42°C/250 cGy	0.9	1.5	1.8	2.0
42°C/500 cGy	1.0	1.3	1.2	0.9
42°C/1000 cGy	0.8	1.2	0.9	1.1

<sup>a</sup>Results of two separate experiments at passage 22

<sup>b</sup>Hyperthermia treatment for 1.5 hours

**Table 3**  
**Effect of Fixation on Flow Cytometric DNA Analysis of 244B Cells**

Fixative	Percent Cell Cycle Distribution			
	GoG1	G2M	S	G2M D/A*
NONE	72	11	17	1.98
0.5% PARAFORMALDEHYDE	64	12	24	1.98
2% PARAFORMALDEHYDE/70% ETOH	57	10	28	1.98
70% ETOH	57	15	33	1.94

\*Ratio G2M diploid/aneuploid cells

**Table 4**  
**Flow Cytometric DNA Analysis of 244B Cell Line<sup>a</sup>**

Cell Cycle	Passage								% Cell Cycle Compartment <sup>b</sup>
	p15*	p22	p24	p29	p32	p33	p35	p47*	
GoG1	69.5	70.4	73.5	76	84	82.6	83.0	72	74.8 (69.5-83)
S	21.0	20.7	19.1	14	10	9.8	10.0	11	12.5 (10-21)
G2M	9.5	8.9	7.4	10	6	7.6	7	17	8.2 (6-17)
D/A <sup>c</sup>	1.98	1.96	1.98	1.98	1.98	1.98	1.98	1.98	1.98 (1.96-1.98)

<sup>a</sup>Results of 8 experiments on live viable cells for passages 15-47

<sup>b</sup>Results are expressed as median score of percent cell compartment with range in parenthesis

<sup>c</sup>Ratio G2M diploid/aneuploid cells

\*Mycoplasma positive cells

**Table 5**  
**Percent Cell Cycle Compartment Distribution<sup>a</sup> of 244B at 24 and 120 hours**  
**Following Exposures**

Exposures	<u>G0G1</u>		<u>S</u>		<u>G2M</u>	
	24h	120h	24h	120h	24h	120h
37°C Control	77.6	87.3	13.8	6.5	8.6	6.2
50 cGy	81.5	84.2	8.1	7.5	10.4	8.3
100 cGy	81.8	82.0	10.4	7.9	7.8	10.1
250 cGy	80.0	80.9	3.7	5.4	16.3	13.7
500 cGy	79.4	78.5	3.0	3.8	17.6	17.7
1000 cGy	84.2	86.1	3.2	2.5	12.6	11.4
42°C Control <sup>b</sup>	77.3	83.9	12.7	7.6	10.0	8.5
42°C/50 cGy	79.8	82.2	7.9	7.7	12.3	10.1
42°C/100 cGy	80.6	80.1	5.7	7.9	13.7	12.0
42°C/250 cGy	80.1	79.5	3.1	5.9	16.8	14.6
42°C/500 cGy	81.7	81.5	2.7	4.0	15.6	14.5
42°C/1000 cGy	84.2	85.6	2.9	3.2	12.9	11.2

<sup>a</sup>Flow cytometric analysis of propidium iodide stained cells

<sup>b</sup>Hyperthermia treatment for 1.5 hours

Table 6  
B-Cell Associated Cell Surface Markers

Antigen Marker	Marker/Function
<i>CONTROLS</i>	
HLA-DR	LYMPHOID STEM CELL
CD19 (B4) <sup>P</sup>	REGULATION B-CELL PROLIFERATION, B-CELL (SIG +) ARE CD-19 + ; LOST ON ACTIVATION; 95KD GLYCOPROTEIN
CD21 (B2) <sup>R</sup>	EBV RECEPTOR BINDING SITE; CR2 RECEPTOR OF C3d FRAGMENT OF COMPLEMENT; 140KD GLYCOPROTEIN RESTRICTED TO MATURE CELL; TRANSMIT/GROWTH PROMOTING SIGNALS; EPI TOPE ON 72KD
CD10 <sup>R</sup>	ALL B-CELL MALIGNANCIES; NOT EXPRESSED IN NORMAL PERIPHERAL BLOOD CELLS
<i>CELL TYPE</i>	
CD20 (B1) <sup>P</sup>	TRANSMEMBRANE EFFECTOR OF SIG BINDING, INDEPENDENT RECEPTOR FOR INTERLEUKIN; 35 KD GLYCOPROTEIN
CD22 <sup>R</sup>	PHENOTYPE MATURE B-CELL; 50% PRE-B, 75% RESTING B-CELL (LOST AFTER ACTIVATION); 135-140KD GLYCOPROTEIN; ADHESION, SIGNAL TRANSDUCTION; EXTRACELLULAR LIGAND OF PROTEIN (CD45) TYROSINE PHOSPHATASE.
CD23 (B6) <sup>R</sup>	ACTIVATED B-CELLS (APPEARS 24HH-PEAK 72H), DISAPPEARS 6-8 DAYS AFTER ACTIVATION; 45KD GLYCOPROTEIN
CD25 (IL-2R)	INTERLEUKIN-2 RECEPTOR ON LYMPHOBLASTOID (B&T-CELLS, ACTIVATED T-CELL PROLIFERATION); 50-57 KD GLYCOPROTEIN
CD45 (R) <sup>R</sup>	PHORBAL MYSTRISTATE OR ANTI- $\mu$ (B-CELL); SPECIFIC STIMULATION PHOSPHATASE SYNTHESIS; CD4 SUBSET; RACIAL VARIANT

Table 6 cont.  
 B-Cell Associated Cell Surface Markers

Antigen Marker	Marker/Function
<i>CELL FUNCTION</i>	
IGG	SUBSEQUENT REARRANGEMENT OF CONSTANT REGION OF HEAVY CHAIN GENES RESULT IN MEMBRANE EXPRESSION IGG,
IGM	PRIMARY B-CELL EXPRESS MEMBRANE IGM, REFLECTS IMMATURE STATUS
IGD	MATURING B-CELL PRODUCES IGD, IGM + IGD + LARGEST NUMBER OF CIRCULATING B-CELLS IN MAN; IGM + IGD + B-CELLS EXPRESS CD19,20,21,41,C3,FC RECEPTORS
KAPPA	B-CELL COMMITMENT, GENE CODING FOR HEAVY AND LIGHT CHAINS, ONLY 1 OF THE 12 LIGHT CHAIN GENES ( $\kappa$ OR $\lambda$ ) ON THE ACTIVE CHROMOSOME IS EXPRESSED

P - Pan B-Cell Marker  
 R - Restricted B-Cell Marker

**Table 7**  
**Phenotypic Cell Surface Characteristics of 244B Cell Line<sup>a</sup>**

<b>Antigen Marker</b>	<b>% Positive Cells<sup>b</sup></b>
HLA-DR	82 (60-86) <sup>c</sup>
CD19	54 (61-70)
CD21	13 (0-19)
CD10	0 (0-12)
CD20	81 (69-90)
CD22	23 (23-35)
CD23	87 (73-87)
CD25	0 (0-29)
CD45	37 (34-44)
IGG	23 (22-36)
IGM	0
IGD	0
Kappa	42 (31-46)

<sup>a</sup>Immunoglobulin nonsecretor; Negative for terminal deoxynucleotidyltransferase (TdT)

<sup>b</sup>Results of 5 flow cytometric experiments on live viable cells for passages 15-43

<sup>c</sup>Results are expressed as median score with range in parenthesis

**Table 8**  
**Effect of Fixation on 244B Cell Surface Markers**

Antigen Marker	% Positive Cells <sup>a</sup>		
	Live Cells	0.5% Paraformaldehyde	70% ETOH
<i>CONTROLS</i>			
HLA-DR	78	55	24
CD19 (B4)	65	20	NEG
CD21 (B2)	NEG	13	17
CD10	NEG	14	95
<i>CELL TYPE</i>			
CD20 (B1)	90	43	14
CD22	23	31	11
CD23 (B6)	87	54	23
CD25 (IL-2R)	NEG	26	91
CD45	33	36	17
<i>CELL FUNCTION</i>			
IGG	27	27	60
IGM	NEG	NEG	26
IGD	NEG	NEG	NEG
KAPPA	31	41	44

<sup>a</sup>FCM using FITC-labeled monoclonal antibodies

Table 9  
244B Cell Surface Marker Analysis 4 Hours Post Exposure

Marker	37°C			42°C		
	control	100cGy	500cGy	control	100cGy	500cGy
HLA-DR	82	79	87	89	86	68
CD-19	64	67	68	61	61	61
CD-21	0	0	0	14	14	14
CD-10	0	0	0	0	0	0
CD-20	83	81	75	85	84	78
CD-22	34	45	35	30	32	17
CD-23	74	75	70	70	70	67
CD-25	0	25	20	0	15	13
CD-45RA	45	44	36	41	39	31
IgG	23	26	27	22	26	21
IgM	0	0	0	0	0	0
IgD	0	0	0	0	0	0
Kappa	40	42	47	39	36	33

Percent Positive Cells

Table 10  
244B Cell Surface Marker Analysis 24 Hours Post Exposure

Marker	37°C			42°C		
	control	100cGy	500cGy	control	100cGy	500cGy
HLA-DR	77	87	80	82	72	69
CD-19	62	70	69	59	66	56
CD-21	0	0	0	12	0	12
CD-10	0	0	0	0	0	0
CD-20	80	74	78	79	81	71
CD-22	36	32	34	25	28	14
CD-23	68	71	71	67	68	64
CD-25	0	0	18	0	10	18
CD-45RA	43	40	48	34	35	30
IgG	20	24	34	22	17	13
IgM	0	0	0	0	0	0
IgD	0	0	0	0	0	0
Kappa	38	42	50	37	37	31

Percent Positive Cells

Table 11  
244B Cell Surface Marker Analysis 120 Hours Post Exposure

Marker	37°C			42°C		
	control	100cGy	500cGy	control	100cGy	500cGy
HLA-DR	51	47	43	60	49	50
CD-19	44	37	30	43	40	25
CD-21	13	8	0	9	9	0
CD-10	0	0	0	0	0	0
CD-20	69	61	54	69	59	50
CD-22	15	10	0	10	0	0
CD-23	57	52	45	58	52	42
CD-25	15	12	12	12	14	9
CD-45RA	20	0	0	12	11	8
IgG	12	12	12	10	13	11
IgM	0	0	0	0	0	0
IgD	0	0	0	0	0	0
Kappa	27	24	26	23	23	20

Percent Positive Cells

Table 12  
Statistical Profile of 244B Cell Surface Marker Panel

Marker	Time	Temperature	Dose	Time•Temp	Time•Dose	Temp•Dose
HLA-DR	↓++	-	-	-	-	-
CD-45RA	↓++	-	-	-	-	-
IGG	↓++	-	-	-	-	-
Kappa	↓++	↓++	-	-	-	↓↑+
CD-20	↓++	-	↓++	-	-	-
CD-22	↓++	↓++	↓+	-	-	-
CD-19	↓++	↓++	↓++	-	↓++	↑↓+
CD-23	↓++	↓++	↓++	-	↓++	-
CD-21	-	↑++	-	↑++	-	-
CD-25	-	-	↓++	-	↑↓++	-

++ Statistical significance ≤ 0.05  
 + Statistical significance ≤ 0.10  
 ↑↓ Increase or decrease at 120 h, 42°C, 500 cGy

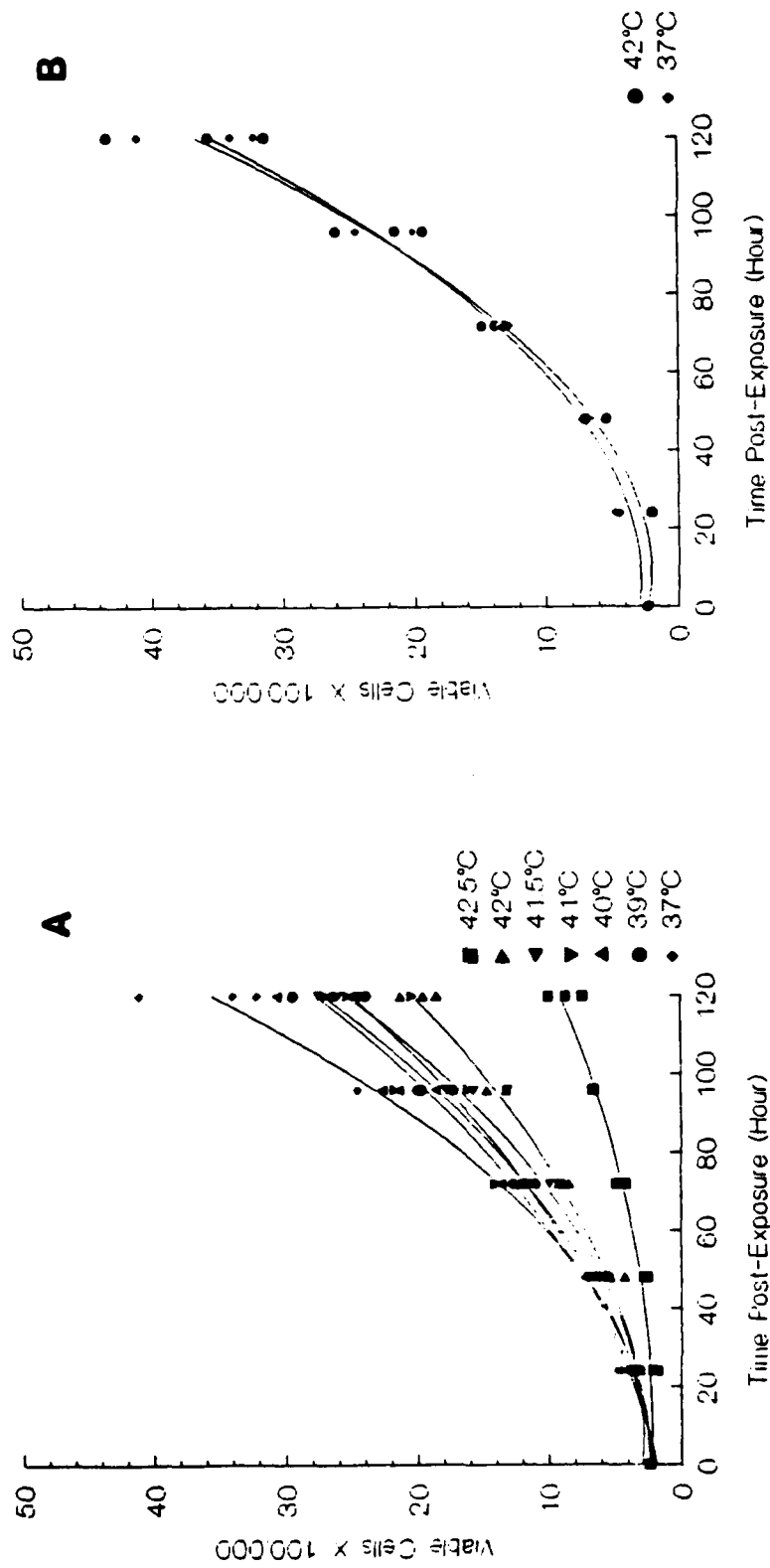


**Figure 1** Effect of hyperthermia on the proliferation of 244B cells. Proliferation of 244B cells was determined as total viable cells  $\times 10^5$  at 24-120 hours after hyperthermia (37°C - 42.5°C) treatment for 2 hours (A) and after 37°C and 42°C hyperthermia treatment for 1.5 hours (B). Time 0 is the pre-exposure time point. Total viable cells were plotted vs time using a computerized quadratic fit  $Y = a + bX + cX^2$  where  $a$  is a constant and  $b$  and  $c$  are slope coefficients.

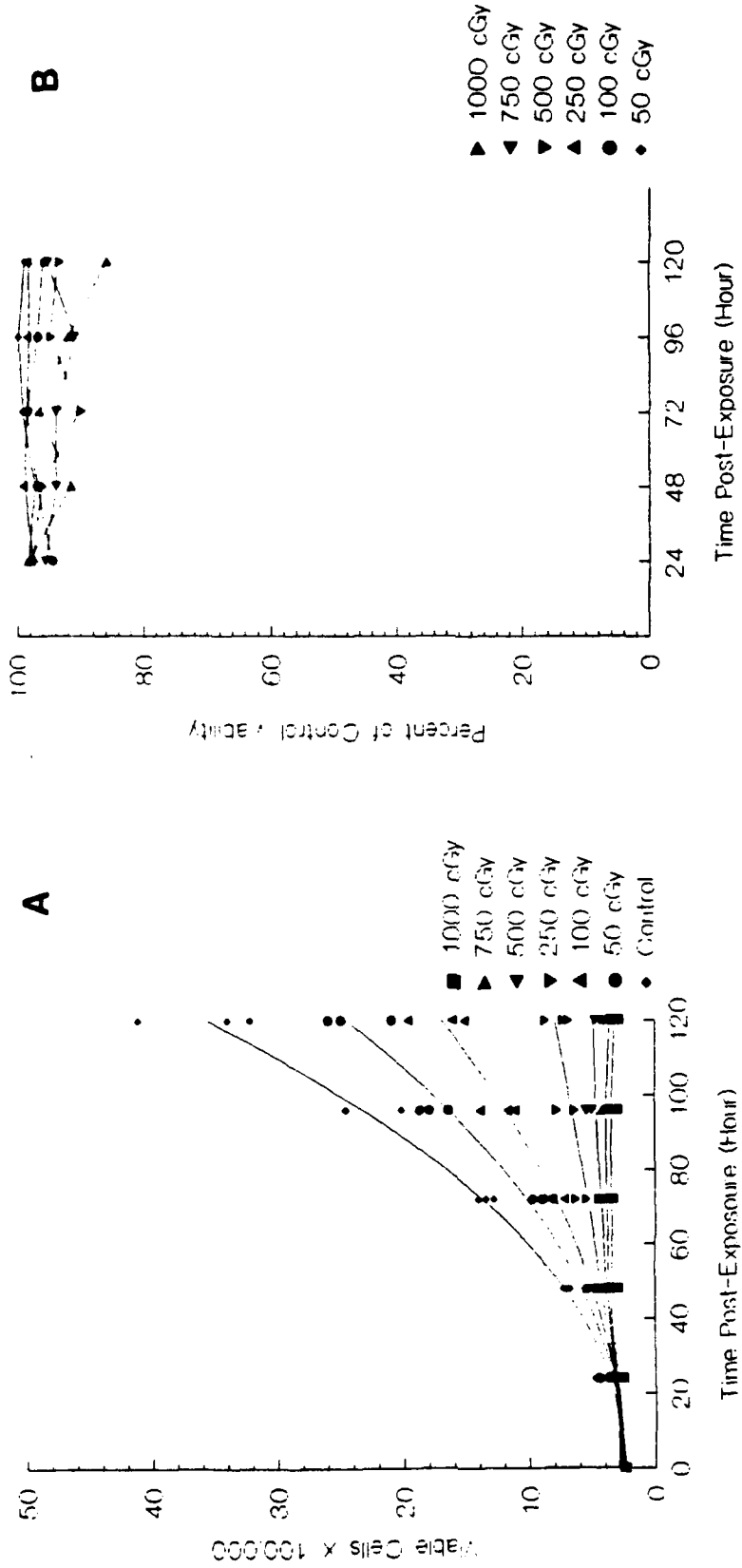
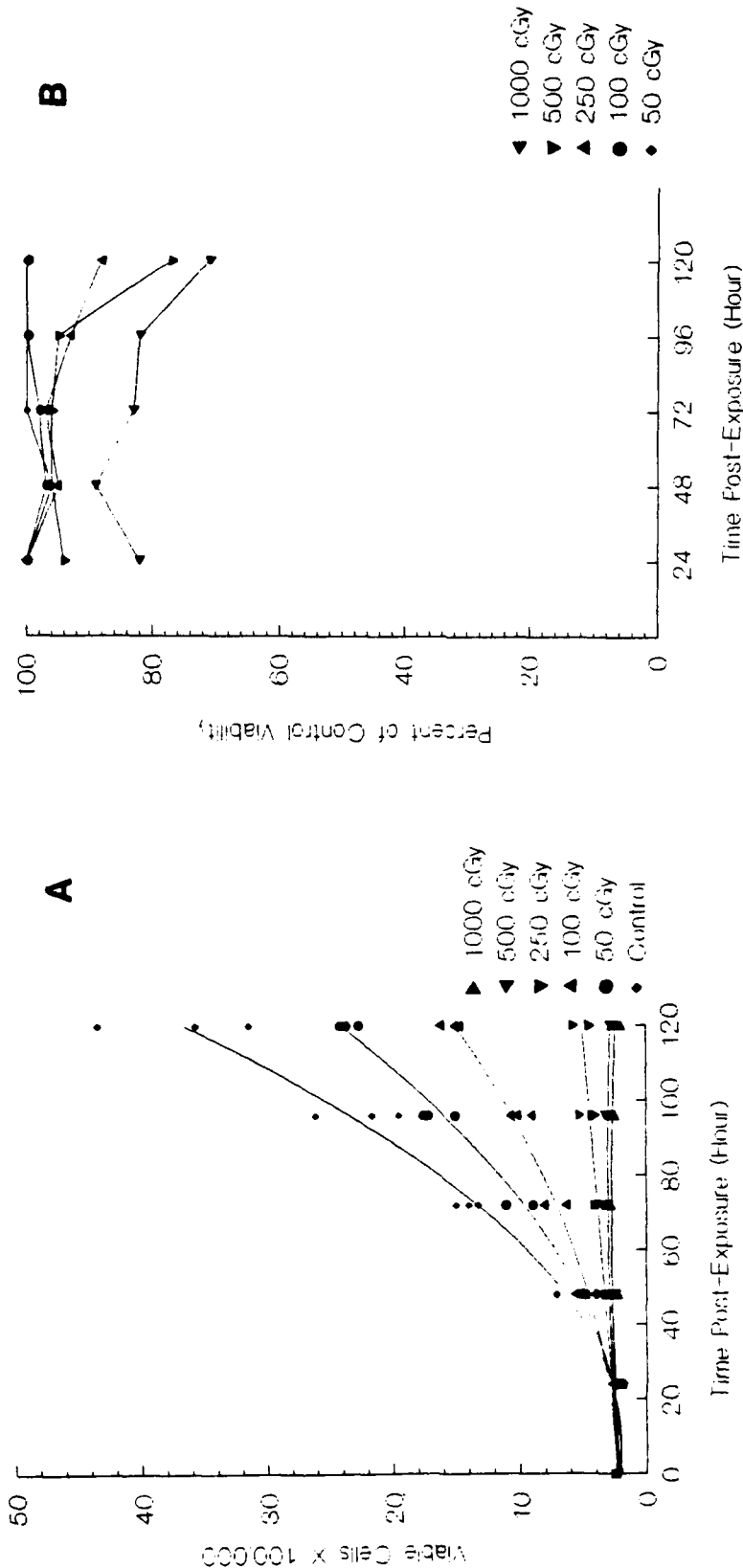


Figure 2 Effect of standard dose rate ionizing radiation on the proliferation of 244B cells. Proliferation of 244B cells was determined as total viable cells  $\times 10^5$  (A) and percent of control viability (B) at 24-120 hours after ionizing radiation exposure (50 cGy - 1000cGy). Time 0 is the pre-exposure time point. Total viable cells were plotted vs time using a computerized quadratic fit  $Y = a + bX + cX^2$  where  $a$  is a constant and  $b$  and  $c$  are slope coefficients.



**Figure 3** Effect of hyperthermia at 42°C sequentially followed by standard dose rate ionizing radiation on the proliferation of 244B Cells. Proliferation of 244B cells was determined as total viable cells X10<sup>5</sup> (A) and percent of control viability (B) at 24-120 hours after hyperthermia treatment at 42°C/1.5 h followed by ionizing radiation exposure (50 cGy - 1000 cGy). Time 0 is the pre-exposure time point. Total viable cells were plotted vs time using a computerized quadratic fit  $Y = a + bX + cX^2$  where  $a$  is a constant and  $b$  and  $c$  are slope coefficients.

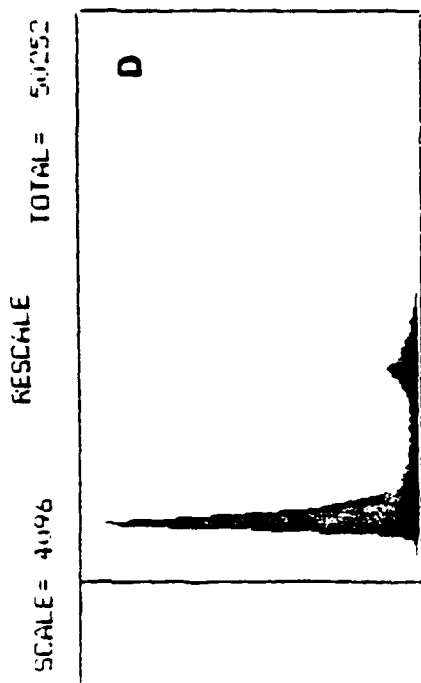
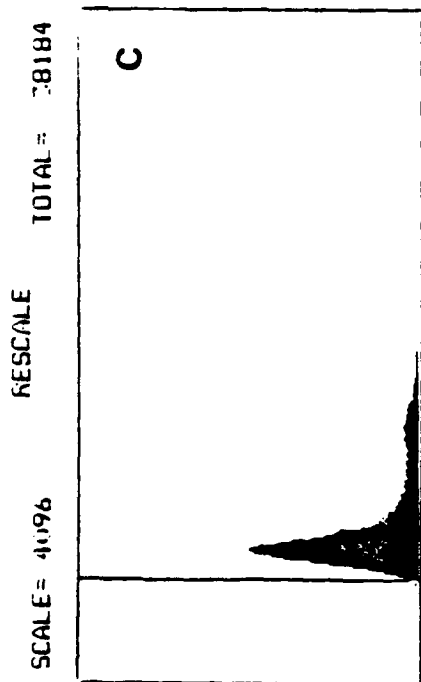
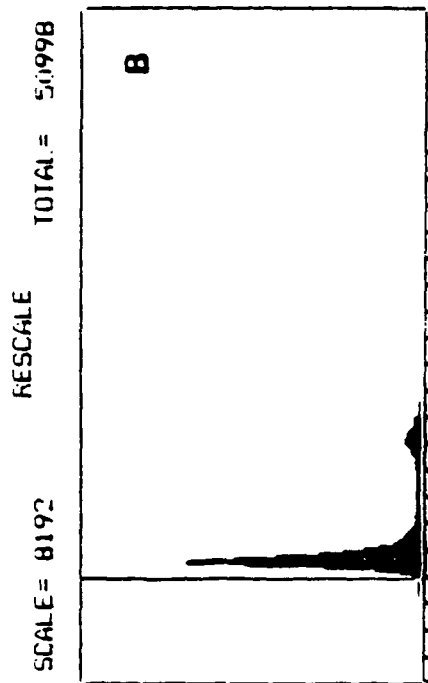
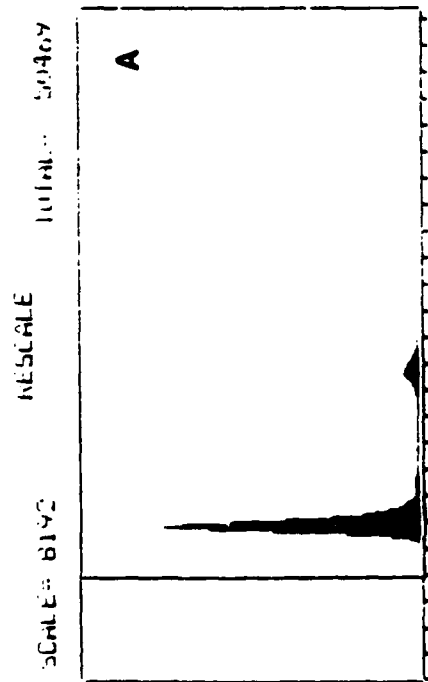


Figure 4 Flow cytometric histograms of 244B cells analysed as live cells (no fixation) (A); 0.5% paraformaldehyde fixed cells (B); 2% paraformaldehyde+70% ETOH (C); and 70% ETOH (D). Scale settings were amplified (8192) for live cell (A) and 2% paraformaldehyde+70% ETOH (B) analysis compared to scale setting (4096) for 0.5% paraformaldehyde fixed cells (C) and 70% ETOH (D) analysis.

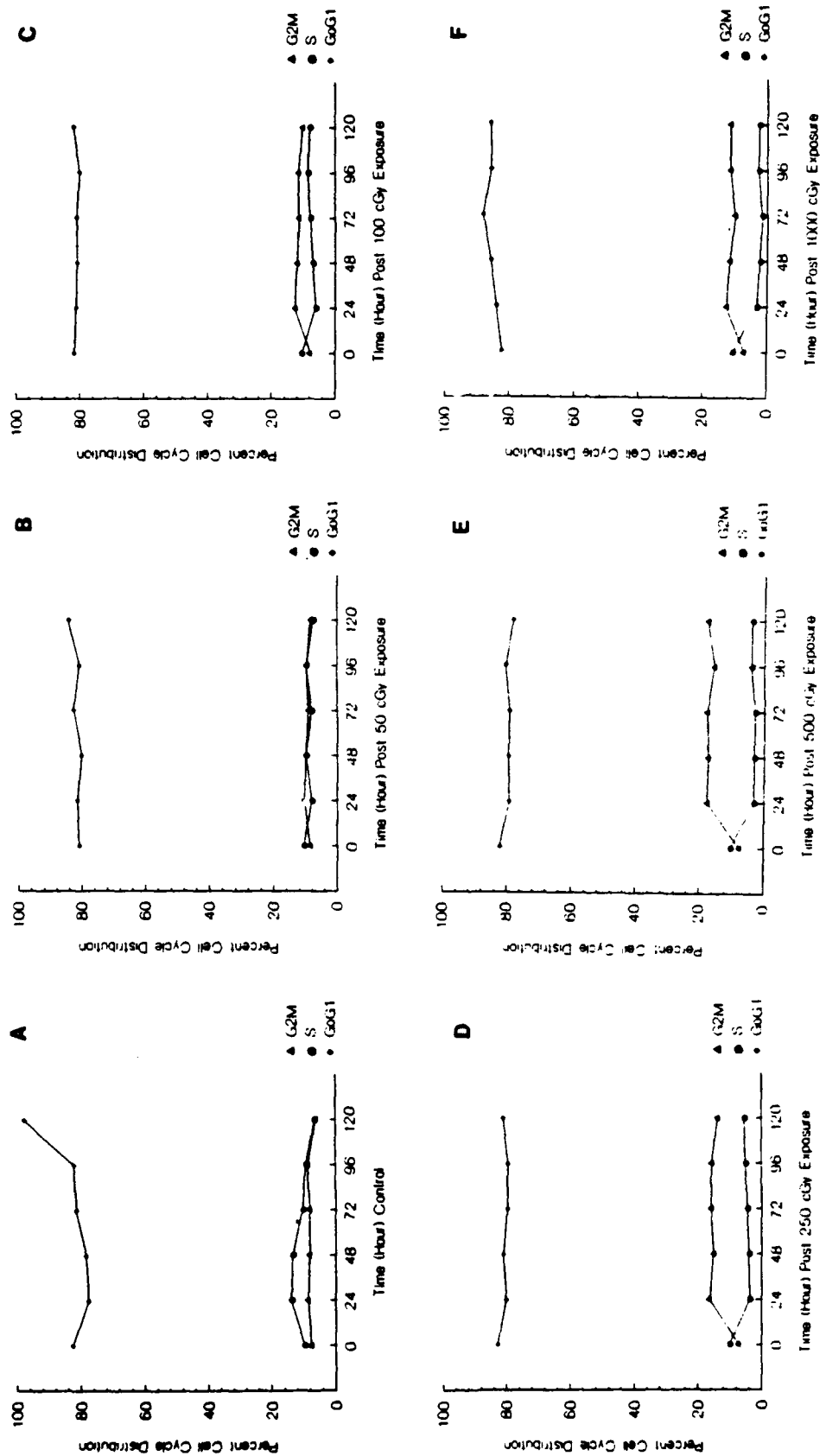
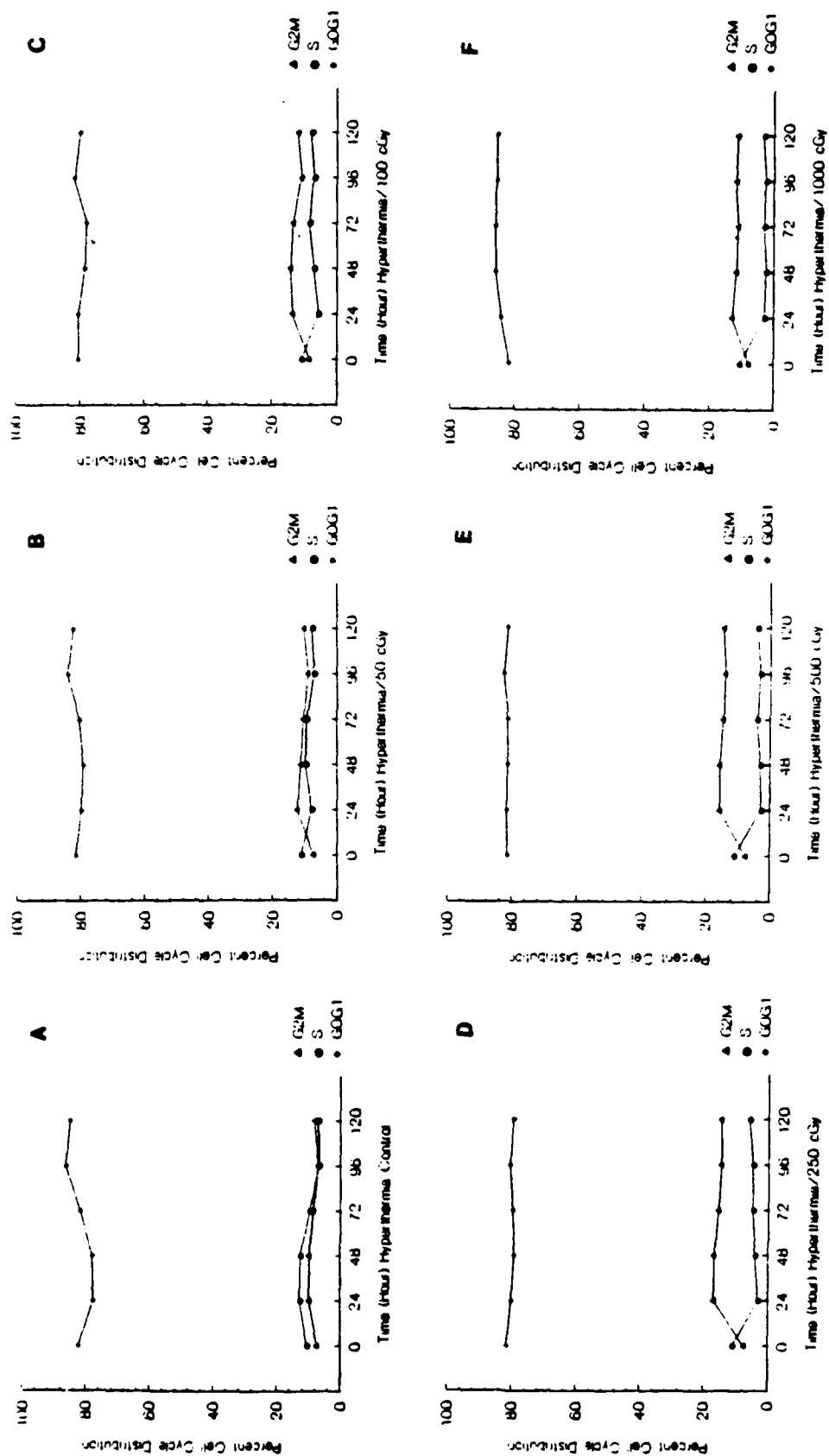


Figure 5 Flow cytometric cell cycle analysis of 244B cells following standard dose rate ionizing radiation exposure. The percent cell cycle distribution of G0G1, S, and G2M compartments was determined for 24-120 h time points following mock 37°C control and 50 cGy, 1000 cGy exposure (A-F).



**Figure 6** Flow cytometric cell cycle analysis on 244B after 42°C hyperthermia treatment for 1.5 h sequentially followed by standard dose rate ionizing radiation exposure. The percent cell cycle distribution of G0G1, S, and G2M compartments was determined for 24-120 h time points following 42°C hyperthermia / 50 cGy - 1000 cGy exposure (A-F).

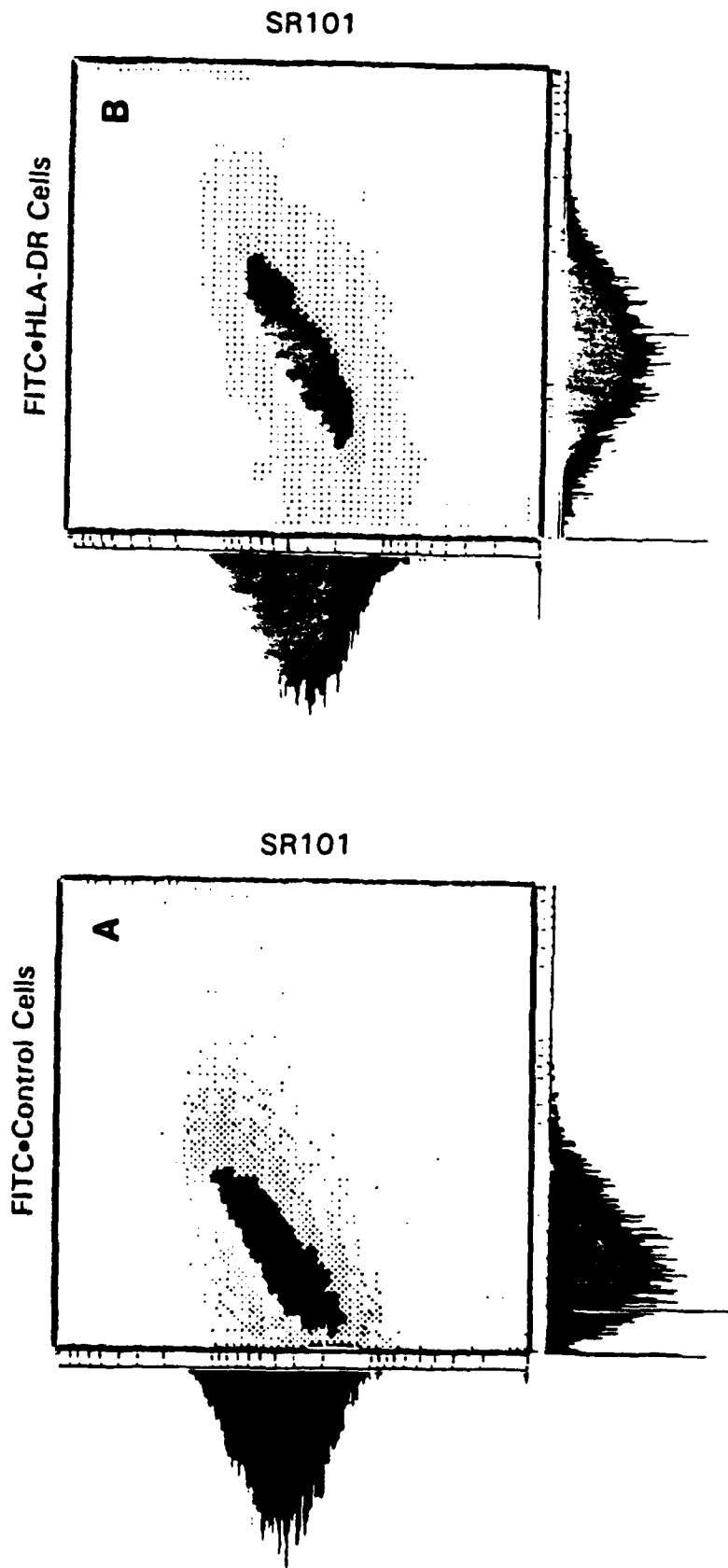


Figure 7 Histogram of SR101 and FITC-anti-HLA-DR dual-labeled 244B cells for determination of total protein and cell surface marker respectively. Panel (A): FITC labeled control cells and SR101 labeled cells; Panel (B): FITC-anti HLA-DR labeled cells and SR101 labeled cells.

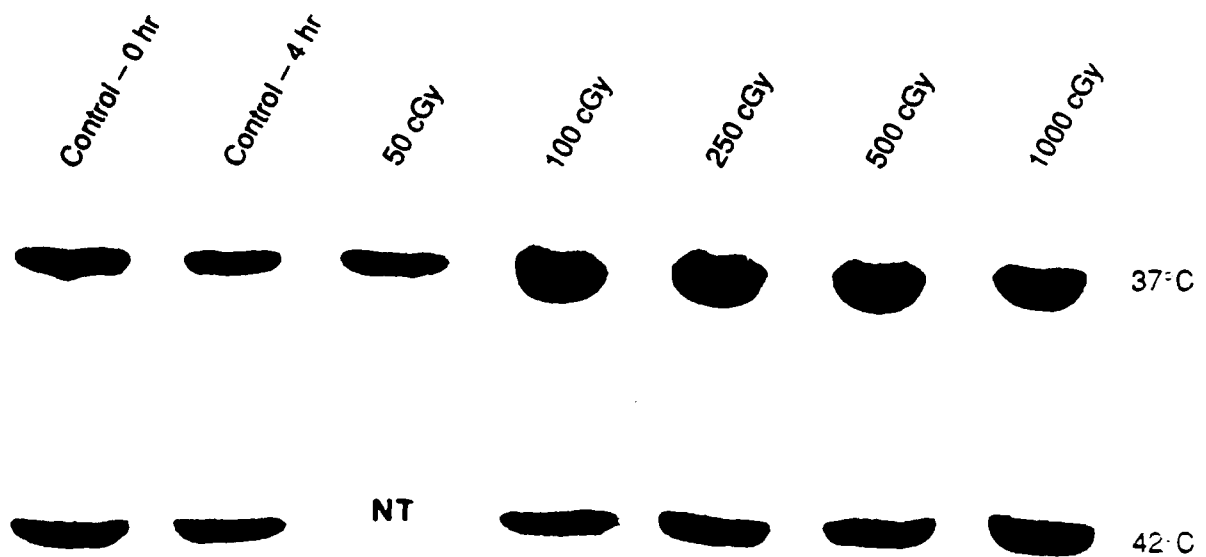
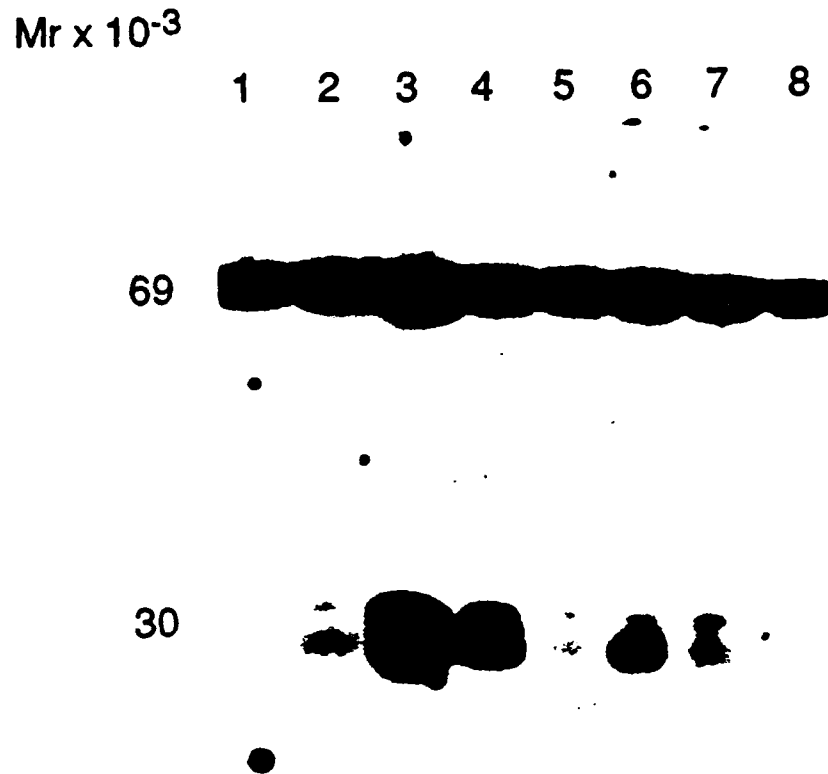


Figure 8 Expression of proliferating nuclear antigen (PCNA) protein after ionizing radiation and hyperthermia/ionizing radiation exposure. Western blot comparison of the expression of PCNA following standard dose rate ionizing radiation (50 cGy - 1000 cGy) exposure at 37°C with the expression of PCNA after 42°C hyperthermia \ 1.5 h followed by standard dose rate ionizing radiation (50 cGy - 1000 cGy) exposure.



**Figure 9** The effect of cell concentration on the expression of HSPs p70 and p27 in 244B cells following hyperthermia, low dose rate ionizing radiation (LDRR) and standard dose rate ionizing radiation (SDRR) exposures. Lane 1: 37°C mock control at  $1 \times 10^6$  cells/ml; Lane 2: 37°C mock control at  $5 \times 10^6$  cells/ml; Lane 3: 42°C/2 h at  $1 \times 10^6$  cells/ml; Lane 4: 42°C/2 h at  $5 \times 10^6$  cells/ml; Lane 5: 100 cGy LDRR at  $1 \times 10^6$  cells/ml; Lane 6: 100 cGy LDRR at  $5 \times 10^6$  cells/ml; Lane 7: 100 cGy SDRR at  $1 \times 10^6$  cells/ml; Lane 8: 100 cGy SDRR at  $5 \times 10^6$  cells/ml. The LDRR exposure rate was 0.5 cGy/minute; the SDRR exposure rate was 116 cGy/minute. A 10% gel was used in this experiment.

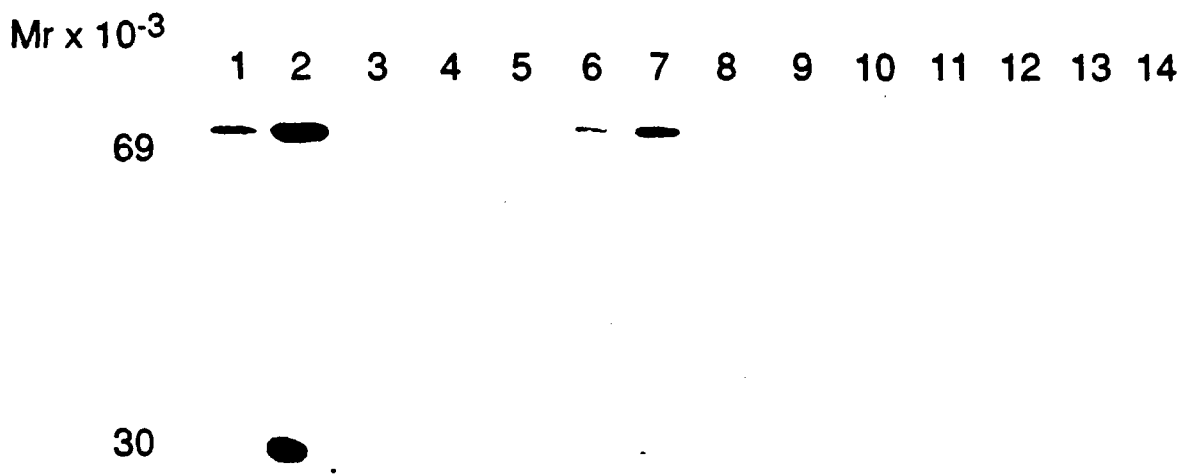


Figure 10 The expression of HSPs p70 and p27 following 50 cGy - 1000 cGy ionizing radiation exposure. HSPs were tested at 0 hour and 4 hour following exposure. Lane 1: 37°C mock control at 4 hours; Lane 2: 42°C control at 4 hours; Lane 3 - 4: 50 cGy at 0 and 4 hours; Lane 5-6: 100 cGy at 0 and 4 hours; Lane 7-8: 250 cGy at 0 and 4 hours; Lane 9-10: 500 cGy at 0 and 4 hours; Lane 11-12: 750 cGy at 0 and 4 hours; Lane 13-14: 1000 cGy at 0 and 4 hours.

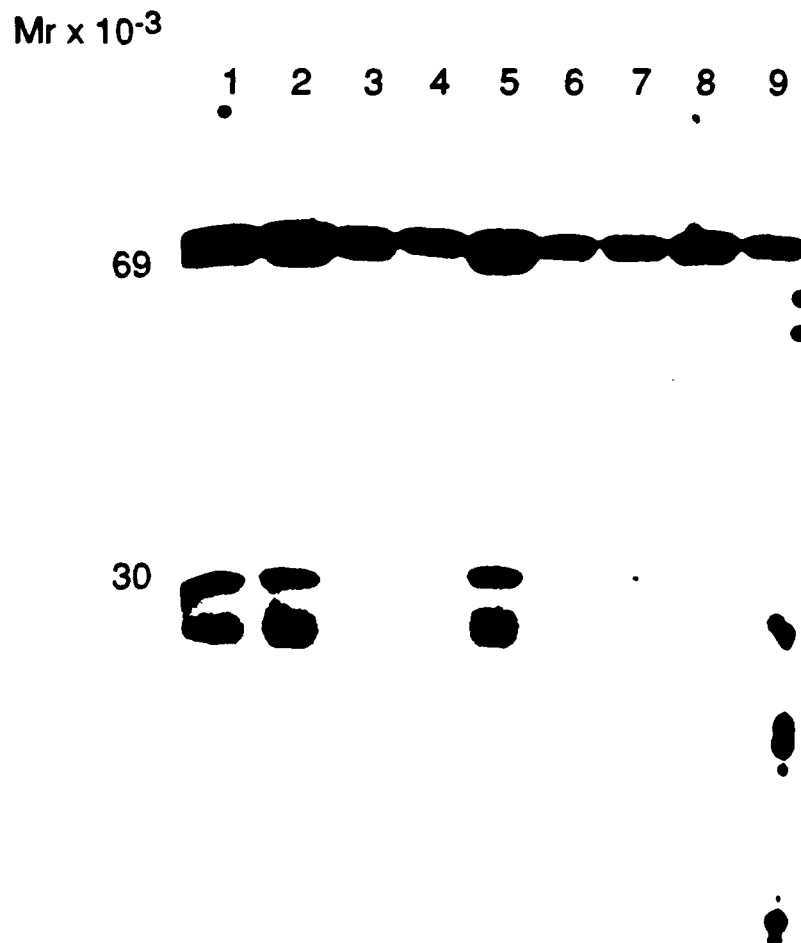


Figure 11 The expression of HSPs p70 and p27 in 244B cells following hyperthermia and 100 cGy ionizing radiation. Expression of HSPs was determined by the pre or post exposure of cell heat treated at 42°C / 2 hours. Lane1: 42°C + 4h•37°C; Lane 2: 42°C + 4h•37°C + 100 cGy; Lane 3: 42°C + 37°C/20 min + 100 cGy + 4h•37°C; Lane 4: 100 cGy + 4h•37°C; Lane 5: 100 cGy + 42°C + 4h•37°C; Lane 6: 42°C + 100 cGy at 42°C + 4h•37°C; Lane 7 -8: mock 37°C controls at 0 hour and 4 hour time points; Lane 9: 42°C heat treated cells at 0 hour.

Hyperthermia Treatment at 42°C / 30 minutes

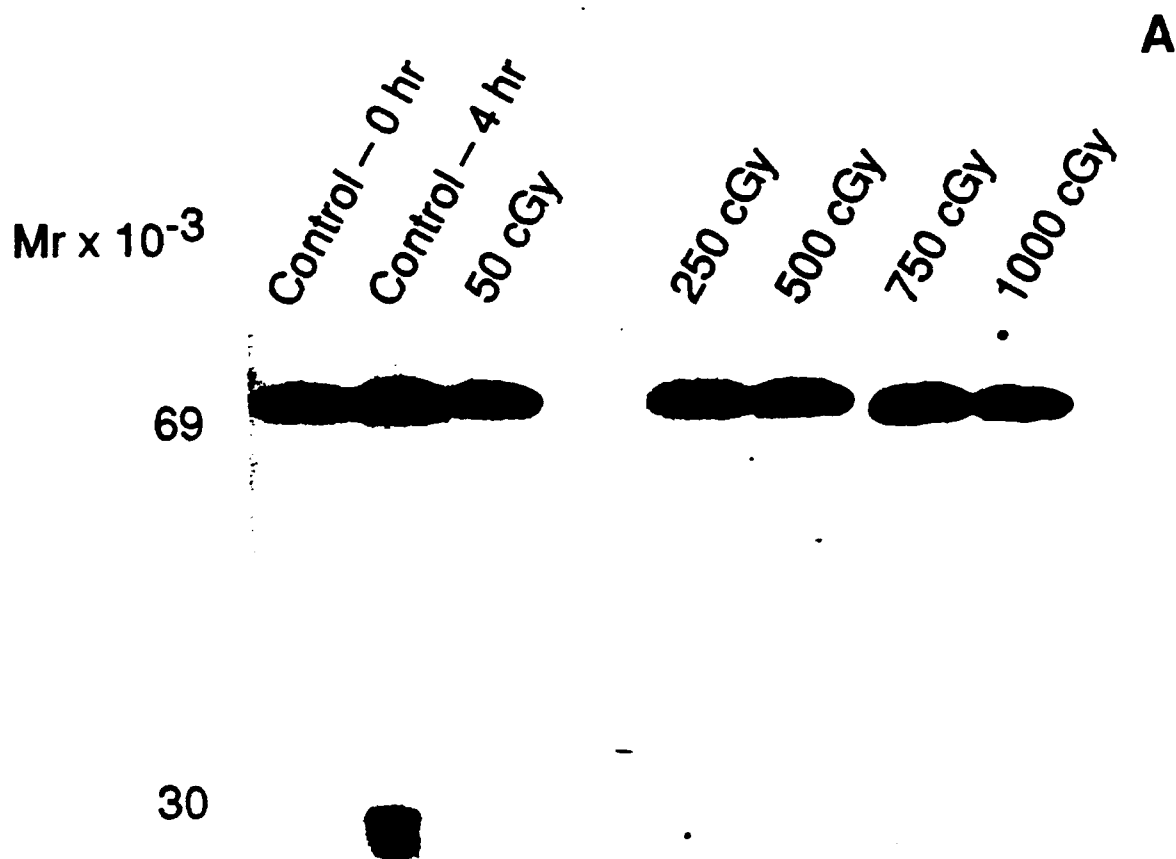


Figure 12 A The expression of HSP p70 and p27 in 244B cells 4 hour after a standard dose rate ionizing radiation exposure. The cells were irradiated immediately after a hyperthermia treatment at 42°C. Hyperthermia treatment time: 30 min. "Control-0 hr" cells were harvested immediately after hyperthermia treatment (0 cGy). "Control-4 hr" cells were allowed to incubate for 4 hours post hyperthermia treatment (0 cGy).

Hyperthermia Treatment at 42°C / 1 hour

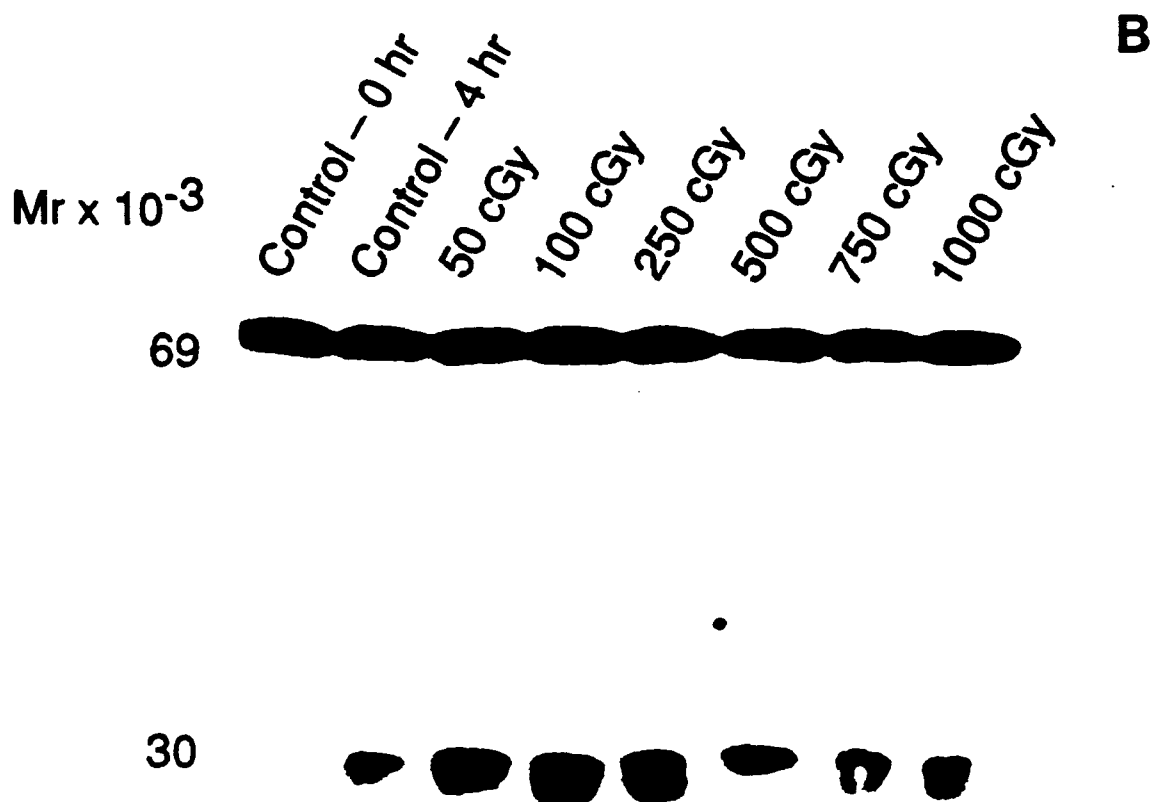


Figure 12 B The expression of HSP p70 and p27 in 244B cells 4 hour after a standard dose rate ionizing radiation exposure. The cells were irradiated immediately after a hyperthermia treatment at 42°C. Hyperthermia treatment time: 1 hour. "Control-0 hr" cells were harvested immediately after hyperthermia treatment (0 cGy). "Control-4 hr" cells were allowed to incubate for 4 hours post hyperthermia treatment (0 cGy).

Hyperthermia Treatment at 42°C / 1.5 hour

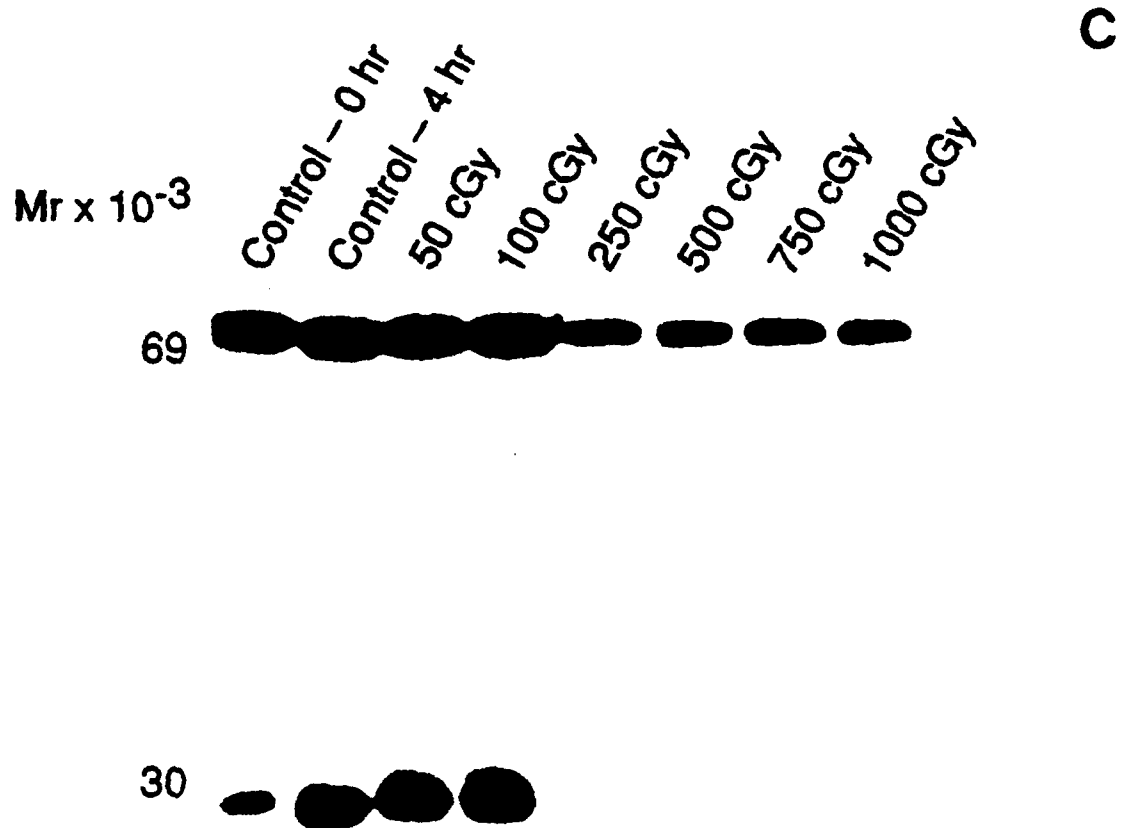


Figure 12 C The expression of HSP p70 and p27 in 244B cells 4 hour after a standard dose rate ionizing radiation exposure. The cells were irradiated immediately after a hyperthermia treatment at 42°C. Hyperthermia treatment time: 1.5 hour. "Control-0 hr" cells were harvested immediately after hyperthermia treatment (0 cGy). "Control-4 hr" cells were allowed to incubate for 4 hours post hyperthermia treatment (0 cGy).

Hyperthermia Treatment at 42°C / 2 hours

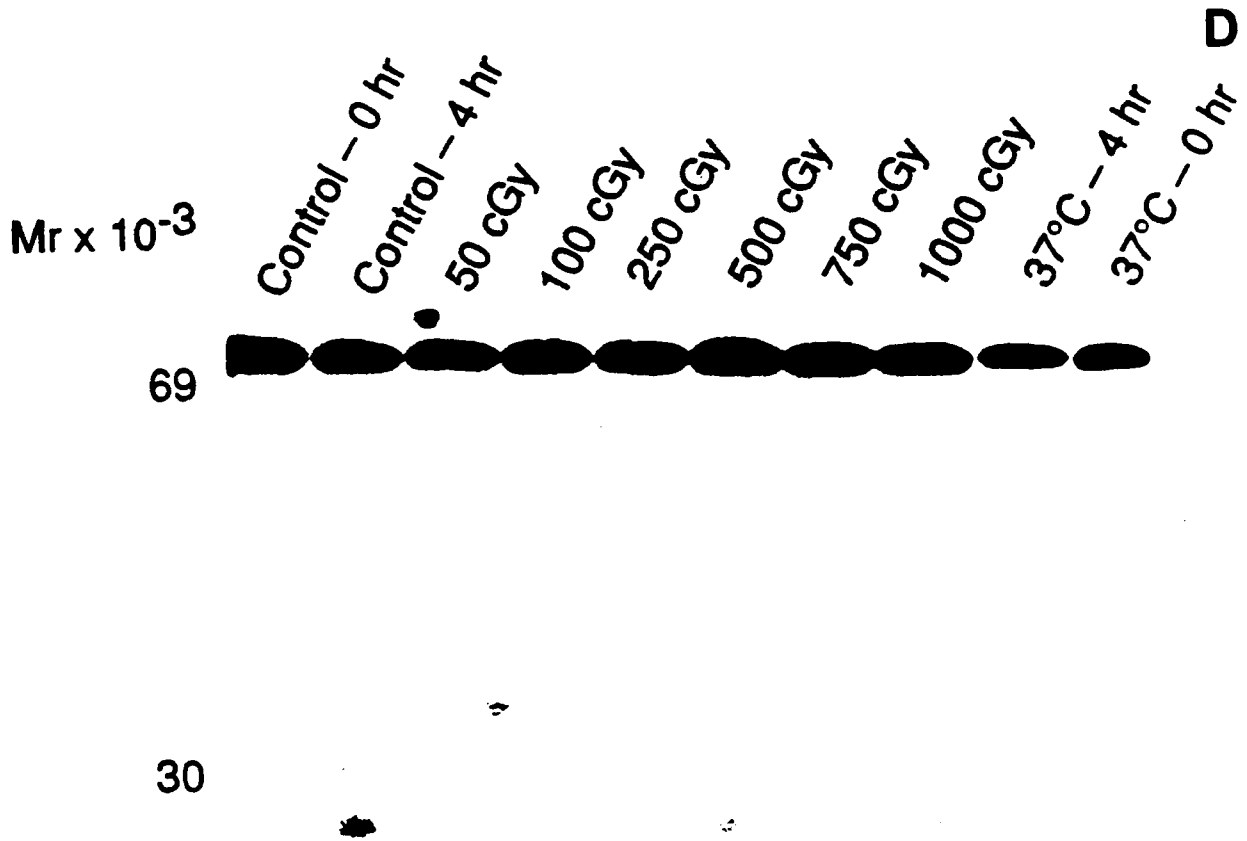
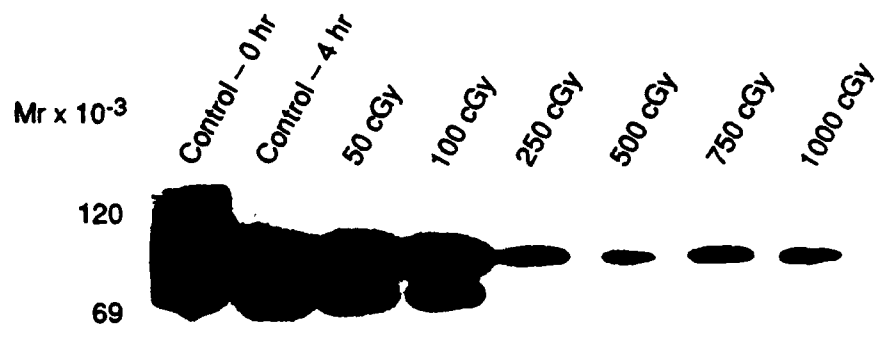


Figure 12 D The expression of HSP p70 and p27 in 244B cells 4 hour after a standard dose rate ionizing radiation exposure. The cells were irradiated immediately after a hyperthermia treatment at 42°C. Hyperthermia treatment time: 2 hours. "Control-0 hr" cells were harvested immediately after hyperthermia treatment (0 cGy). "Control-4 hr" cells were allowed to incubate for 4 hours post hyperthermia treatment (0 cGy).



30

Figure 13 The expression of HSP 90 in 244B cells after 42°C hyperthermia / 1.5 h sequentially followed by 50 cGy -1000 cGy ionizing radiation exposure.



Figure 14 Heat shock transcription factor (HSTF) gel retardation assay following hyperthermia / 1.5 h sequentially followed by standard dose rate ionizing radiation exposure. Lane 1: 37°C control; Lane 2: 42°C control; Lane 3: 42°C/250 cGy.

PART B

STUDIES OF INDUCTION OF NUCLEAR FACTOR  $\kappa$ B (NF- $\kappa$ B) AT DIFFERENT  
CELL DENSITIES AND BY LOW DOSE IONIZING RADIATION, AND INDUCTION  
OF PROTO-ONCOGENES BY LOW DOSE IONIZING RADIATION

Co-Authors: Mohan Natarajan, Ph.D.

Adapa V. Prasad, Ph.D.

Martin L. Meltz

## EFFECT OF LOW DOSE IONIZING RADIATION AND CELL DENSITY ON THE INDUCTION OF NUCLEAR FACTOR NF- $\kappa$ B AND PROTO-ONCOGENES

### BACKGROUND

#### *Biological Response to Low-Dose Ionizing Radiation*

The biological responses to eukaryotic cells to ionizing radiation have tended to focus on cell killing, DNA damage, DNA repair, chromosome damage, mutation and transformation. These phenomena are still not completely understood, although various mechanisms have been proposed (Sagan, 1989). While higher doses can cause enough alterations or destruction of biological molecules of all classes to result in cell death (including apoptosis), lower doses do less damage to DNA and other molecules and can cause mutations (Waldren et al., 1986). The cellular and molecular mechanisms involved in the regulation of these and other effects of ionizing radiation are still enigmatic. Recent studies have taken advantage of modern molecular biology techniques to examine radiation responses at a different level of biological activity. These studies have demonstrated that certain cytokines, including tumor necrosis factor- $\alpha$  (TNF- $\alpha$ , platelet derived growth factor (PDGF), fibroblast growth factor (FGF), interleukin-1 (IL-1) and "immediate early genes" (IEGs) such as the *fos/jun* family (*myc* and *ras*) (Datta et al., 1993; Hallahan et al., 1991). The events responsible for the control of these responses remain unclear. However, ionizing radiation has been postulated to induce such effects by activating the nuclear factor  $\kappa$ B (NF- $\kappa$ B) (Brach et al., 1991). The activation of transcription factors may represent a critical control point in transducing early nuclear signals to longer term changes in gene expression that reflects the response to x-induced damage.

#### *Nuclear/Factor $\kappa$ B ((NF- $\kappa$ B)*

The DNA-binding protein NF- $\kappa$ B is a pleiotropic transcription factor which induces the transcription of specific late response-genes (Baeuerle & Baltimore, 1991; Leonardo & Baltimore, 1989). It exists as a heterodimer (a p50 and p65 complex) in the cytoplasm in an inactive form, complexed to an inhibitor I $\kappa$ B. The disassociation of the heterodimer from I- $\kappa$ B precedes its translocation into the nucleus (Baeuerle & Baltimore, 1991). This event can be accomplished by PKC activation (Baeuerle & Baltimore, 1989), or ROI signalling cascade (Baeuerle & Baltimore, 1988(a); Ghosh & Baltimore, 1990; Meichle, et al., 1990). NF- $\kappa$ B recognizes and binds an 11-bp specific DNA sequence in the enhancer region of the  $\kappa$  immunoglobulin light chain (Schrek, et al., 1991). The activation of transcription factors that bind to specific DNA sequences (Mitchell & Tjian, 1989) results in transcriptional modulation, which plays a major role in the repair of DNA damage, proliferation, and other cellular functions. The study of these gene regulation pathways is of obvious importance, and experimental protocols should be designed to optimize the opportunity to observe the biological events.

#### ***Ionizing Radiation and NF- $\kappa$ B***

Previous reports of NF- $\kappa$ B expression after ionizing radiation exposure of C3 and C5 ABR lymphoblastoid cells (Staal et al., 1990) and human myeloid leukemia cells (Sen & Baltimore, 1986) involved high doses ranging from 2-50 Gy (200 to 5000 cGy) after which significant cell death will occur (Singh & Lavin, 1990). The induction has been attributed to either the activation of the protein kinase C (PKC) signalling pathway or through the reactive oxygen intermediates (ROIs) pathway (Datta et al., 1992; Hallahan, et al., 1991). Although the precise mechanism responsible for the specific gene expression is still unclear.

The majority of these studies on the induction of specific genes by ionizing radiation were associated with very high doses, in the range of 20-50 Gy (2000-5000 cGy) and dose rates above 12 Gy/min, which would result in extensive cell death and delayed progress of the cells through their cell cycle (Wyllie, 1987). There are few reports on specific gene induction at lower doses, in the range of 2 Gy and below, which is close to the level of radiation administered during a single course in fractionated or hyperfractionated radiotherapy (Eldor, et al., 1989), and which is the range where the expression of  $\alpha$ || $\beta$ 3 integrin in melanoma cells has been examined (Onodo, et al. 1992). The latter study suggested that the low doses could be interacting with the cell membrane, leading to a cellular signalling cascade.

#### ***Ionizing Radiation and Immediate Early Genes***

Studies on IEGs, particularly *c-fos/jun*, *c-myc* and *C-Ha-ras* expressions have not been examined after low dose radiation. The proto-oncogene *c-fos* is considered to be a kind of "master switch", acting as a biosensor receiving signals from the membrane receptors coupled to stimulus response, and whose gene activity is central to the cell's capacity to transform short-term responses to long-lasting responses by selective regulation of gene expression (Curran & Morgan, 1987; Turner & Tijian, 1989). The proto-oncogenes *c-fos* and *c-jun* form a hetero- and homo-dimeric complex of the "leucine-zipper" domain, and encode the activator protein-1 (AP-1) (Curran & Franza, 1988; Ranson et al., 1989). This DNA binding protein exhibits both nonspecific and sequence specific - TGA<sup>G</sup>/cTCA - (Franza, et al., 1988) DNA binding activity, and stimulates the transcription of nearby promoters by an unknown mechanism (Curran & Franza, 1988; Sheng & Greenberg, 1990; Lewin, 1991). The human *c-myc* gene is located on chromosome 8, and its activity requires hetero-oligomer-ization in its leucine-zipper domain to a partner protein which is the max DNA binding protein (Dang, 1991). The latter is reported to have a central role in apoptosis (Bissonnett et al., 1992; Evans, et al., 1992). The *c-ras* gene products are reported to be located at the inner surface of the plasma membrane (Willumsen, et al., 1984). The *c-fos/jun* heterodimers may be involved in *c-myc* regulation, and *c-Ha-ras* is reported to have effects on AP-1 activity, regulating *c-fos/jun* phosphorylation (Binetruy, et al., 1991). While *c-fos*, *c-jun* and *c-myc* play a role in the regulation of cell proliferation (Kelly & Siebenlist, 1986, Bravo et al., 1987), *c-Ha-ras* and *c-myc* have a function in cell transformation and

differentiation (Binetruy et al., 1991). These IEGs have the ability of regulating each other's expression (Barbacid, 1987). The induction of these genes is rapid and transient. In many tissues and cells in response to various stimuli (Bravo, et al., 1987), the response involves PKC activation pathway (Sherman, et al., 1990; Imler et al., 1988; Hallahan et al., 1991; Angel & Karin, 1991) and requires no new protein synthesis.

#### ***Effect of Cell Density on the Expression of NF- $\kappa$ B***

Cell density-constraints on the regulation of specific gene expression in different cells have been demonstrated (Kumatori et al., 1991; Kiel et al., 1992; Merenmies, 1992; Phillips et al., 1992; Rollins et al., 1987). For example, the expression of heparin-binding growth associated molecule (HB-GAM), which acts on cell growth and differentiation (Merenmies & Rachivala, 1990) was reported to be enhanced with increasing cell density (Merenmies, 1992). As another example, the proto-oncogenes *c-fos* and *c-myc* were reported to be differentially expressed (Kumaton et al., 1991; Kiel et al., 1992; Merenmies, 1992; Phillips et al., 1992; Rollins et al., 1987) at high cell density. Increased extracellular thiol production at high cell density was also reported in transformed RAW 264.7 mouse macrophages treated with lipopolysaccharide (LPS), and the existence of a redox stress transponding system was discussed (Toledano & Leonard, 1991). However, the mechanism(s) underlying these phenomena have not yet been determined.

#### **OBJECTIVES**

##### **The Objectives Carried Out Are The Following:**

##### ***Induction of NF- $\kappa$ B by Low Dose Ionizing Radiation***

In this report we have demonstrated that NF- $\kappa$ B expression occurs at the lower dose exposures of 0.25, 0.5, 0.75 and 1 Gy, after which cell viability is high. We also describe the time course of the NF- $\kappa$ B expression; its regulation through different signalling pathways; and its p50 and p65 subunit expression. These results were obtained in cells potentially representative of the human immune system, the Epstein-Barr virus (EBV) transformed 244B human lymphoblastoid cell line.

##### ***Induction of Immediate Early Genes by Low Dose Ionizing Radiation.***

Because of the importance of these interrelated regulatory phenomena, we have investigated the effect of low dose ionizing radiation (25-200 cGy) on *c-fos*, *c-jun*, *c-myc* and *c-Ha-ras* proto-oncogene expression and second messenger system (PKC, tyrosine kinase, Ca<sup>++</sup> channel, PKA and ROIs) signalling pathway involvement in Epstein-Barr virus (EBV) transformed 244B human lymphoblastoid cells.

##### ***High Cell Density and NF- $\kappa$ B Expression***

We also determined whether high cell density would interfere with the induction of NF- $\kappa$ B transcription factor. We have observed, and are reporting for the first time, that NF- $\kappa$ B transcription factor

expression can be drastically affected by cell density. Our data demonstrates that NF- $\kappa$ B expression is inhibited at high cell density in Epstein-Barr Virus (EBV) transformed human lymphoblastoid B cells (the 244B cell line) treated with phorbol 12-myristate 13-acetate (PMA). The time course of NF- $\kappa$ B induction was examined, as was its subunit regulation.

#### EXPERIMENTAL DESIGNS AND METHODS

##### *Reagents and chemicals:*

Phorbol 12-myristate 13-acetate (PMA), gentamicin, nifedipine, 2-amino purine, calphostin C, and N-acetylcysteine were purchased from Sigma, St. Louis, MO. Genistein was obtained from Calbiochem, La Jolla, CA. Primary antibodies to NF- $\kappa$ B subunits, rabbit anti-human NF- $\kappa$ B p50 and p65, were purchased from Santa Cruz Biotechnology, Inc., Santa Cruz, CA.

##### *Cell culture:*

EBV transformed 244B human lymphoblastoid cells (originally supplied by Dr. J. Schwartz), were cultured in complete RPMI-1640 medium containing 2mM L-glutamine and 10mM HEPES (Mediatech, Inc., Herndon, VA) and supplemented with 10% fetal bovine serum (Hyclone, Logan, UT) and 50  $\mu$ g/ml gentamicin. The cells used in these experiments were always collected at 72 h after initiation of the cell culture, when they had achieved a density of approximately  $1 \times 10^6$  cells per ml. For each experiment cell viability was determined by the trypan blue dye exclusion method; it was always  $\geq 98\%$ . The cells were transferred to fresh complete media at a cell density of  $1 \times 10^6$  cells/ml and preincubated for 30 min at 37°C in a humidified incubator with 5% CO<sub>2</sub>/95% air in T-25 flasks (Corning, Corning, NY) prior to exposure to ionizing radiation or PMA.

##### *Exposure to ionizing radiation:*

The exponentially growing cells were exposed at room temperature immediately after removal from the 37°C incubator to doses ranging from 0.25-2.0 Gy of <sup>137</sup>Cesium (<sup>137</sup>Cs) gamma rays at a dose rate of 1.17 Gy/min. The irradiations were performed in an Atomic Energy of Canada. Ltd. Gamma Cell-40 irradiator. Immediately after exposure the cultures were again incubated at 37°C in a humidified incubator and harvested at 1, 8, 16, 24, 36 and 72 h.

##### *Second messenger system inducer and inhibitors:*

In the signal transduction studies, various second messenger system inhibitors (nifedipine, 50 $\mu$ M; 2-amino purine, 9mM; calphostin C, 50nM; genistein, 2.6 $\mu$ M) and an anti-oxident (N-acetylcysteine, 30mM) were incubated with the cells for 30 min at 37°C prior to exposure to 0.5 Gy <sup>137</sup>Cs  $\Gamma$ -rays or PMA and continuously for 8 h post-exposure.

##### *Cell harvest:*

After incubation, the cells were harvested from culture medium by centrifugation for 5 min at 250xg and resuspended in phosphate buffered

saline (PBS); they were then washed twice with PBS in a microcentrifuge (Eppendorf, Model 5415C, Rotor S-45-18-11, Westbury, NY) at 14,000 rpm. The resulting pellet was stored at -70°C.

#### ***Electrophoretic Mobility-Shift Assays (EMSAs)***

Nuclear extracts were prepared from the harvested cells using a modification (Hilman et al., 1992) of the Dignam et al. protocol (Dignam, et al., 1983). Protein concentrations were determined using the bicinchonic acid (BCA) method following the manufacturer's protocol (Pierce, Rockford, IL). Fluorescence was measured with an ELISA plate reader (Dynatech MR5000, Chantilly, VA).

Electrophoretic mobility shift assay was performed using an NF- $\kappa$ B binding protein detection system following the manufacturer's protocol (Promega, Madison, WI) with slight modification. Briefly, a double stranded (ds) oligonucleotide containing a tandem repeat of the consensus sequences of -GGGGACTTTC- was end-labeled with T<sub>4</sub> polynucleotide kinase. 1  $\mu$ l of ds oligonucleotide (1.75 pmol/ $\mu$ l), 2  $\mu$ l of 10 x kmase buffer, 11  $\mu$ l of dd H<sub>2</sub>O, 10  $\mu$ l of  $\gamma$ -<sup>32</sup>P(ATP) (100  $\mu$ Ci; 3000 ci/mmol) 1  $\mu$ l of T<sub>4</sub> polynucleotide kinase was incubated at 37°C for 45 min. The reaction was stopped by adding 40  $\mu$ l of STE. Free probe was separated by push column device (strategene, La Jolla, CA). The binding reaction was performed by mixing 20  $\mu$ g of nuclear extract, 1  $\mu$ g of poly (dI-dC) (Pharmacia Fine Chemicals, Nutley, NJ), and  $\delta$ -<sup>32</sup>P (ATP) labeled oligonucleotide probe (30,000 cpm) in binding buffer (10 mM Tris-cl, pH 7.5, 100 mM NaCl, 1mM DTT, 1mM EDTA 20% (v/v) glycerol) and then incubating for 20 min at 22°C. For the competition assay the nuclear extract (20  $\mu$ g) was preincubated with homologous unlabeled NF- $\kappa$ B oligonucleotide for 5 min on ice, followed by addition of <sup>32</sup>P end-labeled NF- $\kappa$ B probe. All samples were subsequently electrophoresed through 6% polyacrylamide gel (acrylamide:bis w/w 29:1) in Tris-glycine buffer (25 mM Tris, 0.19M glycine and 1 mM EDTA). Electrophoreses was performed (at 150 V) until the time required for the free probe to migrate to the bottom of the gels (Hoefer Scientific, San Francisco, CA). The gels were dried and autoradiographed at -70°C with intensifying screens on hyperfilm (Amersham, Arlington Heights, IL).

#### ***Antibodies/Western Blotting***

The specific affinity purified rabbit polyclonal antibodies (Santa Cruz Biotechnology, Inc., Santa Cruz, CA) used in this study were (a) rabbit anti-human NF- $\kappa$ B p50 and b) rabbit anti-human NF- $\kappa$ B p65. These antibodies do not cross react with each other. Immunoblotting was carried out essentially as described by Korc, et al. (Korc et al., 1992). In brief, 30  $\mu$ g of protein samples (an aliquot of nuclear extracts prepared for EMSA) were subjected to 7.5% SDS-PAGE and were then electroblotted onto nitrocellulose membrane (Schleicher and Schuell, Keene, NH) at 30 mA overnight. Nonspecific protein binding was blocked with 10% normal goat serum (Kirkegaard & Perry Labs, Inc., Gaithersburg, MD). The membranes were then incubated for 18 h at 4°C under continuous agitation with the respective primary antibody (5  $\mu$ g/ml). After incubation, the membranes were washed with a buffer containing 20 mM Tris (pH 7.5), 500 mM NaCl and 0.05% v/v Tween-20, and

then again incubated for 2 h with goat anti-rabbit IgG (1:2500 dilution) and further incubation for 2 h with  $^{125}\text{I}$ -protein A (0.33  $\mu\text{Ci/ml}$ ; Amersham). The blots were washed, dried, and analyzed by autoradiography.

#### **Densitometric Analysis**

Autoradiograms were analyzed using a desktop digital imaging method (Griess et al., 1992). Briefly, the autoradiograms were photo-screened by standard video imaging equipment connected to a Macintosh computer (Model IICI) and analyzed using a NIH 1.45 Image Analysis software with an integrated density program. The area analyzed for each band was kept constant for all of the bands in an autoradiogram. Background density on an autoradiogram was subtracted from the densitometric data of each band.

#### **RNA isolation and Northern blot analysis**

Total cellular RNA was isolated by acid guanidinium isothiocyanate-phenol-chloroform extraction method (Chomczynski & Sacchi, 1987). The RNA was quantified spectrophotometrically (ratio of 260 to 280 nm always exceeded 1.8) and aliquots of 20  $\mu\text{g}$  of total cellular RNA were size fractionated by electrophoresis on a 0.8% agarose/2.2 M formaldehyde gel. The RNA were then electroblotted in 0.025 M phosphate buffer (pH 6.5) (New England Nuclear, Boston, MA) onto Gene Screen membrane immobilized by UV cross-linking and prehybridized for 4 h at 42°C in a buffer containing 50% formaldehyde, 0.1% SDS, 5xSSC (1xSSC=150 mM NaCl, 15mM Na Citrate, pH 7.0), 2.5 x Denhardt's (1 x Denhardt's = 0.02% polyvinyl pyrrolidone and 0.02% bovine serum albumin), 250  $\mu\text{g/ml}$  salmon sperm DNA, 50 mM  $\text{Na}_2\text{PO}_4$ , pH 6.5. The membranes were then hybridized at 42°C with specific cDNA probes in the same prehybridization buffer, supplemented with 10% dextran sulfate for at least 16 h. At the end of hybridization, the membranes were washed serially and stringently with 6 x SSPE (1 x SSPE = 150 mM NaCl, 10 mM  $\text{Na}_2\text{HPO}_4$  and 1 mM EDTA)/0.5% SDS (23°C), 1 x SSPE/0.5% SDS (55°C) and 0.1 x SSPE/0.5% SDS (57°C). The membranes were exposed at -80°C on X-ray film (X-Omat AR, Eastman Kodak) with intensifying screens.

cDNA probes: cDNA probes used in this study were as follows: (a) *c-fos*, (b) *c-jun*: a 2.6 kb EcoRI fragment (c) *c-Ha-ras*: 3.0 kb Bam HI fragment (Oncor, Gaithersburg, MD), (d) *c-myc*: a 1.4 kb EcoRI fragment (Oncor), (e) GAPDH (glyceraldehyde3-phosphate dehydrogenase) is used as an internal control. It is constitutively expressed in most tissues and is the most widely accepted internal control for assessing RNA loading and transfer. GAPDH is a 1.2 kb *pst* I (Boehringer Mannheim) with  $^{32}\text{PdCTP}$  (3000 Ci/mmol, Amersham) yielding probes with an activity of  $\sim 1 \times 10^9$  cpm.

## **RESULTS**

### **Dose response expression of NF- $\kappa$ B in low dose ionizing radiation.**

When the expression of NF- $\kappa$ B was observed at 24 hr post-exposure, it was detected at a dose of 0.25 cGy (Fig. 1). The magnitude of this induction reached a maximum at 0.5 Gy, and then decreased at the doses

of 0.75 Gy and 1 Gy. Both the PMA treated and untreated controls acted as expected, i.e., PMA treated samples exhibited a 2-fold increase in NF- $\kappa$ B expression when compared to the constitutive levels in untreated controls. Densitometric analysis revealed (Fig. 2) that the expression after 24 h at 0.25, 0.5, 0.75 and 1 Gy was 1.8, 2.8, 2.2, and 1.6-fold greater than that of the basal level expression, respectively.

***Time-course expression of NF- $\kappa$ B.***

Since the expression of NF- $\kappa$ B was found to be dose-dependent at 24 h post-incubation, we investigated the time-course of its expression after the doses of 0.5, 1 and 2 Gy. The time intervals selected included 1, 8, 16, 24, 36 and 72 h post-exposure. The data is presented in Fig. 3. When the expression at each time point after a dose was compared to the 1 hr value for that dose, NF- $\kappa$ B expression after 0.5 Gy reached its maximum (1.6-fold) at 8 h, decreased (1.2-fold) by 16 h, started increasing (1.3-fold) again at 24 h, and reached a second maximum (1.5-fold) by 36 h; it was at this same level at 72 h. After the 1 and 2 Gy exposures the expression increased equally to a maximum (1.2-fold) at 16 h. After the 1 Gy exposure, it was decreased at 24 h and again increased (1.2-fold) at 36 h, with a decrease at 72 h. After the 2 Gy exposure, the expression was decreased at 24 h, but continued decreasing to a minimum at 36 h; it again rose to its maximum (1.2-fold) at 72 h. The level of expression is clearly time dependent after all three doses.

When the fold comparison was made from the densitometric analysis between the doses, at each time point, the greatest expression was observed after a dose of 0.5 Gy at any given time post-exposure. The expression after 1 Gy was 1.2 and 1.4-fold greater than that of 2 Gy at 8 and 36 h respectively. The expression for 2 Gy was 1.2-fold greater than that of 1 Gy at 24 h and 72 h respectively. The controls exhibited a downward trend as the time increases (data not shown).

***Dose-dependent response of NF- $\kappa$ B subunits p65 and p50.***

Since the previous data revealed the maximum presence of NF- $\kappa$ B at 8 hr after a 0.5 Gy exposure, this time was selected to investigate the expression of the NF- $\kappa$ B subunits p65 and p50 using western blot analysis. The results after exposures of 0.25, 0.5, 1 and 2 Gy (along with unexposed controls) are shown in Figure 4. The expression of both NF- $\kappa$ B subunits in the control was low but detectable. The expression of the p65 subunit after 0.25 Gy was 2.3-fold the control value, was maximum (6.7-fold) after 0.5 Gy, was lower (3-fold) after 1 Gy and was at the control level after 2 Gy. The expression of the p50 subunit exhibited a 4-fold greater response than control after 0.25 Gy, it was maximum (8.8-fold) after 0.5 Gy, and was lower (3-fold) after 1 Gy. In contrast to the p65 subunit response, it again showed a profound increase (6.8-fold) after 2 Gy. When the comparison of the densitometric analysis was made for the expression of p50 and p65, at each dose, the expression of p50 was 1.6, 1.3, 8.3-fold increased over p65 for the doses of 0.25, 0.5 and 2 Gy, respectively. In contrast,

their response after 1 Gy was equal. In the control, both subunits were equally expressed at the constitutive levels (Fig. 5).

**Signal transduction of NF- $\kappa$ B expression after a 0.5 Gy exposure, and comparison to PMA induction.**

The signalling pathway involved in the induction of NF- $\kappa$ B expression at 8 h post-exposure after the dose of 0.5 Gy, and also in PMA treated cells, was studied by using inhibitors for various signalling agents. Our observations are presented in Figure 6A for the PMA treated cells, and Figure 6B for the irradiated cells. For the former, the data shows the inhibition of PMA-induced NF- $\kappa$ B expression by nifedipine (lane 3), calphostin C (lane 5), and genistein (lane 7) when compared to that of PMA-only treated control. The PMA-only treated positive control is shown in lane 1. The expression in NAC (lane 4) and 2-amino purine (lane 6) treated cells was not inhibited. In the irradiated cells, the expression was inhibited only after treatment with calphostin C (lane 4) and genistein (lane 6); it was not inhibited in nifedipine, NAC and 2-amino purine treated samples (lanes 2,3 and 5, respectively). All the samples were run in the same gel and at the same time. Thus, the present data reveal that only PKC and tyrosine kinase were involved in mediating the expression of NF- $\kappa$ B induced after 0.5 Gy, while calcium channels, in addition to PKC and protein tyrosine kinase, were involved in PMA induced NF- $\kappa$ B expression. The densitometric analysis demonstrated that the NF- $\kappa$ B expression in the irradiated cells was reduced 4-fold and 3-fold in calphostin C (lane 5) and genistein (lane 7) treated cells respectively. In PMA treated cells, the expression was reduced 1.7-, 1.3- and 1.9-fold in nifedipine (lane 3), calphostin C (lane 5) and genistein (lane 7) respectively.

**Induction of Immediate Early Genes by Low Dose Ionizing Radiation:**

Since there is a maximum induction of expression of the DNA binding protein NF- $\kappa$ B, at any given time of incubation post-exposures occurred at the dose of 0.5 Gy, we therefore investigated the induction of *c-fos*, *c-jun*, *c-myc* and *c-Ha-ras* after 0.5 Gy, as a function of incubation time post-exposure (0.25, 0.5, 1,2,4,8,12 and 16 h). The data is summarized in Figure 8. It demonstrates this low dose does induce all four proto-oncogenes, and that the maximum induction of all four occurred at 1 h post-exposure. For *c-fos*, the induction is rapid and profound at 1 h, and disappeared by 2 h. For *c-jun*, the expression started at 0.5 h, reached its maximum at 1 h, was decreased at 2 h and had reappeared at 16 h. The induction of *c-myc* and *c-Ha-ras* expression followed the same pattern as that of *c-jun*. The expression of the housekeeping gene GAPDH, which served as a control, was approximately the same at all of the incubation times studied. Since we had observed that 1 h is the maximal response time after the dose of 0.5 Gy for the oncogenes studied, we have further investigated the dose-dependence of their induction at 1 h for the doses of 0.25, 0.5, 0.75, 1 and 2 Gy, along with PMA treated positive and untreated controls. The data is presented in Figure 9. Detectable levels of all four early genes studied were observed in negative controls ("constitutive levels").

The maximum induction of mRNA expression for *c-jun*, *c-myc* and *c-Ha-ras* was at 0.5 Gy dose; for *c-fos*, however, it was at the lower dose of 0.25 Gy. The induction of *c-fos* then decreased in a dose-dependent manner; decreased at 0.75 Gy, while at 1 Gy (and also 2 Gy) it was at basal levels. The expression of *c-jun* and *c-myc* followed identical patterns, i.e., decrease in expression from 0.75 Gy thereby stabilizing at 1 and 2 Gy. Whereas for *c-Ha-ras* the induction was in dose-dependent manner increasing from 0.25 Gy maximum at 0.5 Gy and at .75 Gy reaching levels equivalent to .25 Gy revealing basal level expression at 1 Gy and again reinduction at 2 Gy.

Indeed, the present data has demonstrated that the maximum level of expression for all the four early genes studied was at 1 h and at the dose of 0.5 Gy except for *c-fos* where the dose was at 0.25 Gy. Hence, we have investigated their signalling pathway by using various signalling inhibitors at 1 h for the dose of 0.5 Gy along with that of PMA administered samples. PMA alone and 0.5 Gy alone treated samples without signal transduction inhibitors were used as positive controls respectively for their inhibitor response studies. The data is presented in Figure 10. The data has demonstrated unequivocally that the tyrosine kinase regulation was required for the induction of all four early oncogenes studied in either PMA or 0.5 Gy treated samples. However, several specific signalling pathways were observed for different protooncogenes. For *c-fos* NAC and genestein have inhibited its expression for PMA treated samples suggesting the role of ROIs and tyrosine kinase, but with 0.5 Gy samples nifedipine, calphostine and genestein have inhibited its expression suggesting a role for calcium, PKC and tyrosine kinase.

For *c-jun* expression in PMA treated samples nifedipine and genestein have inhibited its expression suggesting the roles of calcium and tyrosine kinase but not ROIs and PKC. But in 0.5 Gy, NAC and genestein have more inhibitory capacity than nifedipine and calphostine in *c-myc* expression, suggesting that the pathways for both *c-jun* and *c-myc* were similar. However, for *c-Ha-ras* induction, only genestein has inhibited its expression in PMA samples, whereas in 0.5 Gy administered samples nifedipine and genestein have inhibited its expression suggesting a role for tyrosine kinase through calcium channel openings. Thus the whole phenomenon was different for different early genes studied and also behaves differently with PMA and ionizing radiation modulation of IEGs induction.

#### ***Dependence of NF- $\kappa$ B expression on cell density***

The expression of NF $\kappa$ B at 24 h after initiating PMA treatment was investigated using electrophoretic mobility-shift assay (EMSA). The results for PMA treated or untreated 244B cells are shown in Figure 11. The expression was obviously decreased as the cell density was increased. The maximum response was observed at the cell density of  $1 \times 10^6$  cells/ml, and expression was greatly reduced at  $2.5 \times 10^6$  cells/ml and  $5 \times 10^6$  cells/ml. Results from the densitometric analysis are shown in Figure 12. Detectable and equal levels of expression were found in non-PMA treated controls at all cell densities. The response at  $1 \times 10^6$

cells/ml was a 1.9-fold increase over its corresponding non-PMA treated control, while the expression at  $2.5 \times 10^6$  cells/ml and  $5 \times 10^6$  cells/ml was only 1.2-fold greater than their respective non-PMA stimulated controls respectively.

#### *Kinetics of NF- $\kappa$ B expression at different cell densities*

While the NF- $\kappa$ B expression was maximal for  $1 \times 10^6$  cells/ml when assayed at 24 h of exposure to PMA, time course studies for NF- $\kappa$ B expression were done by EMSA for all three cell densities. This allowed us to determine whether NF- $\kappa$ B expression occurred at either earlier or later times at the higher cell densities. Cells were collected for analysis at 1, 8, 16, 36 and 72 h of incubation with PMA; untreated control cells at a density of  $1 \times 10^6$  cells/ml were assayed at the same time points (Fig. 13). For the non-PMA treated controls, an increase in NF- $\kappa$ B expression was observed; it was directly proportional to the incubation time. At each incubation time, the NF- $\kappa$ B expression in the PMA-treated cells was compared to that of the non-PMA treated control cells incubated at  $1 \times 10^6$  cells/ml. The PMA-induced NF- $\kappa$ B expression at the  $1 \times 10^6$  cells/ml density at 8 h was the highest level for all three cell densities and incubation times, a 3.5-fold increase, and gradually decreased to 1.2-fold at 36 h of incubation. At 72 h, the expression was increased slightly to 1.4-fold. The expression of PMA induced NF- $\kappa$ B at the cell densities of 2.5- and  $5 \times 10^6$  cells/ml was maximal at 16 h, a 2-fold increase. The expression at the  $2.5 \times 10^6$  cells/ml density was only slightly decreased at 36 h and 72 h, while at the  $5 \times 10^6$  cells/ml density, the expression started decreasing at 36 h and was at a minimum at 72 h. At the 8 h incubation where the maximum PMA induced expression was observed for  $1 \times 10^6$  cells/ml, the trend in the expression response was  $1.0 > 2.5 > 5.0 > 1 \times 10^6$  cells/ml. The responses at 16 h for all three densities were very similar (2-fold), while at 36 h of incubation the response trend was  $2.5 > 5.0 > 1.0 \times 10^6$  cells/ml (1.9-fold; 1.7-fold; 1.3-fold). The trend remained the same at 72 h. If one looked as early as 1 h of incubation time, the trend in the expression response was  $1 > 5.0 > 2.5 \times 10^6$  cells/ml (3.2-fold; 2.7-fold; 2.4-fold). Furthermore, unstimulated controls showed an increase in NF- $\kappa$ B-DNA binding activity with increasing time in culture at a cell density starting with  $1 \times 10^6$  cells/ml. DNA binding activity was found to be a 2-fold increase compared to 1 h culture. Similarly, at 72 h culture it was doubled, compared to 36 h. The induction of NF- $\kappa$ B-DNA binding activation was correlating very well with cell cycle. The population doubling time of 244B cells under our standard growth conditions was 33-36 h. However, the situation was different when the cells were stimulated with DNA with a starting cell density of  $1 \times 10^6$  cells/ml. There was a transient increase at 8 h culture and started decreasing with time, whereas at an initial cell density of  $2.5 \times 10^6$  cells/ml there was a gradual increase with time. At a starting cell density of  $5.0 \times 10^6$  cells/ml, although the DNA binding activity was found to be less at all time points compared to 1 and  $2.5 \times 10^6$  cells/ml, there was a time-dependent increase similar to unstimulated cells. Specific bands were confirmed by preincubating the samples with cold oligonucleotide before adding  $^{32}$ P-labeled probe as described in

**Experimental Methods.** However, these experiments have to be repeated with negative controls (unstimulated cells) at respective cell densities (1, 2.5 and  $5 \times 10^6$ /ml) at all time points. These controls have to be used to determine fold increase of NF- $\kappa$ B binding activity.

Two discrete complexes were seen in both unstimulated as well as in PMA stimulated 244B cells. The more rapidly migrating complex may contain the p50 and p55 or p50 and p60 proteins, whereas the slower migrating complex contains p50, p55, p75 and p85 proteins. However, these protein complexes have to be confirmed by preincubating the samples with respective antibodies before adding specific oligo probe.

**Expression of NF- $\kappa$ B subunit p50 and p65 at different cell densities**

Since the expression of NF- $\kappa$ B was found to be maximal at 8 h for the  $1 \times 10^6$  cells/ml density with respect to that of any other time and cell density, NF- $\kappa$ B subunit p50 and p65 regulation was investigated using their respective antibodies and western blot analysis at 8 h for all three PMA treated densities. Non-PMA treated cells incubated at  $1 \times 10^6$  cells/ml served as a negative control. The results (Fig. 14) demonstrate the abundance of the p50 subunit of NF- $\kappa$ B at the  $1 \times 10^6$  cells/ml density; its presence was low at  $5 \times 10^6$  cells/ml density. In contrast, the p65 subunit was abundant but unaltered in all three cell densities. The expression of p50-p65 complex was maximal (9-fold) at  $1 \times 10^6$  cells/ml density and minimum (6-fold) at  $5 \times 10^6$  cells/ml in comparison to that of controls. At  $2.5 \times 10^6$  cells/ml density, the increase in expression was 7.8-fold.

**DISCUSSION**

**Induction of NF- $\kappa$ B by Low Dose Ionizing Radiation**

To our knowledge, these results are the first demonstration of the induction of transcription factor NF- $\kappa$ B expression after low doses of ionizing radiation 0.25-2Gy, where cell viability remains high up to 120 h post-exposure (Schneider et al., in preparation). This low dose response pattern was similar to that reported by Onada, et al. (Onada et al., 1992), in which they demonstrated that the  $\gamma$ -radiation induced expression of  $\alpha$ ||bB3 (needs correcting) integrin in melanoma cells exposed to 0.25-2.5 Gy and that it was maximum at 0.5 Gy. Although there are two reports (Singh & Lavin, 1990; Brach et al., 1991) regarding the induction of NF- $\kappa$ B expression by ionizing radiation, both examined the induction after doses ranging from 2-50 Gy (200-5000 cGy), which would likely lead to high cell death (Rauth, 1987). Second, the time course studies of NF- $\kappa$ B expression have demonstrated that the expression is time dependent for the three different doses studied. It was a maximum after 0.5 Gy at 8 h in the first phase and at 36 h in a second phase of expression. After 1 and 2 Gy exposures the maximum expression occurred at 16 h in the first phase and again at 36 h and 72 h, respectively, in a second phase. Our results at these low doses do not correlate with that of two earlier reports (Singh & Lavin, 1990; Brach et al., 1991) in which the maximum induction occurred by 4 h and returned to constitutive level by 6 or 12 h. However, those studies

were done after doses in a highly lethal dose range. Our data is similar to a report (Neumann et al., 1991) which could be considered a biological positive control, in which the maximal induction of NF $\kappa$ B was demonstrated after (TPA) treatment at 8 or more hours. Moreover, our study revealed that the maximum induction of NF $\kappa$ B at any given time post-exposure is at the dose of 0.5 Gy in comparison to 1 and 2 Gy.

#### *Signal Transduction*

We have demonstrated using inhibitors, that the induction of NF- $\kappa$ B expression by ionizing radiation at the low dose of 0.5 Gy requires protein kinase C, as well as tyrosine kinase, but not sequestration channel in the cell membrane, and also not reactive oxygen intermediation. The data from our signal transduction studies, using inhibitors, has demonstrated that both PKC and tyrosine kinase mediate NF- $\kappa$ B expression at 0.5 Gy. This phenomenon can therefore be differentiated from PMA induction, which requires in addition, calcium sequestration channel function. This leaves open the possibility that the 0.5 Gy response might be regulated by the release of internal stores of Ca<sup>++</sup>.

#### *Ionizing Radiation and NF- $\kappa$ B Subunit p65 and p50 Expression*

We have demonstrated the differential regulation of NF- $\kappa$ B subunit p65 and p50 expression after low dose ionizing radiation. The present data on the dose-dependent response of NF- $\kappa$ B subunit (p65 and p50) expression can be examined in light of the known mechanism of the regulation of NF- $\kappa$ B (Friedman et al., 1992). We propose that the maximum response after a dose of 0.5 Gy of ionizing radiation (as well as after 0.25 Gy) is similar to the known mechanism, disassociating the I $\kappa$ B-p65 complex by certain specific pathways, releasing the active p65 to translocate into the nucleus for the DNA binding activity. In contrast, after doses of 1 and 2 Gy, the radiation does not appear to have the signalling pathways which cause the complex to disassociate. In contrast, p50, which is relatively the inactive dimer and requires phosphorylation to disassociate itself from its precursor p105 on the I- $\kappa$ B carboxy-terminus (Friedman et al., 1992; Baeuerle, 1991) was observed to be expressed at all four doses studied. Thus, our subunit data is consistent with the EMSA data (Fig. 1), wherein both p50 and p65 hetero dimer expression could be involved in the DNA binding activity at its maximum, but where the reduced DNA binding activity observed at the 1 and 2 Gy doses is associated mainly with the reduced p65 subunit presence.

It has been suggested that low dose ionizing radiation can interact at the membrane receptor level (Friedman et al., 1986), crosslinking the surface immunoglobulin IgM (Rooney et al., 1992). We suggest that such a phenomenon in turn could activate the NF- $\kappa$ B transcription factor through PKC and tyrosine kinase signalling pathways. In summary, this data has demonstrated for the first time that low dose ionizing radiation modulates NF- $\kappa$ B DNA binding activity through protein kinase C and tyrosine kinase signalling pathways, with the p65 subunit activation being most closely linked to the NF- $\kappa$ B DNA binding activity. This modulation is dependent on the post-exposure time at which the

cells are harvested. In addition, we have established an ionizing radiation signalling response which differs from the well recognized PMA type response.

#### ***High Cell Density Stress and NF- $\kappa$ B Expression***

Recent investigations have demonstrated that certain growth factors such as HB-GAM (Morenmies, 1992) and proto-oncogenes such as c-fos and c-myc, which were regulated by various stimuli (Kumatori et al., 1991; Phillips et al., 1992; Rollins et al., 1987) exhibit cell density-dependent modulation. The expression of HB-GAM in Balb/c 3T3 cells was augmented at high cell density and was reduced when the cells were treated with basic fibroblast growth factor (bFGF) (Morenmies, 1992). Similarly, c-fos induction was profound upon PDGF stimulation at high cell density (Rollins et al., 1987). In contrast, the expression of c-myc was reported to be inversely proportional to the cell density in both rat hepatocytes (Kumatori et al., 1991) and platelet derived growth factor (PDGF) induced Balb/c 3T3 cells (Rollins et al., 1987).

The present data in 244B human lymphoblastoid cells represent the first demonstration of cell density dependent regulation of transcription factor NF- $\kappa$ B DNA binding activity. Investigators use various cell densities, suitable to their laboratory needs and conditions, to obtain their scientific data. The present study achieves considerable significance in that it shows that the NF- $\kappa$ B transcription factor regulation depends on the density of the cells during the induction period and that the results will depend on the time of incubation at which the assay was performed. Our results revealed that in PMA treated 244B cells, NF- $\kappa$ B expression was maximum at 8 h at a density of  $1 \times 10^6$  cells/ml, a density in the range of rapid growth in exponentially growing cultures. At this time (8 h), there was less expression at  $2.5 \times 10^6$  cells/ml, which was at or just beyond the maximum cell density that the 244B cells will normally grow to, and it is minimal at a density of  $5 \times 10^6$  cells/ml, a density not usually reached by these cells when in continuous growth (Holahan et al., 1991). Mechanistically, these results can be considered in light of the recent observation (Kiel et al., 1992) of increased thiol production at a cell density of  $5 \times 10^7$  cells/ml in LPS treated transformed mouse macrophages (RAW 264-7), because if increased thiol production were to occur in the 244B cells at  $5 \times 10^6$  cells/ml, it could decrease the release of reactive oxygen intermediates (ROIs) and thus inhibit the expression of NF- $\kappa$ B (Staal et al., 1990). The cells employed in the present study were in asynchronous growth before being incubated with PMA at different cell densities. Since cell growth would likely be arrested at high cell density, and since the expression of specific genes is dependent on the cell cycle phase in which cell growth was arrested (Kumatori et al., 1991; Rollins et al., 1987), our results may in part be due to cell cycle redistribution and phase specific synthesis of NF- $\kappa$ B (if this occurs in the 244B cells). Our other data regarding the kinetics of NF- $\kappa$ B expression indicate a reappearance of the NF- $\kappa$ B at high cell density after an earlier decrease (an increase between 36 and 72 h (data not shown); this could be due to such a cell cycle redistribution.

The present data on cell density dependent NF- $\kappa$ B subunit regulation is in good agreement with other published observations (Baeuerle & Baltimore, 1991; Angel et al., 1988; Baeuerle & Baltimore, 1989) which demonstrated the need for both p50 and p65 subunits in complex to activate the NF- $\kappa$ B DNA binding activity. We observed that the NF- $\kappa$ B subunit p50 available in the nucleus is modulated by the cell density, decreasing with increased cell density, whereas the p65 subunit available in the nucleus was unaltered with increasing cell density. It is widely accepted that the NF- $\kappa$ B DNA binding activity requires the disassociation of inactive I- $\kappa$ B in the cytoplasm prior to the translocation of the p65-p50 heterodimer into the nucleus (Baeuerle & Baltimore, 1988; Baeuerle & Baltimore, 1988(a), Baeuerle & Baltimore, 1989). The presence of the heterodimer in the nucleus was greatest at the lowest cell density and lowest at the highest cell density. This could be due to the high cell density stress release "a factor" (Kiel et al., 1992), denoted ADF (Wakasugi et al., 1990), that could inhibit the disassociation of p50-p65 complex from I- $\kappa$ B. At the same density at which the heterodimer availability in the nucleus was lowest, the p50 subunit availability was lowest. UV cross-linking studies with these proteins will be required to examine a direct relationship.

In summary, our data revealed that PMA treated EBV transformed 244B human lymphoblastoid cells at high cell density down regulated induced transcription factor NF- $\kappa$ B expression and that this is likely due to the reduction in the expression of the p50-p65 complex; it is very much dependent on the time at which the cells are harvested for assay. The extent of induction of NF- $\kappa$ B and its subunit regulation is important and may play a vital role in cell signalling processes. Our results emphasize that different conclusions may be drawn from laboratories assaying the same biological endpoint at different times and cell densities.

## References:

- Angel, P., Allegretto, E.A., Okino, S.T., Haftori, K., Boyle, W.J., Hunter, T. and Karin, M. (1988) Oncogene *jun* encodes a sequence-specific transactivator similar to AP-1. *Nature* 332, 166-171.
- Angel, P., and Karin, M. (1991) The role of *jun*, *fos* and the AP-1 complex in cell proliferation and transformation. *Biochem. Biophys. Acta* 1072, 129-157.
- Baeuerle, P.A. & Baltimore, D. (1991) In: Hormonal control regulation of gene transcription (Cohen, P. and Foulkes, J.G., eds.) *Mol-Aspects Cell. Regul. Vol. 6*, pp409-432, Elsevier, Amsterdam, New York.
- Baeuerle, P.A. and Baltimore, D. (1989) A 65-KD subunit of active NF- $\kappa$ B is required for inhibition of NF- $\kappa$ B by I $\kappa$ B. *Genes Dev.* 3, 1689-1698.
- Baeuerle, P.A. and Baltimore, D. (1988a) A specific inhibitor of the NF- $\kappa$ B transcription factor. *Science* 241, 1652-1655.
- Baeuerle, P.A. and Baltimore, D. (1988) Activation of DNA-binding activity in an apparently cytoplasmic precursor of the NF- $\kappa$ B transcription factor. *Cell* 53, 211-217.
- Baeuerle P.A. (1991) The inducible transcription activator NF- $\kappa$ B: regulation by distinct protein subunits. *Biochem. Biophys. Acta* 1072, 63-80.
- Barbacid, M. (1987) *ras* genes. *Ann. Rev. Biochem.* 56, 779-827.
- Bin'etruy B., Smeal, T. and Karin, M. (1991) Ha-ras augments c-jun activity and stimulates phosphorylation of its activation domain. *Nature* 351, 122-127.
- Bissonnette, R.P., Echeverri F., Mahbo-Ubi, A. and Green, D.R. (1992) Apoptotic cell death induced by c-myc is inhibited by *bel-2*. *Nature* 359, 552-554.
- Brach, M.A., Hass, R., Sherman, M.L., Gunji, H., Weichselbaum, R.R. & Kufe, D.W. (1991) Ionizing radiation induced expression and binding activity of the nuclear factor  $\kappa$ B. *J. Clin. Invest.* 28:691-695.
- Bravo, R., Neubergh, M., Burckhardt, J., Almendral, J., Wallich, R. and Muller, R. (1987) Involvement of common and cell type-specific pathways in c-fos gene control: stable induction by cAMP in macrophages. *Cell* 48, 251-260.
- Chomezynsky, P. and Sacchi, N. (1987) A single-step method of RNA isolation by acid guanidinium thiocyanate-phenol-chloroform extraction. *Anal. Biochem.* 162, 156-159.

Curran, T. and Franza, B.R. (1988) Fos and jun: the AP-1 connection. Cell 55, 395-397.

Curran, T. In the Oncogene Handbook, E.P. Reddy, A.M. Skalla, T. Curran, eds. (Elsevier, Amsterdam 1988), pp 307-325.

Dang, C.V., Barrett, J., Villa-Garcia, Resar, L.M., Kato, G.J. and Fearon, E.R. (1991) Intracellular leucine zipper interactions suggests c-myc hetero-oligomerization. Mol. Cell Biol. 11, 954-962.

Datta, R., Hallahan, D.E., Kharbanda, S.M., Rubin, B., Sherman, M.L., Huberman, E., Weichselbaum, R.R. & Kufe, D.W. (1992) Involvement of reactive oxygen intermediates in the induction of c-jun gene transcription by ionizing radiation. Biochem. 31, 8300-8306.

Dignan, J.P., Lebovitz, R.M. and Roeder, R.G. (1983) Accurate transcription initiation by RNA polymerase II in a soluble extract from isolated mammalian nuclei. Nucleic Acids Res. 11, 1475-1489.

Eldor, et al. (1989) A novel spatial transcription pattern associated with the segmentation gene, giant, of drosophila.

Franza, B.R., Rauscher, F.J., Josephs, S.F., and Curran, T. (1988) The fos complex and fos-related antigens recognize sequence elements that contain AP-1 binding sites. Science 239, 1150-1153.

Friedman, M., Saunders, D.S., Madden, M.C., Chaney, E.L. and Kwock, L. (1986) The effect of ionizing radiation on the pulmonary endothelial cell uptake of  $\alpha$ -aminoisobutyric acid and synthesis of prostacyclin. Radiat. Res. 106, 171-181.

Ghosh, S. and Baltimore, D. (1990) Activation in vitro of NF-Kappa B by phosphorylation of its inhibitor I $\kappa$ B. Nature 344, 678-682.

Griess, G.A., Moreno, E.T. and Serwer, P. (1992) In: Desktop digital imaging (Biomeister, M. and Ulanovsky, L. eds) Methods in Mol. Biol. Vol 12, pp173-181, Humana, Totowa, New Jersey.

Hallahan, D.E., Sukhatme, V.P., Sherman, M.L., Virudachalam, S., Kufe, D.W. & Weichselbaum, R.R. (1991) Protein kinase C mediates X-ray inducibility of nuclear signal transducers. EGR1 and Jun, Proc. Natl. Acad. Sci. USA 88:2156-2160.

Hilman, K., Jiahua, G., Siegel, J.N., Rodriguez, G., Blackburn, R., Manischewitz, J., Norcross, M. and Gelding, H. (1992) Reduced susceptibility to HIV-1 infection of ethyl-methanesulfonate-treated CEM subclones correlates with a blockade in their protein kinase C signaling pathway. J. Immunol. 148, 3991-3998.

- Holahan, P.K., Eagan, P. and Meltz, M.L. (1991) Hyperthermic effects on viability and growth kinetics of human lymphoblastoid cells. *Int. J. Hyperthermia* 7, 849-856.
- Imler, J.L., Ugarte, E., Wasylyk, C. and Wasylyk, B. (1988) v-jun is a transcriptional activator, but not in all cell lines. *Nucleic acids Res* 16, 3005-3012.
- Korc, M., Chandrasekar, B., Yamanaka, Y., Friess, H., Puechler, M. and Beger, H.G. (1992) Overexpression of the epidermal growth factor receptor in human pancreatic cancer is associated with concomitant increases in the levels of epidermal growth factor and transforming growth factor alpha. *J. Clin. Invest.* 90:1352-1360.
- Kumatori, A., Nakamura, T. and Ichihara, A. (1991) Cell density dependent expression of the c-myc gene in primary cultured rat hepatocytes. *Biochem. Biophys. Res. Commun.* 178, 480-485.
- Leonardo, M.J. and Baltimore, D. (1989) A pleiotropic mediator of inducible and tissue-specific gene control. *Cell* 58, 227-229.
- Meichle, A., Schutze, S., Hensel, G., Brunsing, D. & Kronke, M. (1990) Protein kinase C-dependent activation of nuclear factor  $\kappa$ B by tumor necrosis factor. *J. Biol. Chem.* 265, 8339-8343.
- Mitchell, P.J. & Tjian, R. (1989) Transcriptional regulation in mammalian cells by sequence-specific DNA binding proteins. *Science* 245, 371-378.
- Onoda, J.M., Piechocki, M.P. and Honn, K.V. (1992) Radiation-induced increase in expression of the  $\alpha_{v}\beta_{3}$  integrin in melanoma cells: effects on metastatic potential. *Radiat. Res.* 130, 281-288.
- Ransone, L.J., Visvader, J., Sassone-Corisi, P., Verma, I.M. (1989) Fos-jun interaction: mutational analysis of the leucine zipper cloning of both proteins. *Gene Dev.* 3(6), 770-781.
- Rauth, A.M. (1987) Radiation carcinogenesis. In: *Basic Science of Oncology*. I.F. Tannock and R.P. Hill, ed., Pergamon Press, Inc., Elmsford, N.Y. 106-124.
- Rollins, B.J., Morrison, E.D. and Stiles, C.D. (1987) A cell-cycle constraint on the regulation of gene expression by platelet derived growth factor. *Science* 238, 1269-1271.
- Rooney, J.W., Dubois, P.M. and Sibley, C.H. (1992) Cross-linking of surface IgM activates NF- $\kappa$ B in B lymphocyte. *Eur. J. Immunol.* 21, 2993-2998.
- Sagan, L.A. (1989) On radiation, paradigms, and hormesis. *Science* 11:245, 574 & 621.

Schrek, R., Rieber, P. & Baeuerle, P.A. (1991) Reactive oxygen intermediates as apparently widely used messengers in the activation of the NF $\kappa$ B transcription factor of HIV-1. *EMBO J.* 10, 2247-2258.

Sen, R. & Baltimore, D. (1986) Inducibility of Kappa immunoglobulin enhancer-binding protein NF-Kappa B by a post-translational mechanism. *Cell* 47, 921-928.

Sherman, M.L., Datta, R., Hallahan, D.E., Weichselbaum, R.R. & Kufe, D.W. (1990) Ionizing radiation regulates expression of the c-jun protooncogene. *Proc. Natl. Acad. Sci. USA* 87, 5663-5666.

Singh, S.P. & Lavin, M.F. (1990) DNA binding protein activated by gamma radiation in human cells. *Mol. Cell. Biol.* 10, 5279-5285.

Staal, F.J., Roederer, M., Herzenberg, L.A. and Herzenberg, L.A. (1990) Intracellular thiols regulate activation of nuclear factor Kappa B and transcription of human immunodeficiency virus. *Proc. Natl. Acad. Sci. USA*, 87, 9943-9947.

Turner, R. and Tjian, R. (1989) Leucine repeats and an adjacent DNA binding domain mediate the formation of functional c-fos - c-jun heterodimers. *Science* 243, 1689-1694.

Wakasugi, N., Tagaya, Y., Wakasugi, H., Mitsui, A., Michiyuki, M., Yodoi, J. and Tursz, T. (1990) Adult T-cell leukemia-derived factor/thioredoxin, produced by both human T-lymphotropic virus type I- and Epstein-Barr virus-transformed lymphocytes, acts as an autocrine growth factor and synergizes with interleukin 1 and interleukin 2. *Proc. Natl. Acad. Sci. USA* 87, 8282-8286.

Waldren, C., Correll, L., Sognier, M.A., Puck, T.T. (1986) Measurement of low level X-ray mutagenesis in relation to human doses. *Proc. Natl. Acad. Sc. USA* (13):4839-4843.

Williamsen, B., Christensen, A., Hubbert, N.L., Papageorge, A.G. and Lowry, D.R. (1984) The p21 ras C-terminus is required for transformation and membrane association. *Nature* 310, 583-586.

Wyllie, A.H. (1987) Apoptosis: cell death in tissue regulation. *J. Pathol.* 153, 313-316.

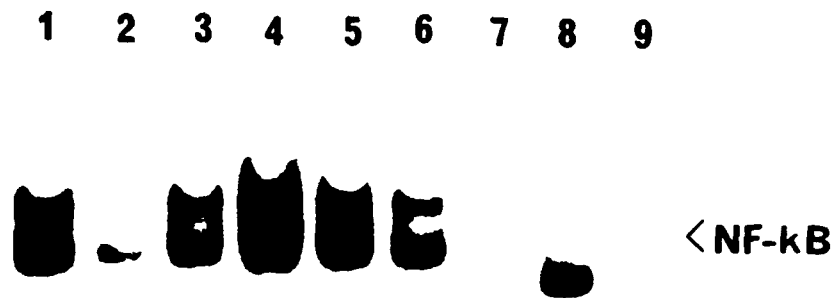


**Figure 1:** Dose dependent activation of NF- $\kappa$ B by low dose ionizing radiation. Electrophoretic mobility-shift assay was performed by incubating the nuclear protein (20 $\mu$ g) obtained from 24 h culture of 244B cells with g-<sup>32</sup>P (ATP) labeled (30,000 cpm) NF- $\kappa$ B specific ds-oligonucleotide on 6% poly acrylamide gel. Autoradiogram of native gel is shown. Lanes 1 & 2: Nuclear extract derived from the cell in the presence (lane 1) or absence (lane 2) of PMA; Lanes 3-6: Nuclear extract derived from the cells exposed to 0.25 Gy (lane 3), 0.5 Gy (lane 4), 1.0 Gy (lane 5) and 2.0 Gy (lane 6) exposure; Lane 7: Nuclear extract (20 $\mu$ g) was preincubated with homologous unlabeled NF- $\kappa$ B specific ds-oligonucleotide competitor for 5 min on ice followed by the addition of <sup>32</sup>P end labeled NF- $\kappa$ B probe. Lane 8: Hela cell extract as positive control; and Lane 9 shows free probe. Complexes tested for specific binding are indicated by arrowhead.

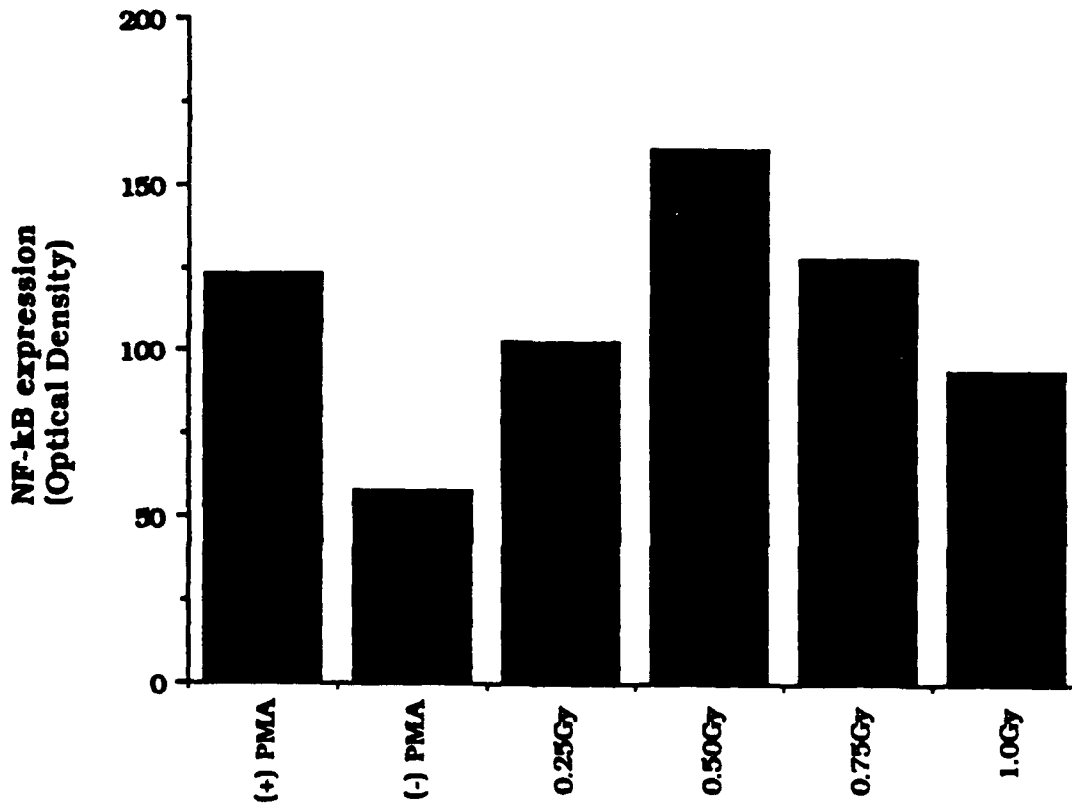


**Figure 2:** Quantitation of dose dependent DNA-binding activity of NF-κB by densitometric analysis. The autoradiograph in Figure 1 was photoscreened by a desktop digital imaging method and analyzed using NIH 1.45 image analysis software with an integrated density program. Data shown is representative of three individual experiments and expressed as optical density values.

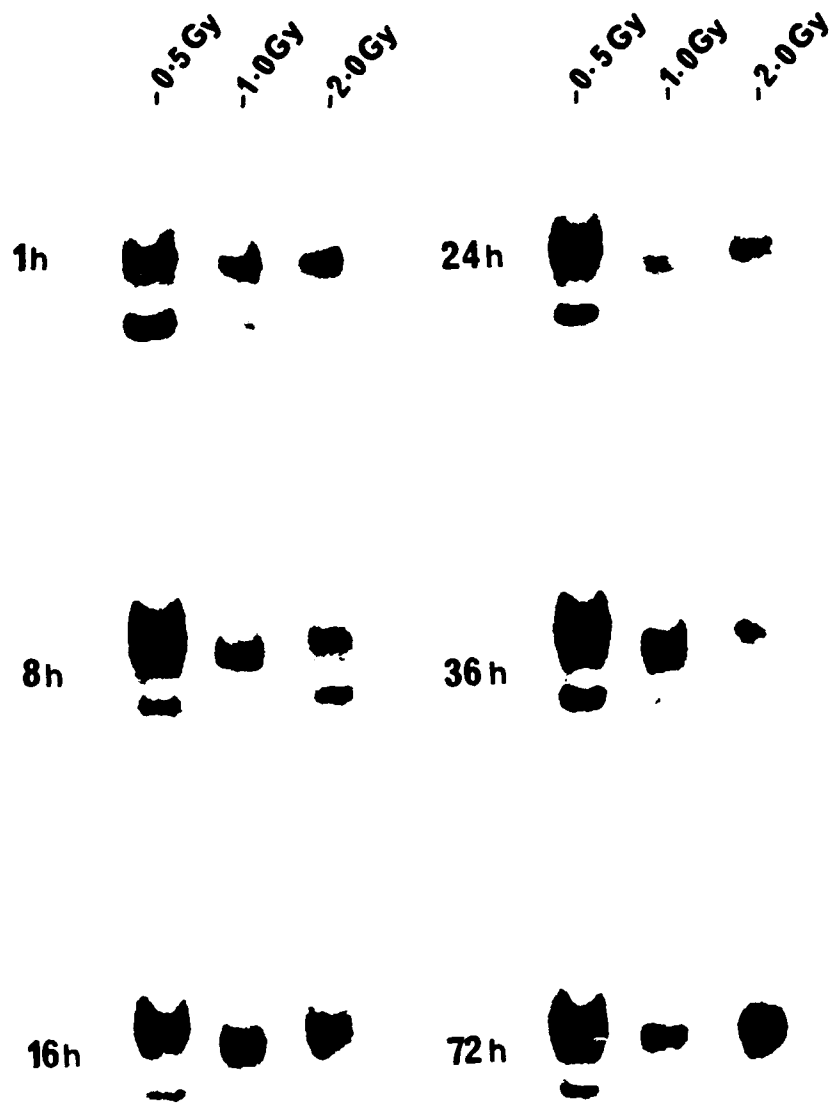


**Figure 3:** Kinetics with increasing time of binding of nuclear factor NF- $\kappa$ B from 244B cells treated with ionizing radiation ranging from 0.5, 1.0 and 2.0 Gy for the time periods as indicated. Twenty micrograms of nuclear protein were incubated with end labeled ds-oligonucleotide containing the NF- $\kappa$ B binding site as described in Figure 1. Autoradiograms of native gel are shown.

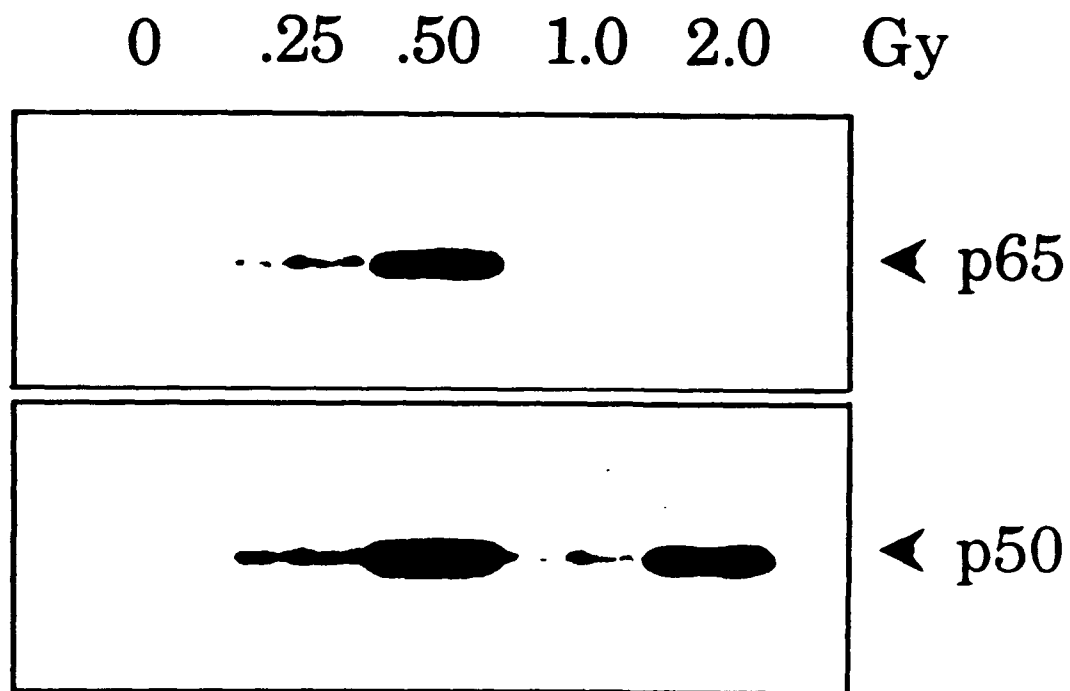


**Figure 4:** Differential regulation of transcription factor NF- $\kappa$ B p50 and p65 subunits expression by various doses of ionizing radiation in EBV transformed 244B lymphoblastoid cells. Thirty micrograms of whole cell extracts were subjected to SDS-PAGE analysis and electroblotted onto nitrocellulose membrane. The relative levels of p50 and p65 subunit expression were detected using polyclonal antibodies against p65 (upper panel) and p50 (lower panel) subunits and second antibody followed by  $^{125}$ I protein A.

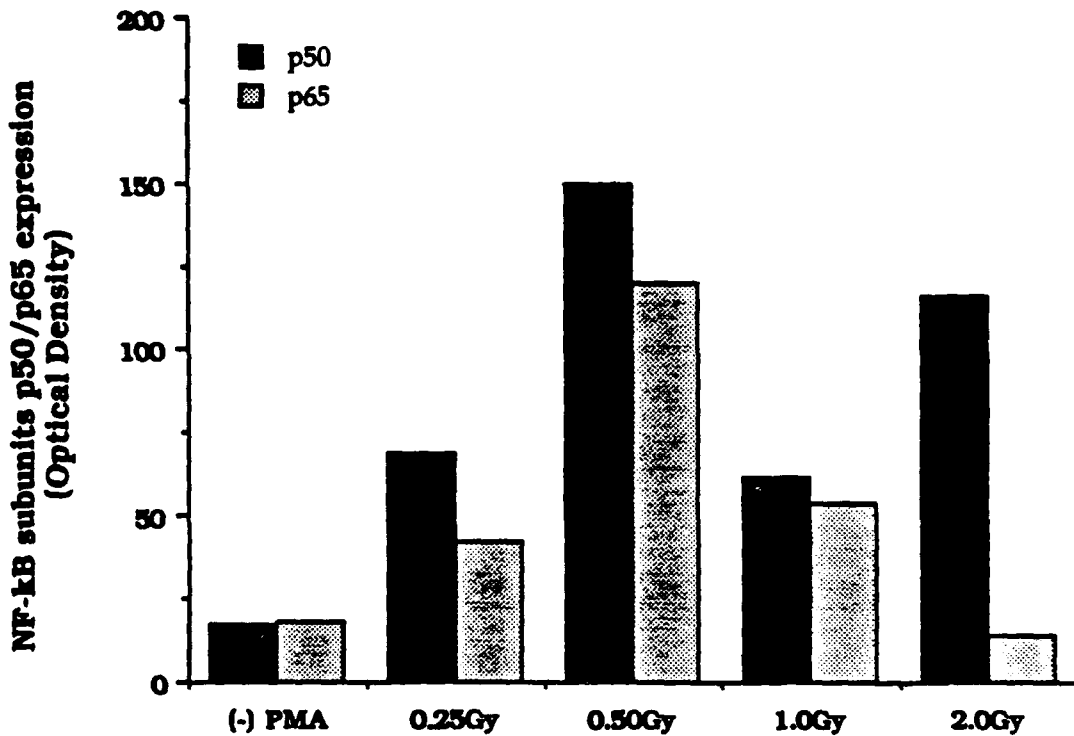


**Figure 5:** Densitometric analysis of NF-κB subunit p50/p65 expression after low dose ionizing radiation. The autoradiograph in Figure 5 was photoscreened by a desktop digital imaging method and analyzed using NIH 1.45 image analysis software with an integrated density program. Data shown is representative of three individual experiments and expressed as optical density values.

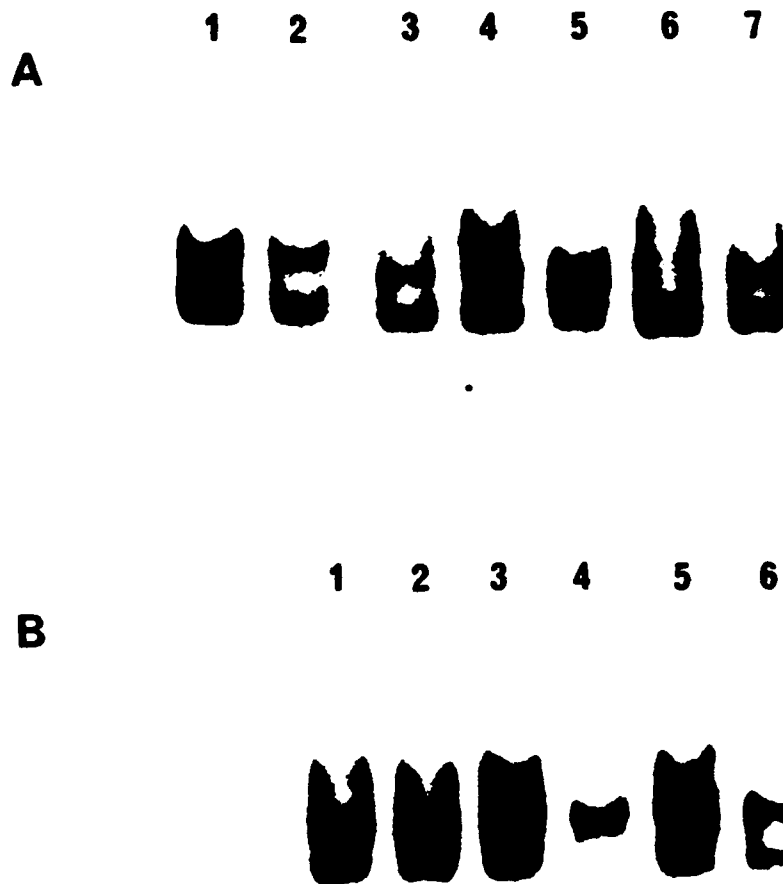


**Figure 6:** The effect of low dose ionizing radiation on signal transduction. Effect of signal transduction inhibitors in PMA treated or irradiated 244B cells were analyzed by EMSA.

A) 244B cells were treated with PMA (lane 1), nifedipine (lane 3), NAC (lane 4), calphostin (lane 5), 2-aminopurine (lane 6), genistein (lane 7) or unstimulated (lane 2) for 8 h in culture. B) Irradiated 244B cells were treated with nifedipine (lane 2), NAC (lane 3), calphostin C (lane 4), 2-aminopurine (lane 5) for 8 h. Lane 1 shows 244B cells irradiated with 50 cGy exposure alone.

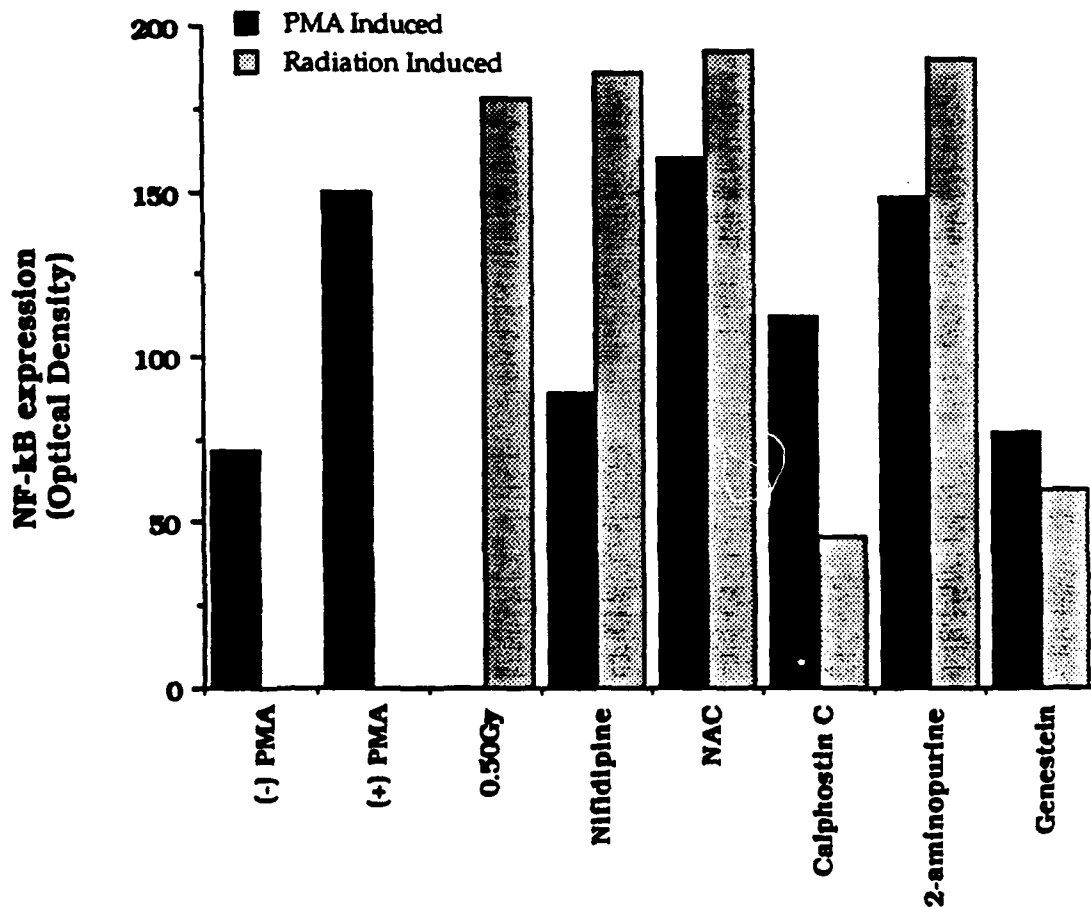


**Figure 7:** Densitometric analysis of NF- $\kappa$ B expression in the presence of signal transduction inhibitors.

The autoradiograph in Figure 6 was photoscreened by a desktop digital imaging method and analyzed using NIH 1.45 image analysis software with an integrated density program. Data shown is representative of three individual experiments and expressed as optical density values.

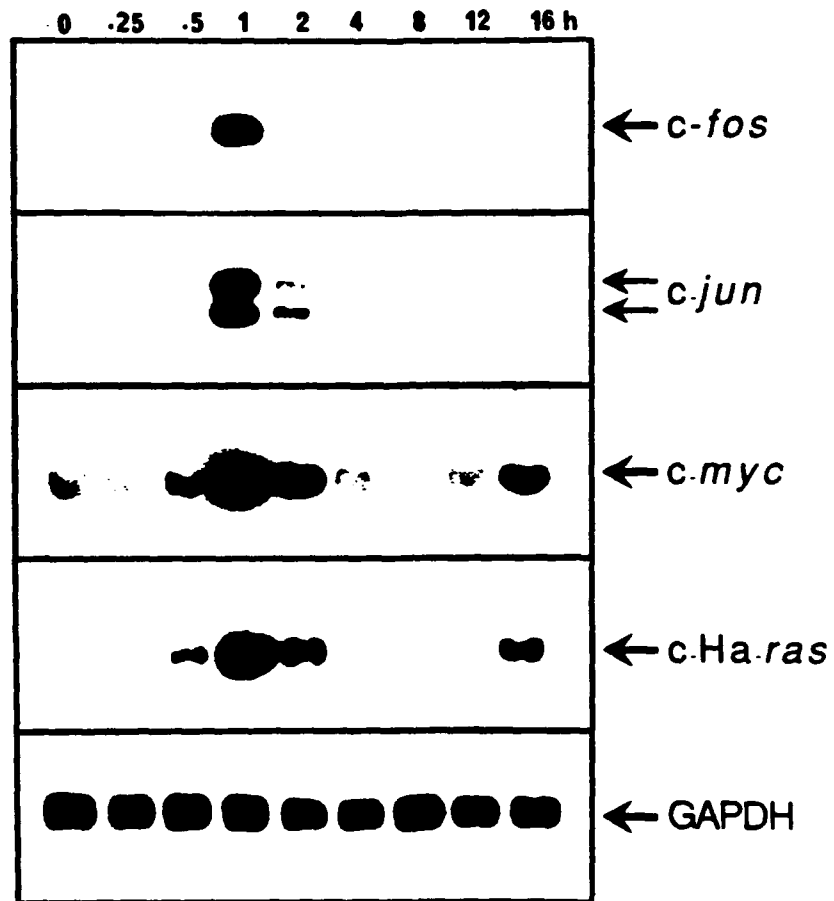


**Figure 8:** Time kinetics of *c-fos*, *c-jun*, *c-myc* and *c-Ha-ras* expression after low dose ionizing radiation exposure. Northern blot analysis was carried out as described in experimental methods.

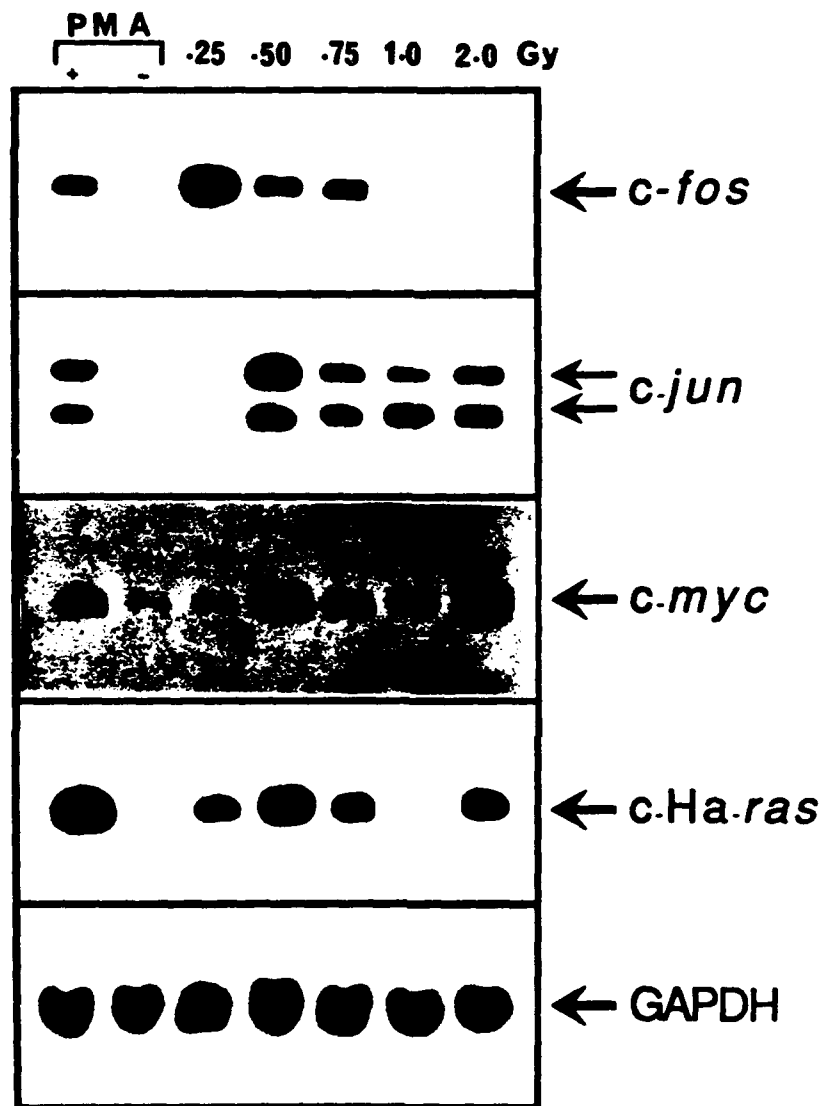


**Figure 9:** Dose dependent induction of immediate early gene transcripts (*c-fos*, *c-jun*, *c-myc* and *c-Ha-ras*) by low dose ionizing radiation. Northern blot analysis was carried out as described in experimental methods.

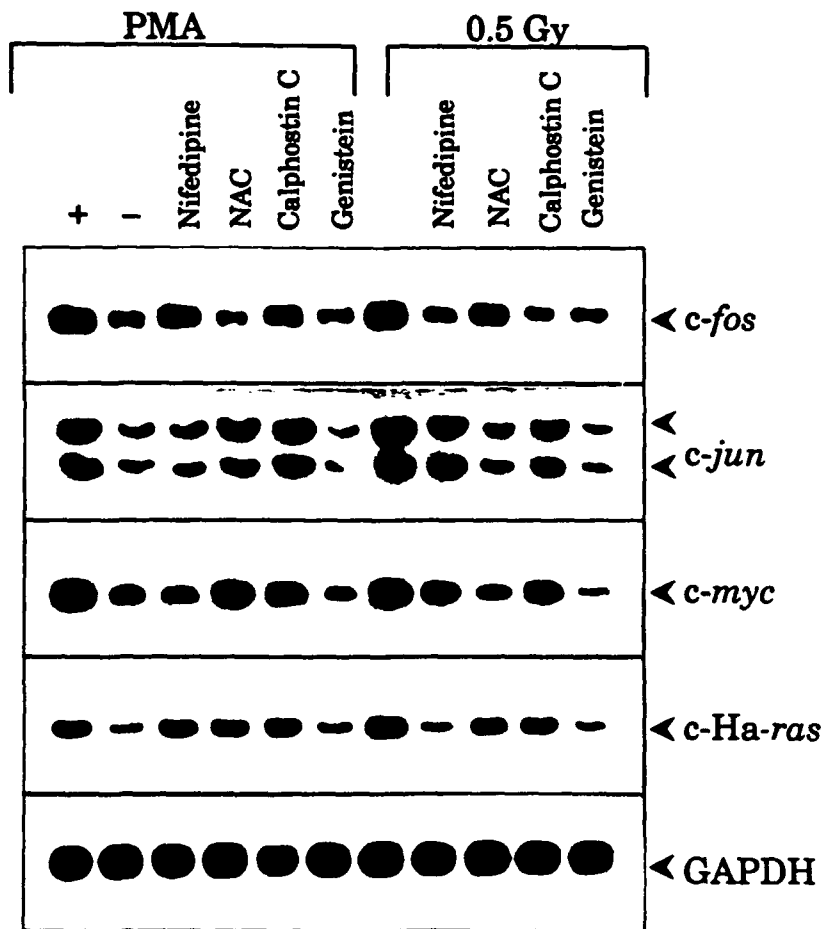


**Figure 10:** Signal transduction mechanism in the induction of immediate early gene in response to PMA or low dose ionizing radiation (50 cGy) exposure.

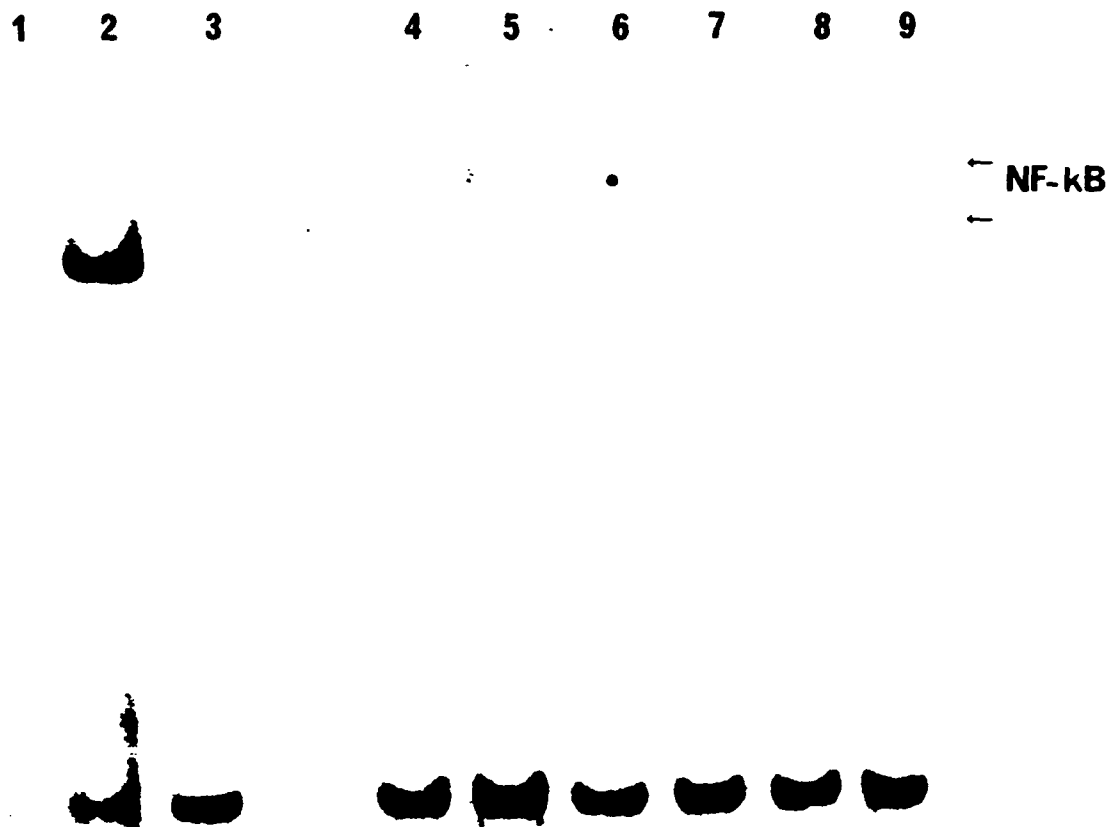


**Figure 11.** Density dependent NF- $\kappa$ B protein expression in 244B human lymphoblastoid cells. An electrophoretic mobility shift analysis was performed using 20  $\mu$ g of nuclear extract of 244B cells cultured in the presence or absence of PMA (20 ng/ml). Lane 1: Free probe; Lane 2: Hela cell nuclear extract as positive control; Lane 3: Competition assay using homologous unlabeled NF- $\kappa$ B specific oligonucleotide probe showing knocking off of the specific band; Lanes 4 & 5: Extracts derived from  $1 \times 10^6$  cells/ml in the absence or presence of PMA; Lanes 6 & 7: Extract derived from  $2.5 \times 10^6$  cells/ml in the absence or presence of PMA. Lanes 8 & 9: Extracts derived from  $5.0 \times 10^6$  cells/ml in the absence or presence of PMA. Arrow represents the position of gel shift complexes.

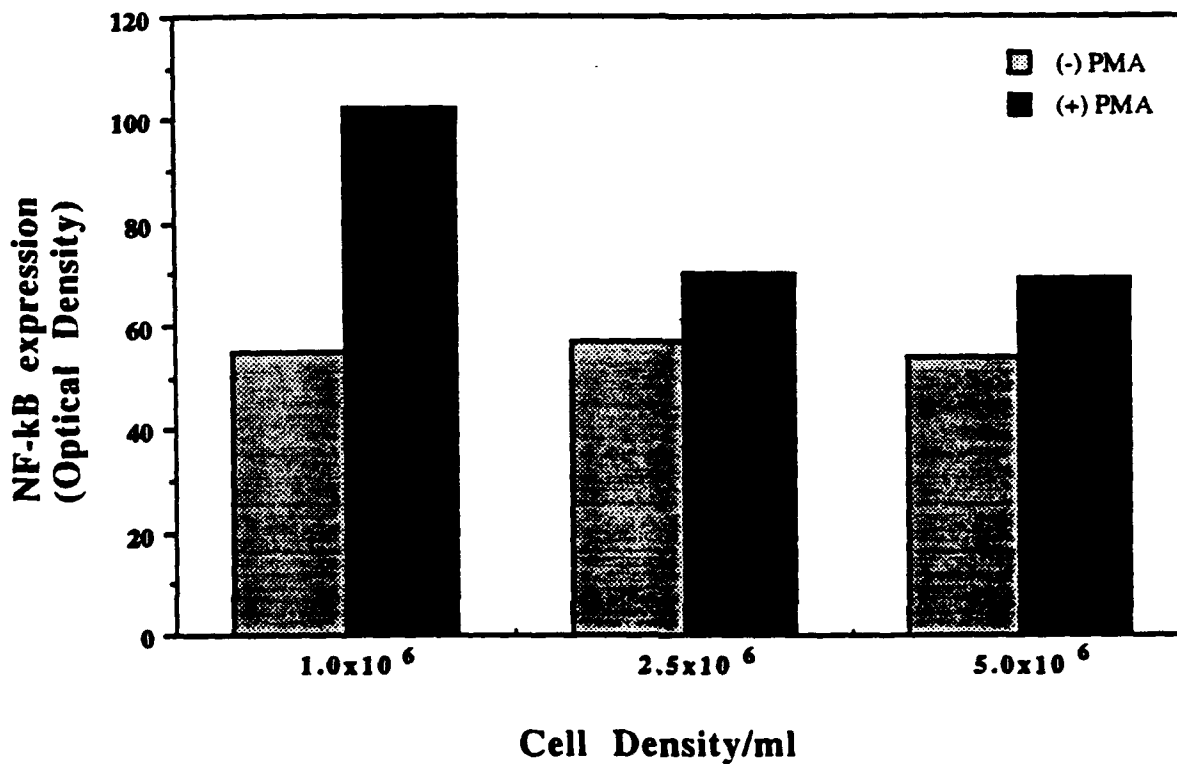


**Figure 12.** Densitometric analysis. The autoradiographs in Figure 11 was photoscreened by a desk top digital imaging method and analyzed using NIH 1.45 image analysis software with an integrated density program. Data shown is representative of three individual experiments and expressed as optical density values.

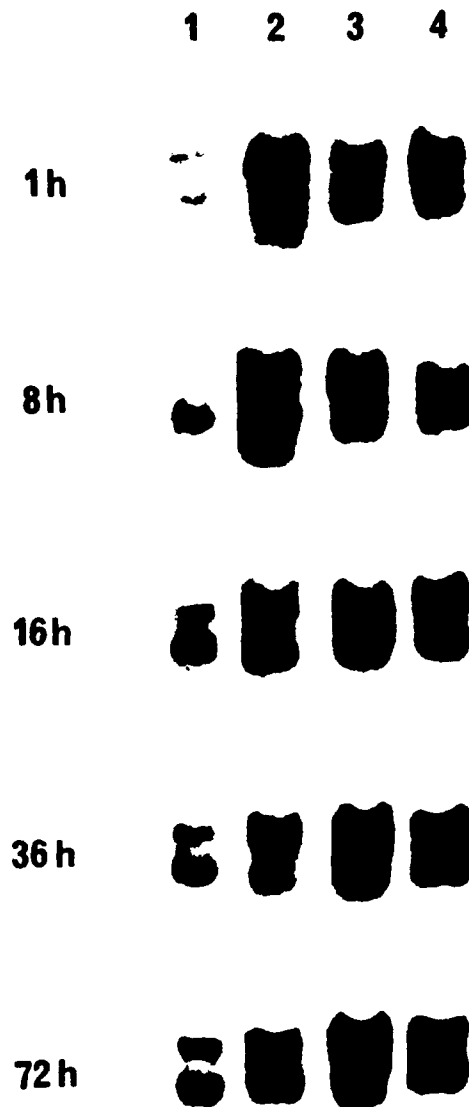


**Figure 13.** Kinetics of transcription factor NF- $\kappa$ B expression in the presence of PMA in  $1.0 \times 10^6$  cells/ml (lane 2),  $2.5 \times 10^6$  cells/ml (lane 3) and  $5.0 \times 10^6$  cells/ml (lane 4). Human lymphoblastoid cells (244B) at different cell densities were treated with 20 ng/ml of PMA for 1h, 8h, 16h, 36h and 72h. The cells were analyzed for the induction of transcription factor NF- $\kappa$ B by gel mobility shift assay. Lane 1 represents the constitutive levels of NF- $\kappa$ B in the absence of PMA initially at  $1 \times 10^5$  cells/ml.

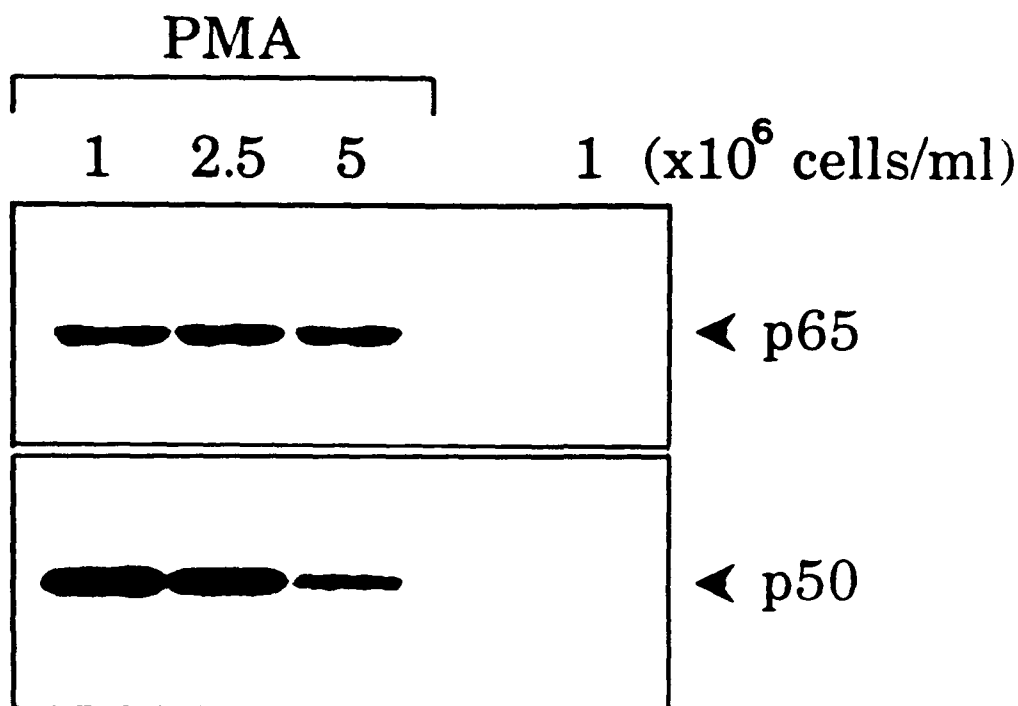


**Figure 14.** Western blot analysis of 244B cells incubated with PMA (20 ng/ml) at the indicated cell densities. Protein samples (30  $\mu$ g) from the nuclear extracts prepared for EMSA were analyzed by SDS-PAGE under reducing condition, and electroblotted onto nitrocellulose membrane. The immobilized proteins were then processed according to the protocol described under Materials and Methods. After washing, the membrane was autoradiographed. The upper panel shows the p65 subunit, which was exposed for 72 h at  $-70^{\circ}\text{C}$  to visualize the band. The lower panel shows the p50 subunit, which was exposed for 4 h at  $-70^{\circ}\text{C}$ . Lanes 1, 2 and 3 are extracts from PMA induced 244B cells at a density of  $1 \times 10^6$ ,  $2.5 \times 10^6$  and  $5.0 \times 10^6$  cells/ml respectively. Lane 4 shows subunit pattern in induced control.